P-124

Variable Sweep Transition Flight Experiment (VSTFE) — Unified Stability System (USS) Description and User's Manual

R. A Rozendaal
R. Behbehani

July 1989

████████████████████The limitations contained in this legend will be considered void after
July 1991. This legend shall be marked on any reproduction of these data in whole or in part.

for
Laminar Flow Control Project Office
NATIONAL AERONAUTICS AND SPACE ADMINISTRATION

NASA

National Aeronautics and
Space Administration

Langley Research Center
Hampton, Virginia 23665-5225

NASA CR-181918

Variable Sweep Transition Flight Experiment (VSTFE) — Unified Stability System (USS) Description and User's Manual

R. A Rozendaal
R. Behbehani

July 1989

for
Laminar Flow Control Project Office
NATIONAL AERONAUTICS AND SPACE ADMINISTRATION

NASA

National Aeronautics and
Space Administration

Langley Research Center
Hampton, Virginia 23665-5225

CONTENTS

1. Report No. NASA CR-181918	2. Government Accession No.	3. Recipient's Catalog No.
4. Title and Subtitle Variable Sweep Transition Flight Experiment (VSTFE) — Unified Stability System (USS) Description and Users' Manual		5. Report Date June 1990
		6. Performing Organization Code
7. Author(s) Rodger A. Rozendaal and Roxanna Behbehani		8. Performing Organization Report No. D6-54961
		10. Work Unit No. 505-60-41-01
9. Performing Organization Name and Address The Boeing Company P.O. Box 3707 Seattle, WA 98124		11. Contract or Grant No. NAS1-15325
12. Sponsoring Agency Name and Address National Aeronautics and Space Administration Washington, DC 20546-0001		13. Type of Report and Period Covered Contractor Report October 1985-May 1990
		14. Sponsoring Agency Code

15. Supplementary Notes

Technical Monitors: D. W. Bartlett
D. V. Maddalon
NASA/Langley Research Center

16. Abstract

NASA initiated the Variable Sweep Transition Flight Experiment (VSTFE) to establish a boundary layer transition database for laminar flow wing design. For this experiment, full-span upper surface gloves were fitted to a variable sweep F-14 aircraft. The Boeing Company is under contract to NASA to provide design and analyses support for the program. This report documents the development of an improved laminar boundary layer stability analysis system called the Unified Stability System (USS) and shows results of its use on the VSTFE flight data. The USS consists of eight computer codes. The theoretical background of the system is described herein, as is the input, output, and usage hints. The USS is capable of analyzing boundary layer stability over a wide range of disturbance frequencies and orientations, making it possible to use different philosophies in calculating the growth of disturbances on sweptwings.

17. Key Words (Suggested by Author(s)) ● Computational fluid dynamics ● Crossflow disturbances ● Transition ● Linear stability theory ● Boundary layer ● Natural laminar flow (NLF) ● Wing glove ● Tollmein-Schlichting disturbances ● F-14 ● Flight test ● Computer code		18. Distribution Statement FEDD Distribution Subject Category 02	
19. Security Classif. (of this report) Unclassified FEDD	20. Security Classif. (of this page) Unclassified	21. No. of pages	22. Price*

*For sale by the National Technical Information Service, Springfield, VA 22161

1.0 SUMMARY

Flight testing of aircraft with natural laminar flow experiments in the last 10 years has brought this means of drag reduction closer to practical application on small to medium-sized transports. To assist in forming a database relating the length of natural laminar flow to various wing design parameters, NASA initiated the Variable Sweep Transition Flight Experiment (VSTFE) in 1983. This experiment involved flight testing different gloves on the F-14 aircraft and correlating the measured transition results with analytical disturbance growth calculations. The Boeing Company has been under contract to support NASA in several phases of the VSTFE. This report describes a new laminar boundary layer stability analysis computer system, called the Unified Stability System (USS), developed by Boeing, and documents USS analyses of 24 flight test cases from the VSTFE and earlier experiments.

Intelligent design of laminar flow airplanes requires the ability to predict the effect of the selection of airplane design parameters such as sweep, airfoil, and flight condition on the extent of laminar flow. Since the current state of the art for transition does not permit rigorous predictions, a semiempirical approach is required. The most successful correlations use disturbance amplification factors given by stability theory as the correlating parameter. This approach, originated in the 1950s, is quite straightforward for simple situations, but in modern applications there are many ways in which this method could be applied: following a particular disturbance along a streamline, or at some preferred direction, or some preferred wavelength or frequency, combinations of different disturbances, or some other approach as yet untried. The determination of the best method requires a statistical approach wherein a battery of reliable data are analyzed in various ways to see which is the most successful. With previous stability methods, this has involved an impractically large amount of labor. The analysis of a single transition data point requires many stability theory runs for each of the several approaches under consideration. Previous stability codes have required much human intervention in the form of initial guesses or in the selection of physically meaningful results from among a large number of solutions, some of which were spurious. The result is that previous transition correlations have not been exhaustively compared against all data. The purpose of the USS is to automate stability calculations, making statistical comparisons feasible.

The USS was developed to analyze spatial laminar boundary layer stability over a wide range of disturbance frequencies and orientations. In doing so it would overcome the limitations of old stability methods, which analyzed only enough disturbance conditions to satisfy particular growth philosophies. In the USS, these growth philosophies are included only in the final disturbance growth integrations, not in the stability analyses. This allows new philosophies to be tried without recomputing stability characteristics. In addition to the automatic calculation of a wide range of stability characteristics, the USS is intended to be easier to use than previous stability analysis codes.

The USS consists of eight separate computer codes that set up the run as desired by the user and carry out the boundary layer analysis, stability analyses, and integrations of disturbance growth as necessary. The laminar boundary layer is determined using a finite difference infinite sweep method with taper corrections and can account for forward sweep. The boundary layer stability is investigated using techniques developed by Dr. L. M. Mack and involves numerical integration of the disturbance equations through the boundary layer with disturbance eigenvalues that must be iteratively determined so the boundary conditions can be met. After the disturbance characteristics are calculated over a large range of frequencies and orientations, the total growth of various

disturbances using different growth philosophies is calculated. Presently, Tollmien-Schlichting (TS) growth at constant wave angle, crossflow (CF) growth using "irrotationality," and "maximum amplification" growth can be calculated.

Although the USS was intended to be easy to use, the wide range of boundary layer conditions that it may encounter made this difficult. The resulting system is reasonably expensive in computer time, and a new user should read the usage sections of this report carefully and completely before using the USS. The system creates many files that can be used to examine the details of laminar boundary layers and their associated stability with regard to various disturbances.

Fifteen conditions from the F-14 VSTFE flight tests were analyzed by the USS to determine disturbance growth and correlate it to the experimental transition points. These crossflow and Tollmien-Schlichting disturbance growth N-factors at transition were combined with N-factors from earlier laminar flow flight experiments on the F-111 and 757, which were reanalyzed using the USS. This group of transition N-factors scatter over a wide range, which makes their use as a prediction method for future laminar flow wing design questionable. The sensitivity of transition N-factors to small wing pressure field changes can account for some of this scatter. Some researchers consider the addition of curvature terms to the boundary layer stability equations to be important in establishing a transition criterion with less scatter. Adding curvature terms arising from surface and streamline curvature to the USS is straightforward, but curvature arising from the path of the disturbance followed on a surface is dependent on the growth philosophy chosen by the user. This would involve an iterative procedure.

Despite the scatter in the transition N-factor correlation presented in this report, the wide range of disturbances examined by the USS makes it a useful tool for analyzing the nature of disturbance growth in laminar boundary layers. The USS is recommended for general use in understanding the stability of laminar boundary layers on wings at speeds up to about a sonic freestream.

2.0 INTRODUCTION

Laminar flow investigations in the last 10 years have increased the optimism about obtaining significant areas of laminar flow on small- to medium-sized transports with little or no boundary layer suction. Intelligent design of laminar flow airplanes requires the ability to predict the effect of the selection of airplane design parameters such as sweep, airfoil, and flight condition on the extent of laminar flow. To significantly add to existing flight data regarding laminar flow on sweptwings, NASA initiated the Variable Sweep Transition Flight Experiment (VSTFE). The VSTFE is an effort involving the NASA Langley Research Center and the NASA Ames/Dryden Flight Research facility, with The Boeing Company providing design and analysis support under contract to Langley. Starting in 1986, flight tests were conducted at Dryden with an F-14 fitted with full-span upper surface wing gloves. Transition was measured for a wide range of flight conditions and wing sweep angles. Two gloves of different designs were examined: a "cleanup" or minimum modification glove and a 0.7-Mach glove designed by NASA Langley. Early results from flight tests with the cleanup glove are reported in reference 1. Boundary layer stability calculations were done on the VSTFE cleanup glove flight data by Boeing and were combined with measured transition locations to provide a transition prediction method. Reference 2 reports on the Boeing support of the VSTFE carried out before the flight testing. Reference 3 describes Langley's design of the 0.7-Mach glove.

The application of these data to airplane design requires adjustment for differences between conditions of the experiments and those of the intended application. Ideally, this adjustment would be made through a rigorous theory. Since a rigorous theory does not exist, an empirical or semi-empirical approach is required. The most successful approaches so far developed use disturbance amplification factors given by stability theory as the correlating parameter. This approach, originated in the 1950s, is quite straightforward for simple situations, but in modern applications there are many ways in which this method could be applied: following a particular disturbance along a streamline, or at some preferred direction, or some preferred wavelength or frequency, combinations of different disturbances, or some other approach as yet untried. The determination of the best method requires a statistical approach wherein a battery of reliable data are analyzed in various ways to see which is the most successful. With previous stability methods, this has involved an impractically large amount of labor. The analysis of a single transition data point requires many stability theory runs for each of the several approaches under consideration. Previous stability codes have required much human intervention in the form of initial guesses or in the selection of physically meaningful results from among a large number of solutions, some of which were spurious. The result is that previous transition correlations have not been exhaustively compared against all available data.

2.1 OBJECTIVE AND SCOPE

As part of the flight data analysis task of the VSTFE, NASA contracted with Boeing to improve and expand the capability of using linear stability theory to determine disturbance growth in sweptwing laminar boundary layers. The desirability of expanding on available methods was due in part to the different philosophies used by different researchers in the industry.

One philosophy used presently (refs. 2 and 4) investigates two classes of disturbances, those more or less aligned with the local external flow (called Tollmien-Schlichting (TS) disturbances), and those nearly perpendicular to the local external flow (called crossflow (CF) disturbances). This philosophy involves choosing a wave angle at which to analyze the TS disturbances. This is similar

3

to the "Option 6" growth calculation in the COSAL stability analysis program, reference 5. The angle is usually chosen to give the greatest growth throughout the range of important frequencies. In addition, this philosophy considers the zero frequency (stationary) crossflow disturbances to be the most important in causing transition and calculates the growth of stationary crossflow waves for which the component of spanwise wavelength is constant. This is the "irrotational" method described by Mack in reference 6.

Another philosophy of calculating disturbance growth does not distinguish between TS and CF wave classes, but calculates the growth of disturbances of different frequencies at whatever wave angle gives the maximum growth rate at each point on the wing. This is the philosophy used in "Option 1" of COSAL, reference 5. As shown in figure 1, both philosophies just described require only a partial knowledge of the boundary layer stability characteristics.

The objective of the stability analysis procedure described in this report is to automatically determine stability characteristics over a wide enough range of disturbance orientation and frequency so either of the disturbance growth philosophies mentioned above or any new approach could be evaluated.

The stability analysis system developed during this task was to be used in examining the new high-quality flight transition data taken during the VSTFE. Disturbance growth would then be calculated by the philosophies described above to determine their viability as transition criteria.

2.2 APPROACH

The laminar boundary layer stability analysis procedure described in this report consists of eight computer codes and is called the Unified Stability System (USS). Figure 2 shows the sequence of
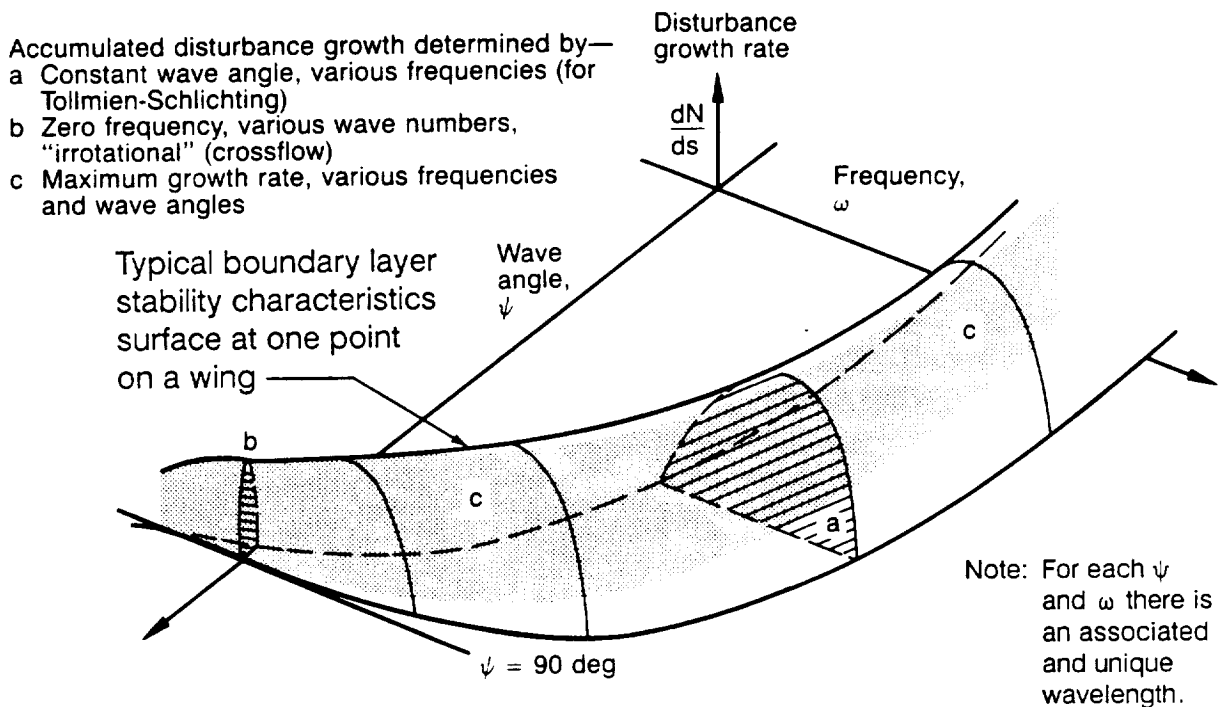

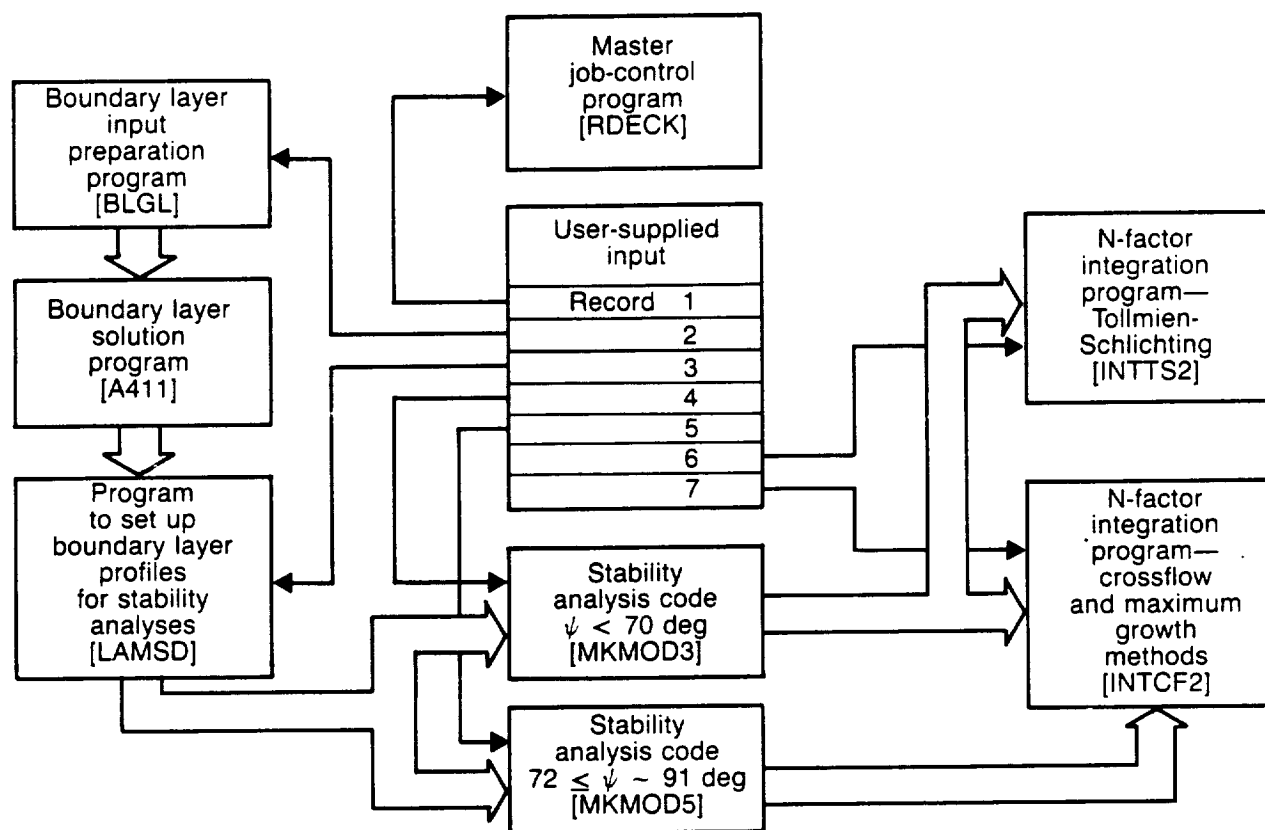Figure 1. — Philosophies of Determining Disturbance Growth

Figure 2. — The Unified Stability System

execution of the eight codes. A master program sets up the job control statements to carry out the calculations desired by the user. Three programs set up the input for the boundary layer analysis, carry out the analysis, and prepare the boundary layer information for stability analysis. The boundary layer analysis is a finite difference method that can account for conventional or inverse wing taper. The boundary layer analysis and stability analysis codes were based on existing codes and only modified as necessary to satisfy the requirements of the USS.

Two different computer codes are used to calculate the boundary layer stability. The mathematical basis and solution procedure in both are almost identical, but one is tailored to analyze disturbances with wave angles below 70 deg and the other disturbances with wave angles between 72 deg and about 91 deg. This range of wave angles covers the disturbances of primary interest to stability analysts for most cases on sweptwings. In choosing a stability analysis code for the USS, two existing methods were examined: COSAL, a temporal technique using matrix solution methods (ref. 5) and MACK, a method that can solve for temporal or spatial stability using numerical integration through the boundary layer (ref. 7). After considerable work with both methods, the MACK method was chosen for calculating the spatial stability required in the USS.

The mathematical development of the linear stability theory used in the MACK method parallels that for the Orr-Sommerfeld equation, but compressibility is included and the spanwise dimension is added. Disturbances in the boundary layer are characterized as having some wave length, λ, frequency, ω, wave direction relative to the local external flow, ψ, and a spatial growth rate,

dN/ds. N is the exponent of "e" in describing disturbance growth as: disturbance amplitude at some point = e^N times (amplitude of that disturbance when it first starts to be amplified). The introduction of that disturbance into the compressible, 3D boundary layer equations results in an eighth-order system of equations with four unknowns; λ, ω, ψ, dN/ds. Typically, wave length or frequency and wave orientation are chosen by the user, and the other two unknowns are solved for. This is an eigenvalue problem because solutions exist only for certain combinations of the unknowns. In the MACK method, guesses for the eigenvalues start an iterative solution process that uses the Newton-Raphson procedure to refine the eigenvalues until the system of equations is solved to within some adequate tolerance. In the USS, the initial guessing of values that will successfully converge to eigenvalues has been automated based on the work of previous authors and experience with the MACK method.

When spatial disturbance growth rates for different disturbance frequencies and orientations have been calculated along the wing surface, the integration to find total disturbance growth is done by two different programs in the USS. Both constant wave angle (TS) and "irrotational" (CF) disturbance growths are calculated, and the "maximum amplification" philosophy is also implemented. The constant wave angle integration is similar to "Option 6" of COSAL, and the "maximum amplification" integration is similar to "Option 1" of COSAL. However, with the USS, all the stability analyses are done before the disturbance growth integrations, so calculating disturbance growth for a range of frequencies does not require different stability program runs, as it does with COSAL.

The programs of the USS generate numerous files. Some only transfer information between programs, but several are available to the user for detailed examination and plotting of the laminar boundary layer and its stability characteristics.

Data for 15 flight conditions from the VSTFE cleanup glove testing were used to analyze laminar boundary layer disturbance characteristics for different wing sweep angles, freestream conditions, and wing pressure fields. The USS was used to calculate disturbance growth rates over a wide range of disturbance orientations and frequencies. Then downstream amplification of the disturbances using the constant wave angle approach for TS waves, the irrotational stationary wave approach for crossflow waves, and for some cases the maximum amplification approach was carried out. The amplification of TS and CF disturbances at the flight-measured transition point was plotted on a graph of N_{TS} versus N_{CF} for each case analyzed in order to establish transition criteria that could be used for laminar flow wing design. To further define the transition criteria using a consistent analysis method, several cases from earlier laminar flow flight tests on an F-111 (ref. 8) and a 757 (ref. 9) were reanalyzed with the USS.

3.0 SYMBOLS AND ABBREVIATIONS

Abbreviations:

CF	crossflow.
TS	Tollmien-Schlichting.
USS	Unified Stability System.
VSTFE	Variable Sweep Transition Flight Experiment.

Symbols:

c	wing section chord length.
C_p	wing section pressure coefficient.
H	boundary layer shape parameter, δ^*/θ. However, H (crossflow) is defined for the crossflow velocity profile as the ratio of (1) height at which the crossflow velocity is greatest to (2) the height at which the crossflow velocity is $\frac{1}{10}$ of its maximum value.
M_∞	freestream Mach number
N	accumulated growth of a disturbance in the laminar boundary layer. Also called N-factor.
Re_{CF}	Reynolds number based on maximum crossflow velocity, edge kinematic viscosity, and distance from the surface to the height at which the crossflow velocity is $\frac{1}{10}$ the magnitude of the maximum crossflow velocity.
Re_{TR}	Reynolds number based on freestream conditions and the length of laminar flow at a wing section.
Re_δ	Reynolds number based on local boundary layer thickness, δ, edge velocity, and edge kinematic viscosity.
Re_{δ^*}	similar to Re_δ with δ replaced by displacement thickness, δ^*.
s	distance along an airfoil section surface from the attachment line.
u	a velocity component in the "x" coordinate direction.
x	distance along an airfoil section chord line.
z	distance perpendicular to the airfoil chord line.
α	angle of attack.
α_r	real part of the nondimensional disturbance wave number in the "x" direction, see figure 9. In the rotated coordinate system, this is also the magnitude of the real part of the wave number.
α_i	imaginary part of the nondimensional disturbance wave number in the "x" direction, see figure 9. In a coordinate system with x aligned with the group velocity, α_i is the negative of spatial disturbance growth rate.

α_{r_s}	the spanwise component of α_r. This is used only with the unrotated coordinate system, and therefore, equals β_r in that system.
β_r	real part of the nondimensional disturbance wave number in the "z" direction. Equals zero by definition in a coordinate system with x aligned with the group velocity.
$\beta_{(F-S)}$	Falkner-Skan boundary layer pressure gradient parameter.
δ	boundary layer thickness, defined to be the distance from the surface at which the local velocity is 99% of the local edge velocity.
δ^*	boundary layer displacement thickness.
θ	boundary layer momentum thickness.
Λ	sweep angle.
ν	local kinematic viscosity.
$(\rho v)_{wall}$	suction mass flow rate.
$(\rho U)_\infty$	mass flow rate of the freestream.
$(\rho Q)_e$	local mass flow rate at the edge of the boundary layer.
ψ	an angle that defines the disturbance orientation, see figure 9.
$\overline{\psi}$	an angle that defines the orientation of the group velocity of a disturbance. This is the direction in which the disturbance grows in space.
ω	disturbance frequency.
λ	disturbance wavelength.

Subscripts:

CF	denotes a parameter associated with crossflow disturbances
e	denotes the local value of a parameter at the edge of the boundary layer.
LE	denotes the value of a parameter at the wing leading edge.
TR	denotes value of a parameter at boundary layer transition.
TS	denotes a parameter associated with Tollmien-Schlichting (low wave angle) disturbances.

Superscript:

*	denotes a dimensional quantity.

The following symbols are only applicable to section 4.2. They are presented separately because section 4.2 has the most complicated set of symbols in this report.

Symbols:

$A_i^{(j)}$	components of the characteristic vector of the compressible stability equations outside the boundary layer. The subscript denotes the component of the solution vector and the superscript denotes the number of the independent solution associated with this component.
A_o	Initial disturbance amplitude in equation (21).
a_{ij}	Components of the eight first-order differential equations that the compressible stability equations can be reduced to. The subscripts vary from 1 to 8 and denote the position of a in the 8 by 8 matrix of terms.
c_v, c_p	specific heat at constant volume and pressure, respectively.
D	$\dfrac{d(\quad)}{dy}$, D^2 is the second derivative.
e_{ij}	components of the rate of strain tensor, see equation (2a).
H (crossflow)	crossflow boundary layer shape factor. The ratio of (1) the height at which the crossflow velocity is greatest to (2) the height at which the crossflow velocity is $\frac{1}{10}$ of its maximum value.
i	the imaginary number $\sqrt{-1}$.
$\vec{k}_c$	the complex wave number vector. Without the subscript, it refers to the real part of the wave number.
L	reference length.
M	Mach number.
P	pressure, mean value.
p	pressure.
R	Reynolds number.
R_{CF}	Reynolds number based on δ_{10}, maximum crossflow velocity, and edge kinematic viscosity.
R_{δ^*}	Reynolds number based on δ^*, edge velocity, and edge kinematic viscosity.
r	density, time fluctuating part.
S	a "normalized" redefinition of Z done by the Gram-Schmidt ortho-normalization algorithm, see equations (18) and (19).
T	temperature.
t	time.
U (U,V,W)	the three components of mean velocity. U can also be used as the mean velocity vector.

u (u,v,w)	the three fluctuating components of velocity. u can also be used as the fluctuating velocity vector and, when used with the bar (−), is the total time-varying velocity vector.
x_i (x,y,z)	the three component directions. x can also be any of the three orthogonal directions when used with a subscript.
Z_i	redefined variables in the stability equations that form a system of 8 first-order differential equations. The index varies from 1 to 8.
α	component of the complex disturbance wave number in the x direction.
β	component of the complex disturbance wave number in the z direction.
$\beta_{(F-S)}$	Falkner-Skan boundary layer pressure gradient parameter.
γ	ratio of specific heats.
$\Delta(\ )$	denotes a finite change in the parameter in the parentheses.
δ^*	boundary layer displacement thickness.
δ_{10}	height in the boundary layer at which the crossflow velocity is $\frac{1}{10}$ the magnitude of the maximum crossflow velocity.
δ_{ij}	Dirac delta function.
Θ	in the normal mode form of disturbances, Θ is the function in the exponent of e, see equations (7) and (21).
θ	temperature, time-varying part.
κ	coefficient of thermal conductivity.
λ	second coefficient of viscosity.
λ_i	characteristic values that form the solutions to the system of first-order differential equations of stability outside the boundary layer. The index varies from 1 to 8 although only $i = 1,3,5$ and 7 are physically reasonable.
μ	coefficient of viscosity.
ρ	density.
σ	Prandtl number.
τ_{ij}	stress tensor.
ψ	an angle that defines the disturbance orientation, see figure 9.
$\overline{\psi}$	an angle that defines the orientation of the group velocity of a disturbance. This is the direction in which the disturbance grows in space.
ω	disturbance frequency.

Subscripts:

CRITICAL   value of a parameter at which the disturbance it is associated with
                  has its maximum growth rate. This also applies to the value of a
                  parameter when there is some disturbance that is unstable.

i,j   both i and j are used to denote one of the three component
                  directions.

i   the imaginary part of a parameter.

r   the real part of a parameter.

1   denotes value of parameter at the edge of the boundary layer.

Superscripts:

*   denotes a dimensional quantity except for δ^*.

'   denotes the fluctuating part of a variable.

Special designators:

^   caret, denotes the part of a variable that is a function of y only in
                  the normal mode disturbance designation. See equation (7).

—   overbar, denotes a parameter that varies with time.

~   tilde, denotes a change of variable definition in equation (8).

4.0 USS THEORETICAL DEVELOPMENT

The three main functions of the Unified Stability System (USS) are laminar boundary layer analysis, boundary layer stability analysis, and disturbance growth calculations. The first two of these functions use computer programs that were developed previously and described in the literature. The boundary layer method is described in detail in reference 10, and therefore only a brief outline of it is repeated here. The stability analysis uses a method developed by Dr. L. M. Mack, and it is explained in reference 7. However, that reference gives a more general background of stability theory than is used in the USS, so the development of the method that pertains to the USS is presented in this report. The disturbance growth calculations use computer code developed completely under this contract and are explained herein.

4.1 BOUNDARY LAYER ANALYSIS

The boundary layer program is essentially the same code, with some improvements and corrections, that was delivered to NASA in 1979 and reported in reference 10. It is a general-purpose 3D finite-difference code that has been applied to wings, fuselages, inlets, wind tunnel walls, and propfan blades. In the present application, the code is used in the infinite-span-wing mode with taper effects, in which it solves the special form of the 3D boundary layer equations applicable to the coordinate system shown in figure 3. It is assumed that the isobars of the sweptwing flow lie along lines of constant percent chord, or that pressure is constant along the spanwise x-coordinate lines.

It is further assumed that the boundary layer solution is similar along x-coordinate lines and that the boundary layer thickness varies with the local chord in a prescribed way ($\sqrt{c}$ for laminar flow). The x-direction derivatives in the 3D equations can then be expressed in terms of derivatives normal to the surface, and spanwise finite differences are not required. The 3D solution can be generated by integration along a single chordwise arc.

The same similarity arguments are applied to the flow in the neighborhood of the leading edge attachment line, leading to a special form of the attachment line boundary layer equations that the program solves to start the solution near the leading edge. Thus, for laminar flow the equations solved are equivalent to those solved by the special-purpose code of Kaups and Cebeci (ref. 11). Running the 3D code in this mode requires specialized inputs. The z-coordinate is defined as arc length measured from the attachment line along the intersection of the wing surface and a sphere of radius r_0 centered at point A, normalized by c, the local chord at the intersection of the arc and the trailing edge. The metric coefficients consistent with this choice are as follows:

$$h_1 = 1$$
$$h_3 = c$$
$$K_{13} = 0$$
$$K_{31} = -1/r_0$$

The boundary conditions required along the arc are velocity vectors at the boundary layer edge that are consistent with the tapered wing similarity assumption. These are calculated by the input preprocessing program, BLGL, using airfoil section geometry and a pressure (Cp) distribution from a 2D or 3D outer flow solution or from experimental measurements. Because the attachment line of the flow generally falls between input data points, a special curve-fitting technique is used in the preprocessor to locate the attachment line and define flow quantities in its neighborhood, so

12

Analysis Section—Rear View
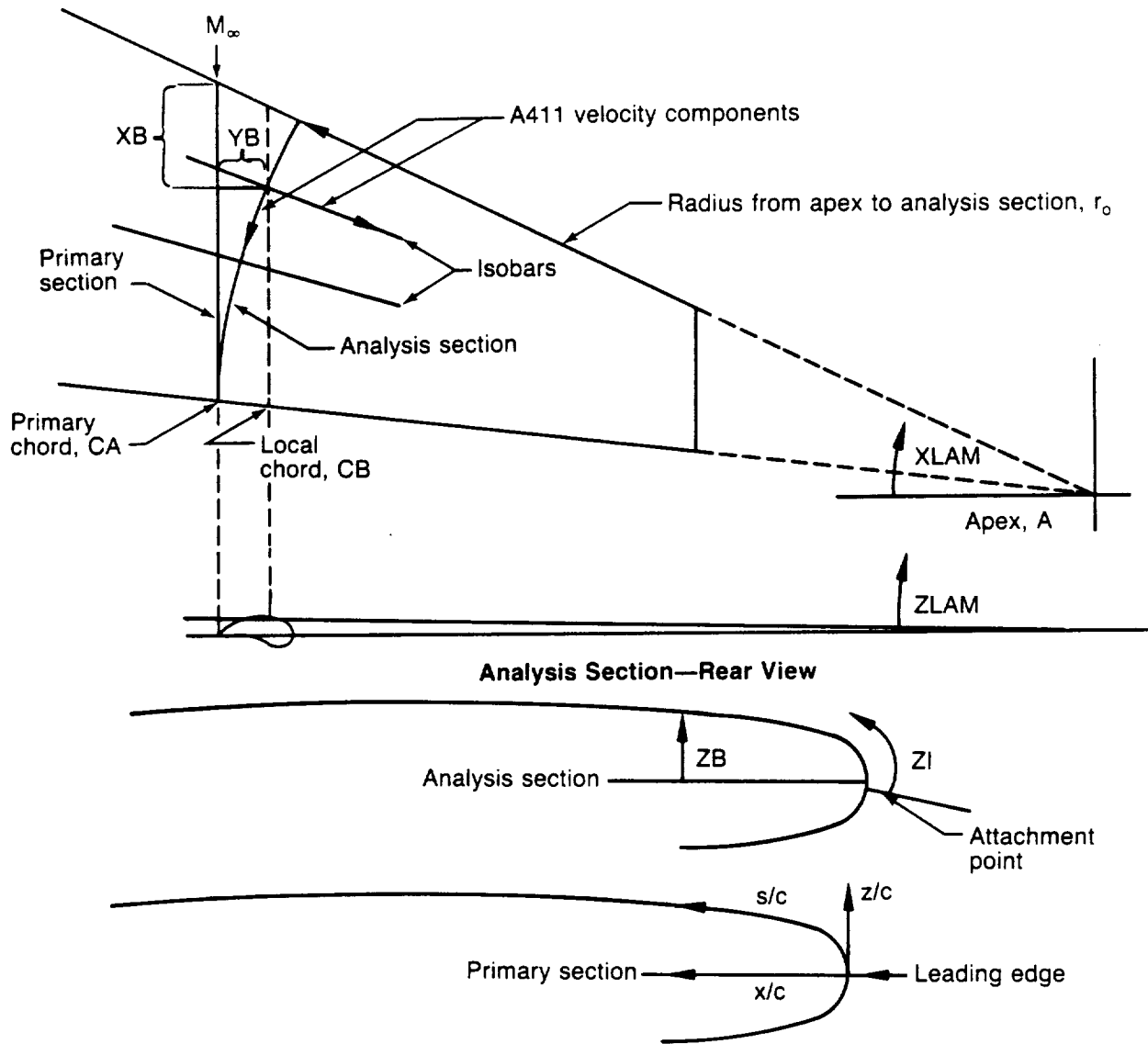
Figure 3. — A411 Geometric Definitions

the boundary layer code computes correct flow derivatives and obtains a correct solution for the attachment line flow. For most laminar flow applications it is not adequate simply to assume that the attachment line coincides with the leading edge.

Subsequent stability analysis of the boundary layer requires that the velocity profiles be defined along a different chordwise path than the arc along which the boundary layer code generates the solution for the velocity field. A postprocessing program, LAMSD, performs the transformation of the velocity profiles (a simple normal coordinate stretching) to the spanwise locations desired for the stability analysis.

13

4.2 STABILITY ANALYSIS

The material presented in this section is an abbreviated form of what Dr. L. M. Mack gave in his AGARD paper (ref. 7). The important mathematical points pertinent to the USS stability analysis codes MKMOD3 and MKMOD5 are outlined. For more detail, reference 7 should be consulted.

Compressible stability theory starts with the derivation of the governing equations from the Navier-Stokes equations for a viscous, heat-conducting, perfect gas, which in dimensional form are:

$$\frac{\partial \bar{u}_i}{\partial t^*} + \bar{u}_j^* \frac{\partial \bar{u}_i}{\partial x_j^*} = \frac{1}{\bar{\rho}^*} \frac{\partial \bar{\tau}^*_{ij}}{\partial x_j^*} \quad , \tag{1a}$$

$$\frac{\partial \bar{\rho}^*}{\partial t^*} + \frac{\partial}{\partial x_j^*}(\bar{\rho}^* \bar{u}_j^*) = 0 \quad , \tag{1b}$$

$$\rho^* c_v^* \left[\frac{\partial T^*}{\partial t^*} + \bar{u}_j^* \frac{\partial T^*}{\partial x_j^*} \right] = \frac{\partial}{\partial x_j^*} \left[\bar{\kappa}^* \frac{\partial T^*}{\partial x_j^*} \right] + \bar{\tau}^*_{ij} \bar{e}^*_{ij} \quad , \tag{1c}$$

$$\bar{p}^* = \bar{\rho}^* R^* T^* \tag{1d}$$

where

$$\bar{e}^*_{ij} = \frac{1}{2} \left[\frac{\partial \bar{u}_i^*}{\partial x_j^*} + \frac{\partial \bar{u}_j^*}{\partial x_i^*} \right] \quad , \tag{2a}$$

$$\bar{\tau}^*_{ij} = 2\bar{\mu}^* \bar{e}^*_{ij} + \left[\frac{2}{3}(\bar{\lambda}^* - \bar{\mu}^*)\bar{e}^*_{kk} - \bar{p}^* \right] \delta_{ij}. \tag{2b}$$

The asterisks denote dimensional quantities, overbars denote time-dependent quantities, and tensor summation convention has been adopted. The equations are, respectively, of momentum, continuity, energy, and state.

The stability equations are obtained from the Navier-Stokes equations by the following procedure. First, all quantities are divided into mean flow and fluctuating terms. With primes used to denote fluctuations of the transport coefficients,

$$\begin{aligned}
\bar{u}^* &= U^* + u^*, & \bar{p} &= P^* + p^*, \\
\bar{T}^* &= T^* + \theta^*, & \bar{\rho}^* &= \rho^* + r^*, \\
\bar{\mu}^* &= \mu^* + \mu'^*, & \bar{\kappa}^* &= \kappa^* + \kappa'^*, & \bar{\lambda}^* &= \lambda^* + \lambda'^*.
\end{aligned} \tag{3}$$

where the first variable on each RHS is a steady mean-flow quantity, and the second is an unsteady fluctuation.

Next, the equations are linearized, the mean-flow terms are subtracted out, and, finally, the parallel-flow assumption is made. The resulting equations are then made dimensionless with respect to the local freestream velocity U^*_1, a reference length L^*, and the freestream values of all state

14

variables (including the pressure). Both viscosity coefficients are referenced to μ_1^*, and κ^* is referenced to $c_p \mu_1^*$, where c_p is the specific heat at constant pressure. The transport coefficients are functions only of temperature so their fluctuations can be written

$$\mu' = \left(\frac{d\mu}{dT}\right)\theta, \quad \kappa' = \left(\frac{d\kappa}{dT}\right)\theta, \quad \lambda' = \left(\frac{d\lambda}{dT}\right)\theta. \tag{4}$$

Therefore, μ, κ, and λ in the following equations along with ρ are mean-flow quantities, not fluctuations. The dimensionless, linearized x-momentum equation is

$$\rho\left(\frac{\partial u}{\partial t} + U\frac{\partial u}{\partial x} + v\frac{dU}{dy} + W\frac{\partial u}{\partial z}\right) = -\frac{1}{\gamma M_1^2}\frac{\partial p}{\partial x} + \frac{1}{R}\left[2\mu\frac{\partial^2 u}{\partial x^2} + \mu\left(\frac{\partial^2 u}{\partial y^2} + \frac{\partial^2 u}{\partial z^2} + \frac{\partial^2 v}{\partial x\partial y} + \frac{\partial^2 w}{\partial x\partial z}\right)\right. \tag{5a}$$

$$+ \frac{2}{3}(\lambda - \mu)\left(\frac{\partial^2 u}{\partial x^2} + \frac{\partial^2 v}{\partial x\partial y} + \frac{\partial^2 w}{\partial x\partial z}\right) + \frac{d\mu}{dT}\frac{dT}{dy}\left(\frac{\partial u}{\partial y} + \frac{\partial v}{\partial x}\right) + \frac{d\mu}{dT}\left(\frac{d^2 U}{dy^2}\theta + \frac{dU}{dy}\frac{\partial\theta}{\partial y}\right) + \frac{d^2\mu}{dT^2}\frac{dT}{dy}\frac{dU}{dy}\theta\right].$$

The y-momentum equation is

$$\rho\left(\frac{\partial v}{\partial t} + U\frac{\partial v}{\partial x} + W\frac{\partial v}{\partial z}\right) = -\frac{1}{\gamma M_1^2}\frac{\partial p}{\partial y} + \frac{1}{R}\left[2\mu\frac{\partial^2 v}{\partial y^2} + \mu\left(\frac{\partial^2 v}{\partial x^2} + \frac{\partial^2 v}{\partial z^2} + \frac{\partial^2 u}{\partial x\partial y} + \frac{\partial^2 w}{\partial y\partial z}\right)\right. \tag{5b}$$

$$+ \frac{2}{3}(\lambda - \mu)\left(\frac{\partial^2 u}{\partial x\partial y} + \frac{\partial^2 v}{\partial y^2} + \frac{\partial^2 w}{\partial y\partial z}\right) + \frac{d\mu}{dT}\left(2\frac{dT}{dy}\frac{\partial v}{\partial y} + \frac{dU}{dy}\frac{\partial\theta}{\partial x} + \frac{dW}{dy}\frac{\partial\theta}{\partial z}\right)$$

$$+ \frac{2}{3}\left(\frac{d\lambda}{dT} - \frac{d\mu}{dT}\right)\frac{dT}{dy}\left(\frac{\partial u}{\partial x} + \frac{\partial v}{\partial y} + \frac{\partial w}{\partial z}\right)\right].$$

The z-momentum equation is

$$\rho\left(\frac{\partial w}{\partial t} + U\frac{\partial w}{\partial x} + v\frac{dW}{dy} + W\frac{\partial w}{\partial z}\right) = -\frac{1}{\gamma M_1^2}\frac{\partial p}{\partial z} + \frac{1}{R}\left[2\mu\frac{\partial^2 w}{\partial z^2} + \mu\left(\frac{\partial^2 w}{\partial y^2} + \frac{\partial^2 w}{\partial x^2} + \frac{\partial^2 v}{\partial y\partial z} + \frac{\partial^2 u}{\partial x\partial z}\right)\right. \tag{5c}$$

$$+ \frac{2}{3}(\lambda - \mu)\left(\frac{\partial^2 w}{\partial z^2} + \frac{\partial^2 v}{\partial y\partial z} + \frac{\partial^2 u}{\partial x\partial z}\right) + \frac{d\mu}{dT}\frac{dT}{dy}\left(\frac{\partial w}{\partial y} + \frac{\partial v}{\partial z}\right) + \frac{d\mu}{dT}\left(\frac{d^2 W}{dy^2}\theta + \frac{dW}{dy}\frac{\partial\theta}{\partial y}\right) + \frac{d^2\mu}{dT^2}\frac{dT}{dy}\frac{dW}{dy}\theta\right].$$

The continuity equation is

$$\frac{\partial r}{\partial t} + \varrho\left(\frac{\partial u}{\partial x} + \frac{\partial v}{\partial y} + \frac{\partial w}{\partial z}\right) + v\frac{d\varrho}{dy} + U\frac{\partial r}{\partial x} + W\frac{\partial r}{\partial z} = 0. \tag{5d}$$

15

The energy equation is

$$\rho\left(\frac{\partial\theta}{\partial t} + U\frac{\partial\theta}{\partial x} + v\frac{dT}{dy} + W\frac{\partial\theta}{\partial z}\right) = -(\gamma-1)\left(\frac{\partial u}{\partial x} + \frac{\partial v}{\partial y} + \frac{\partial w}{\partial z}\right) \tag{5e}$$

$$+ \frac{\gamma\mu}{\sigma R}\left[\frac{\partial^2\theta}{\partial x^2} + \frac{\partial^2\theta}{\partial y^2} + \frac{\partial^2\theta}{\partial z^2} + \frac{1}{\kappa}\frac{d\kappa}{dT}\frac{d^2T}{dy^2}\theta + \frac{2}{\kappa}\frac{d\kappa}{dT}\frac{dT}{dy}\frac{\partial\theta}{\partial y} + \frac{1}{\kappa}\frac{d^2\kappa}{dT^2}\left(\frac{dT}{dy}\right)^2\theta\right]$$

$$+ \gamma(\gamma-1)M_1^2\frac{1}{R}\left[2\mu\frac{dU}{dy}\left(\frac{\partial u}{\partial y} + \frac{\partial v}{\partial x}\right) + 2\mu\frac{dW}{dy}\left(\frac{\partial v}{\partial z} + \frac{\partial w}{\partial y}\right) + \frac{d\mu}{dT}\left(\frac{dU}{dy}\right)^2\theta + \frac{d\mu}{dT}\left(\frac{dW}{dy}\right)^2\theta\right].$$

The equation of state is

$$p = r/\varrho + \theta/T. \tag{5f}$$

New terms that appear in these equations are M, γ, and $\sigma = \dfrac{\mu^{\bullet}c_p^{\bullet}}{\kappa^{\bullet}}$, the Prantl number, which is a function of temperature.

Equations (5) are the compressible counterparts of the incompressible stability equations and are valid for a 3D disturbance in a 3D mean flow. It should be noted that unlike most compressible stability analyses, equation (5e), the energy equation, is valid for a variable Prandtl number. The constant Prandtl number form is recovered by replacing κ with μ in the three terms in which it occurs.

The boundary conditions at y = 0 are

$$u(0) = 0, \quad v(0) = 0, \quad w(0) = 0, \quad \theta(0) = 0. \tag{6a}$$

The boundary conditions on the velocity fluctuations are the usual no-slip conditions, and the boundary condition on the temperature fluctuation is suitable for a gas flowing over a solid wall. For almost any frequency, it is not possible for the wall to do other than to remain at its mean temperature. The only exception is for a stationary, or near-stationary, crossflow disturbance when $\theta(0) = 0$ is replaced by $D\theta(0) = 0$. The boundary conditions at $y \to \infty$ are

$$u(y), \quad v(y), \quad w(y), \quad p(y), \quad \theta(y) \text{ are bounded as } y \to \infty \tag{6b}$$

This boundary condition is less restrictive than requiring all disturbances to be zero at infinity, but, in supersonic flow, waves may propagate to infinity, and we wish to include those that do so with constant amplitude.

Normal-Mode Equations. Except for the asymptotic suction boundary layer, most boundary layers grow in the downstream direction, and even for a wave of constant frequency, the disturbances are all functions of x (and z in a general 3D boundary layer). What we have to deal with is a problem of wave propagation in a nonuniform medium. Because the complete linearized equations are not separable, they do not have the normal modes as solutions. The most straightforward

16

approach is to simply set the nonparallel terms to zero on the grounds that the boundary layer growth is small over a wavelength, and it is the local boundary layer profile that will determine the local wave motion. This approach, called the quasi-parallel or locally parallel theory, has been almost universally adopted. It retains the parallel-flow normal modes as local solutions but is, of course, an extra approximation beyond linearization and leaves open the question of how important the admittedly slow growth of the boundary layer really is. We now specialize the disturbances to normal modes,

$$[u, v, w, p, r, \theta]^T = [\hat{u}(y), \hat{v}(y), \hat{w}(y), p(y), \hat{r}(y), \hat{\theta}(y)]^T \exp[i \left(\int \alpha dx + \beta dz - \omega t \right)], \quad (7)$$

where we have adopted the quasi-parallel form of the complex phase function. The normal modes may grow either temporally or spatially or both depending on whether ω, or $\overline{k}$, or both are complex. If α and β are real and ω is complex, the amplitude will change with time; if α and β are complex and ω is real, the amplitude will change with x. The former case is referred to as the temporal amplification theory; the latter as the spatial amplification theory. If all three quantities are complex, the disturbance will grow in space and time. The original, and for many years the only, form of the theory was the temporal theory. However, in a steady mean flow the amplitude of a normal mode is independent of time and changes only with distance. The spatial theory that was introduced by Gaster (refs. 12, 13, and 14), gives this amplitude change in a more direct manner than does the temporal theory.

When equations (7) are substituted into equations (5) and linear combinations of the x and z momentum equations formed for the variables,

$$\bar{\alpha}\hat{u} = \alpha\hat{u} + \beta\hat{w}, \quad \bar{\alpha}\hat{w} = \alpha\hat{w} - \beta\hat{u}, \quad (8)$$

we obtain a system of equations. The momentum equation in the direction parallel to the wave number vector $\overline{k}$ is

$$\rho\left[i(\alpha U + \beta W - \omega)\bar{\alpha}\hat{u} + (\alpha DU + \beta DW)\hat{v}\right] = -i(\alpha^2 + \beta^2)(\beta/\gamma M_1^2) \quad (9a)$$

$$+ \frac{\mu}{R}\left[\bar{\alpha}D^2\hat{u} + (\alpha^2 + \beta^2)(iD\hat{v} - 2\bar{\alpha}\hat{u})\right] + \frac{2}{3}\frac{\lambda - \mu}{R}(\alpha^2 + \beta^2)(iD\hat{v} - \bar{\alpha}\hat{u})$$

$$+ \frac{1}{R}\left\{\frac{d\mu}{dT}(\alpha D^2 U + \beta D^2 W)\hat{\theta} + \left(\frac{d\mu}{dT}D\hat{\theta} + \frac{d^2\mu}{dT^2}DT\hat{\theta}\right)(\alpha DU + \beta DW)\right.$$

$$\left. + \frac{d\mu}{dT}DT[\bar{\alpha}D\hat{u} + i(\alpha^2 + \beta^2)\hat{v}]\right\}.$$

The y momentum equation is

$$i\rho\,(aU + \beta W - \omega)\hat{v} = -D\beta/\gamma M_1^2 + \frac{\mu}{R}\left[2D^2\hat{v} + i\dot{a}D\hat{u} - (a^2 + \beta^2)\hat{v}\right] \tag{9b}$$

$$+\frac{2}{3}\frac{\lambda - \mu}{R}(D^2\hat{v} + i\dot{a}\hat{u}) + \frac{1}{R}\left[i\frac{d\mu}{dT}(aDU + \beta DW)\hat{\theta} + 2\frac{d\mu}{dT}DTD\hat{v}\right.$$

$$\left.+\frac{2}{3}\frac{d}{dT}(\lambda - \mu)DT(D\hat{v} + i\dot{a}\hat{u})\right].$$

The momentum equation in the direction normal to $\overline{k}$ is

$$\rho\left[i(aU + \beta W - \omega)\dot{a}\hat{w} + (aDW - \beta DU)\hat{v}\right] = \frac{\mu}{R}\left[\dot{a}D^2\hat{w} - (a^2 + \beta^2)\dot{a}\hat{w}\right] \tag{9c}$$

$$+\frac{1}{R}\left[\frac{d\mu}{dT}DT\,\dot{a}D\hat{w} + \frac{d\mu}{dT}(aD^2W - \beta D^2U)\hat{\theta} + \left(\frac{d\mu}{dT}d\hat{\theta} + \frac{d^2\mu}{dT^2}DT\hat{\theta}\right)(aDW - \beta DU)\right].$$

The continuity equation is

$$i(aU + \beta W - \omega)\hat{r} + \varrho(D\hat{v} + i\dot{a}\hat{u}) + D\varrho\hat{v} = 0. \tag{9d}$$

The energy equation is

$$\rho\left[i(aU + \beta W - \omega)\hat{\theta} + DT\hat{v}\right] = -(\gamma - 1)(D\hat{v} + i\dot{a}\hat{u}) \tag{9e}$$

$$+\frac{\gamma\mu}{\sigma R}\left\{D^2\hat{\theta} - (a^2 + \beta^2)\hat{\theta} + \frac{1}{\kappa}\left[\frac{d\kappa}{dT}D^2T + \frac{d^2\kappa}{dT^2}(DT)^2\right]\hat{\theta} + \frac{1}{\kappa}\frac{d\kappa}{dT}DTD\hat{\theta}\right\}$$

$$+\gamma(\gamma - 1)M_1^2\frac{1}{R}\left\{i2\mu(aDU + \beta DW)\hat{v} + \frac{d\mu}{dT}(DU^2 + DW^2)\hat{\theta}\right.$$

$$\left.+\frac{2\mu}{a^2 + \beta^2}\left[(aDU + \beta DW)\dot{a}D\hat{u} + (aDW - \beta DU)\dot{a}D\hat{w}\right]\right\}.$$

The equation of state is

$$\hat{p} = \hat{r}/\rho + \hat{\theta}/T. \tag{9f}$$

To reiterate, in these equations the eigenfunctions of the fluctuations are functions only of y and are denoted by a caret or a tilde; the mean-flow velocities U and W are also functions of y as are the other mean-flow quantities: density $\rho(= 1/T)$, temperature T, viscosity coefficients μ and λ, thermal conductivity coefficient κ, and Prandtl number. The specific heats are constant. The reference velocity for U and W is the same as for R and M_1, and the reference length for y is the same as in R.

Numerical Solution Procedure

Eighth-Order System. Equations (9) are the basic equations of the compressible stability theory, but are not yet in a form suitable for numerical computation. For this purpose we need a system of first-order differential equations with the dependent variables defined by

$$Z_1 = a\hat{u} + \beta\hat{w}, \quad Z_2 = DZ_1, \quad Z_3 = \hat{v},$$
$$Z_4 = \beta/\gamma M_1^2, \quad Z_5 = \hat{\theta}, \quad Z_6 = D\hat{\theta},$$
$$Z_7 = a\hat{w} - \beta\hat{u}, \quad Z_8 = DZ_7, \tag{10}$$

Equations (9) can be written as eight first-order differential equations

$$DZ_i(y) = \sum_{j=1}^{8} a_{ij}(y)Z_i(y), \quad (i = 1, 8), \tag{11}$$

and the fact that this reduction is possible proves that equations (9) constitute an eighth-order system. The lengthy equations for the matrix elements are listed in reference 7.

The boundary conditions at the wall are

$$Z_1(0) = 0, \quad Z_3(0) = 0, \quad Z_5(0) = 0, \quad Z_7(0) = 0, \tag{12}$$

$$Z_1(y), \quad Z_3(y), \quad Z_5(y), \quad Z_7(y) \text{ bounded as } y \to \infty.$$

Uniform Mean-Flow Boundary Conditions. To solve equations (11) we also need to know the "boundary" conditions outside the boundary layer. In the flow outside the boundary layer, $U = U_1$, $W = W_1$, $T = 1$, $\mu = 1$, $\kappa = 1/\sigma_1$, all y derivatives of mean-flow quantities are zero, and equations (11) reduce to a system of equations with constant coefficients. In spite of the greater complexity of these equations compared to those for incompressible flow, we are still able to arrive at analytical solutions. The lengthy derivation is given in reference 7. The exact freestream solutions are the ones to use to calculate the outer boundary values for a numerical integration of equations (11), but they do not lend themselves to a ready physical interpretation. For this purpose we examine the limit of large Reynolds numbers. The characteristic values simplify to

$$\lambda_{1,2} = \mp [a^2 + \beta^2 - M_1^2(aU_1 + \beta W_1 - \omega)^2]^{1/2}, \tag{13a}$$

$$\lambda_{3,4} = \mp [iR(aU_1 + \beta W_1 - \omega)]^{1/2}, \tag{13b}$$

$$\lambda_{5,6} = \mp [i\sigma R(aU_1 + \beta W_1 - \omega)]^{1/2}, \tag{13c}$$

$$\lambda_{7,8} = \lambda_{3,4}. \tag{13d}$$

We can now identify our solutions as, in order, the inviscid solution, the first viscous velocity solution, a viscous temperature solution that does not appear in the incompressible theory, and

19

the second viscous velocity solution. We shall only use the upper signs in what follows, as these are the solutions that enter the eigenvalue problem.

The components of the characteristic vector of the inviscid solution are

$$A_1^{(1)} = -i(\alpha^2 + \beta^2)^{1/2}, \tag{14a}$$

$$A_3^{(1)} = [\alpha^2 + \beta^2 - M_1^2(\alpha U_1 + \beta W_1 - \omega)^2]^{1/2}/(\alpha^2 + \beta^2)^{1/2} \tag{14b}$$

$$A_4^{(1)} = i(\alpha U_1 + \beta W_1 - \omega)/(\alpha^2 + \beta^2)^{1/2}, \tag{14c}$$

$$A_5^{(1)} = i(\gamma - 1)M_1^2(\alpha U_1 + \beta W_1 - \omega)/(\alpha^2 + \beta^2)^{1/2}. \tag{14d}$$

The normalization has been changed to correspond to incompressible solutions. It can be noted that these expressions are correct when we set $M_1 = 0$.

The components of the characteristic vector corresponding to the viscous velocity solution are

$$A_1^{(3)} = 1, \tag{15a}$$

$$A_3^{(3)} = -i/[iR(\alpha U_1 + \beta W_1 - \omega)]^{1/2}, \tag{15b}$$

$$A_4^{(3)} = 0, \quad A_5^{(3)} = 0. \tag{15c}$$

This solution is identical to the λ_3 incompressible solution only in the limit of large Reynolds numbers.

The components of the characteristic vector corresponding to the viscous temperature solution are

$$A_1^{(5)} = 0, \tag{16a}$$

$$A_3^{(5)} = -i(\alpha U_1 + \beta W_1 - \omega)^{1/2}/(i\sigma R)^{1/2}, \tag{16b}$$

$$A_4^{(5)} = 0, \quad A_5^{(5)} = 1, \tag{16c}$$

The components of the characteristic vector corresponding to the second viscous velocity solution are

$$A_1^{(7)} = 0, \quad A_3^{(7)} = 0, \quad A_4^{(7)} = 0, \quad A_5^{(7)} = 0, \tag{16a}$$

$$A_7^{(7)} = 1, \tag{16b}$$

$$A_8^{(7)} = -[\alpha^2 + \beta^2 + iR(\alpha U_1 + \beta W_1 - \omega)]^{1/2}. \tag{16c}$$

This solution is exact and is the same spanwise viscous wave solution as in incompressible flow.

20

We may observe that the viscous velocity solutions have only fluctuations of velocity, not of pressure or temperature. The velocity fluctuations in the x, z plane are in the direction of $\bar{K}$ for the first solution and are normal to $\bar{K}$ for the second solution, which is periodic only in time. The viscous temperature solution has no velocity fluctuations in the x, z plane, or pressure fluctuations. We may regard these solutions as the responses to sources of $\hat{u}$, $\hat{w}$, and $\hat{\theta}$; and to emphasize this fact the respective solutions have been normalized to make these quantities unity. The second viscous velocity solution still has the interpretation of a normal vorticity wave, as in incompressible flow, but this wave cannot exist as a pure mode in the boundary layer (Squire mode) because of the dissipation term that couples the latter two of equations (11) to the first six equations.

Since the early 1960s, the asymptotic theories developed by Tollmien (ref. 15) and Lin (ref. 16) have been largely superseded as a means of predicting numerical results in favor of direct solutions of the governing differential equations on a digital computer. The numerical methods that have been employed fall roughly into three categories: (1) finite-difference methods, used first by Thomas (ref. 17) in his pioneering numerical work on plane Poiseuille flow, and later, by Kurtz (ref. 18), Osborne (ref. 19), and Jordinson (ref. 20), among others; (2) spectral methods, used first by Gallagher and Mercier (ref. 21) for Couette flow with Chandrasekhar and Reid functions, and later improved by Orszag (ref. 22) with the use of Chebyshev polynomials; and (3) shooting methods, used first by Brown and Sayre (ref. 23). All of these methods have advantages and disadvantages that show up in specialized situations, but they are all equally able to do the routine eigenvalue computations required in transition-prediction calculations. However, a shooting method used by Mack is what will be described here.

The Shooting Method. Various integrators have been used to implement the shooting method. Perhaps the most common is some form of the Runge-Kutta method, but the Adams-Moulton and Keller box method have also been used. One choice that has to be made is whether to use a fixed or variable step-size integrator. The latter is better in principle, but it adds to the computational overhead, and thus to the expense, and it may be as difficult to construct a proper error test and then choose the error limits as it is to select the proper fixed step size. The integration method used in the USS is a modified fourth-order Runge-Kutta scheme described in reference 24, which eliminates some of the function evaluations required by the classical fourth-order method while preserving accuracy. This is a change to what Dr. Mack used in his computer code and is helpful in reducing computer time, since a high percentage of the effort of finding eigenvalues involves repeated applications of this integration scheme.

Gram-Schmidt Orthonormalization. The early applications of shooting methods suffered from the problem of parasitic error growth. This growth arises because of the presence of a rapidly growing solution in the direction of integration that is associated with the large characteristic value λ_3 in the freestream, which the numerical round-off error will follow. The parasitic error eventually completely contaminates the less rapidly growing solution associated with the characteristic value λ_1 in the freestream. The essential advance in coping with this problem, which had previously limited numerical solutions to moderate Reynolds numbers, was made by Kaplan (ref. 25). The Kaplan method "purifies" the contaminated solution by filtering out the parasitic error whenever it becomes large enough to destroy the linear independence of the solutions.

A widely used method, which was originally developed for systems of linear differential equations by Godunov (ref. 26) and Bellman and Kalaba (ref. 27) and applied to the boundary layer stability problem by Radbill and Van Driest (ref. 28) and Wazzan, Okamura, and Smith (ref. 29), is that of Gram-Schmidt orthonormalization. This method has the advantage that it is easier to generalize to higher order systems than is the Kaplan filtering technique. However, the geometri-

21

cal argument often adduced in its support, that this procedure preserves linear independence by keeping the solution vectors orthogonal, cannot be correct because the solution vector space does not have a metric. In such vector spaces, vectors are either parallel or non parallel. The concept of orthogonality does not exist. Instead, the orthonormalization method works on exactly the same basis as Kaplan filtering: the "small" solution is replaced by a linear combination of the "small" and "large" solutions, which is itself constrained to be "small."

For the simplest case of a 2D wave in a 2D boundary layer, there are two solutions, $Z^{(1)}$ and $Z^{(3)}$, each consisting of four components. In the freestream, $Z^{(1)}$ is the inviscid and $Z^{(3)}$ the viscous solution. Although this identification is lost in the boundary layer, $Z^{(3)}$ continues to grow more rapidly with decreasing y than does $Z^{(1)}$. The parasitic error will follow $Z^{(3)}$, and when the difference in the "magnitudes" of $Z^{(3)}$ and $Z^{(1)}$ as defined by an arbitrarily assigned metric becomes sufficiently large, $Z^{(1)}$ will no longer be independent of $Z^{(3)}$. Well before this occurs, the Gram-Schmidt orthonormalization algorithm is applied. The "large" solution $Z^{(3)}$ is normalized component by component to give the new solution

$$S^{(3)} = Z^{(3)} / \{Z^{(3)*} Z^{(3)}\}^{1/2} \ , \tag{18}$$

where an asterisk refers to a complex conjugate and {} to a scalar product. The metric adopted for the vector space is the usual Euclidian norm. The scalar product of $Z^{(1)}$ and $S^{(3)}$ is used to form the   vector

$$S^{(1)} = \left[Z^{(1)*} - \left(S^{(3)*} Z^{(1)}\right) S^{(3)}\right] / \left(\overline{S}^{(1)*} \overline{S}^{(1)}\right)^{1/2}, \tag{19}$$

which replaces $Z^{(1)}$ and where $\overline{S}$ refers to the quantity in the numerator.

The numerical integration continues with $S^{(1)}$ and $S^{(3)}$ in place of $Z^{(1)}$ and $Z^{(3)}$, and when in turn $S^{(3)}$ exceeds the set criterion of, say, 10^5 with single precision arithmetic and a 36-bit computer word, the orthonormalization is repeated. With homogeneous boundary conditions at the wall, it makes no difference in the determination of the eigenvalues whether the $Z^{(i)}$ or $S^{(i)}$ are used. A linear combination of the two solutions satisfies the u(0) = 0 boundary condition, but the v(0) = 0 boundary condition will in general not be satisfied unless α, β, and ω are eigenvalues of the problem.

Although the orthonormalization procedure has no effect on the method of determining eigenvalues, it does complicate the calculation of the eigenfunctions. The solution vectors of the numerical integration are linear combinations of the original solution vectors $Z^{(1)}$ and $Z^{(3)}$, and it is necessary to "unravel" these combinations.

Newton-Raphson Search Procedure. The Newton-Raphson method has been found to be satisfactory for obtaining the eigenvalues. The boundary condition on $Z^{(1)}$ [or $S^{(1)}$] is satisfied at the conclusion of each integration by a linear combination of the two solutions at y = 0. The guess value of one of the eigenvalues is perturbed by a small amount and the integration repeated. Then the other eigenvalue is perturbed and the integration repeated again.

The corrections to the initial guesses of the eigenvalues, for example a_r and a_i, are obtained from the residual $\hat{v}(0)$ and the numerical (linear) approximations to the partial derivatives by

$$\left[\partial \hat{v}_r(0)/\partial a_r\right] \Delta a_r - \left[\partial \hat{v}_r(0)/\partial a_i\right] \Delta a_i = -\hat{v}_r(0) \ , \tag{20}$$
$$\left[\partial \hat{v}_i(0)/\partial a_r\right] \Delta a_r - \left[\partial \hat{v}_i(0)/\partial a_i\right] \Delta a_i = -\hat{v}_i(0).$$

The corrected a_r and a_i are used to start a new iteration, and the process continues until Δa_r and Δa_i have been reduced below a preset criterion. The values in this criterion are a compromise between solution accuracy and computing time. These values were examined during the development of the USS and are given in the descriptions of output from programs MKMOD3 and MKMOD5 in section 7.0.

Starting Guesses for the Eigenvalue Search. The search procedure for eigenvalues requires initial guesses for the eigenvalues. Depending on the nature of the boundary layer, the guesses may have to be quite accurate for the iterative search procedure to converge to actual eigenvalues rather than diverge. In developing the USS, a substantial part of the effort was automating successful eigenvalue guessing.

The MKMOD3 program examines low wave angle stability. In this program frequency and wave angle are chosen, the imaginary part of β is assumed to be zero, and the remaining eigenvalues to be found are the real and imaginary parts of α. Reference 29 has been extremely helpful in estimating the stability characteristics of low wave angle disturbances. These estimates are used to determine (1) when to begin searching for unstable disturbances during boundary layer growth, (2) what frequency range will likely have unstable disturbances, and (3) the guess for α_r to use in starting the eigenvalue search procedure.

Stability calculations begin in the MKMOD3 program when boundary layer R_{δ^*} is 500 less than the critical R_{δ^*} given in reference 29. The critical R_{δ^*} is a function of pressure gradient and is illustrated in figure 4. The R_{δ^*} and $\beta_{(F-S)}$ are characteristics of the boundary layer profile which is perpendicular to the local isobars, since the reference 29 results are for Falkner-Skan boundary layers. The value of 500 subtracted from the critical R_{δ^*} was determined by experience with
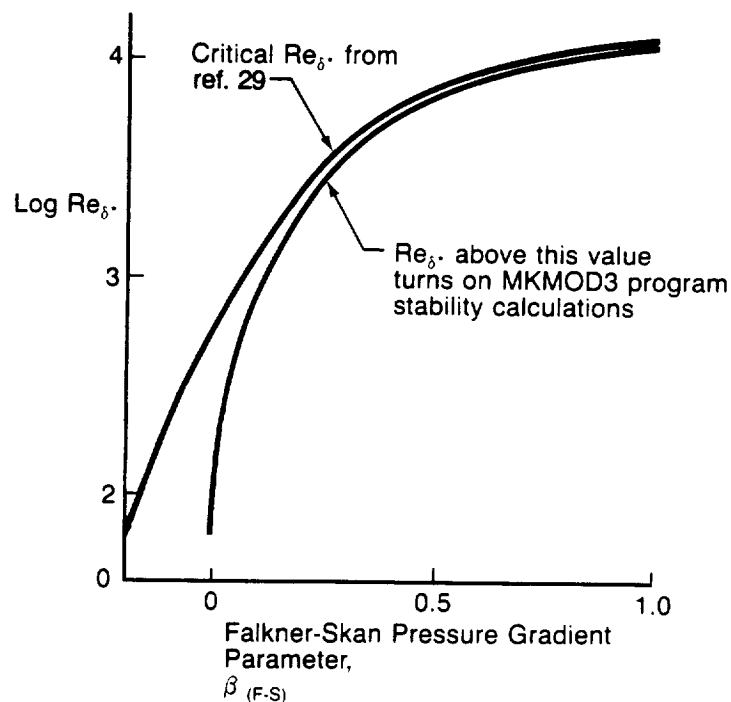
Figure 4. — *Critical Reynolds Number for MKMOD3 Program*

MKMOD3. This helps ensure a successful start to the calculations because unstable eigenvalues are easier to converge on.

The frequency range over which to search for eigenvalues is also found from information presented in reference 29. Again, it is related to $R\delta^*$ and $\beta_{(F\text{-}S)}$ by:

$$\log \omega_{HIGH} - \log \omega_{LOW} = f\left(\left[\log R_\delta^* - \log R_\delta^*_{CRITICAL} \right], \; \beta_{(F\text{-}S)} \right).$$

The function f is shown graphically in figure 5. This frequency range is distributed around a critical frequency found from an empirically determined equation, which is

$$\log \omega_{CRIT} = -1.46 \log R_\delta^*_{CRIT} + 0.37$$

The α_r initial guess is another value empirically derived from reference 29 and experience with MKMOD3 and is:

$$a_r \text{ (initial)} = a_{r_{CRIT}} - \Delta a_r - 0.06$$

$a_{r_{CRIT}}$ is a function of $R_\delta^*_{CRIT}$ as given in figure 6. Δa_r is a function of $\left(\log R_\delta^* - \log R_\delta^*_{CRIT} \right)$ and $\beta_{(F\text{-}S)}$ and is graphed in figure 7. This guess is for the lowest frequency in the array of ω and ψ at the first point in the boundary layer that is analyzed because this is the starting point of the whole eigenvalue search.
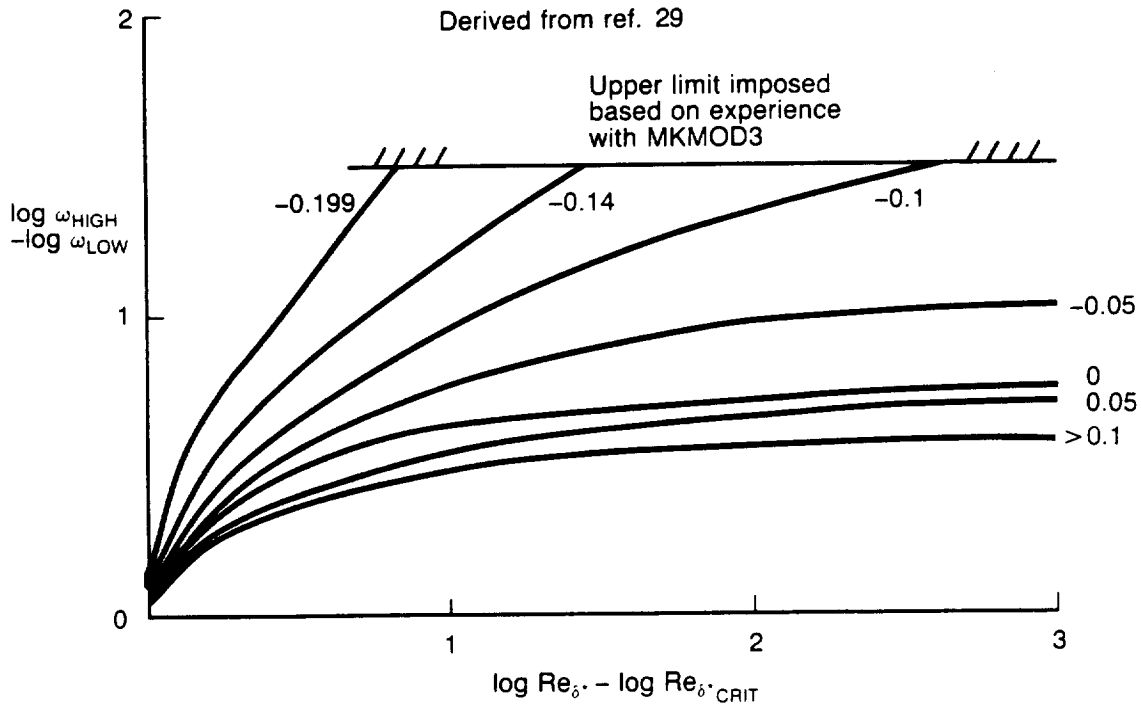
Figure 5. — Unstable Frequency Range Used in MKMOD3

24
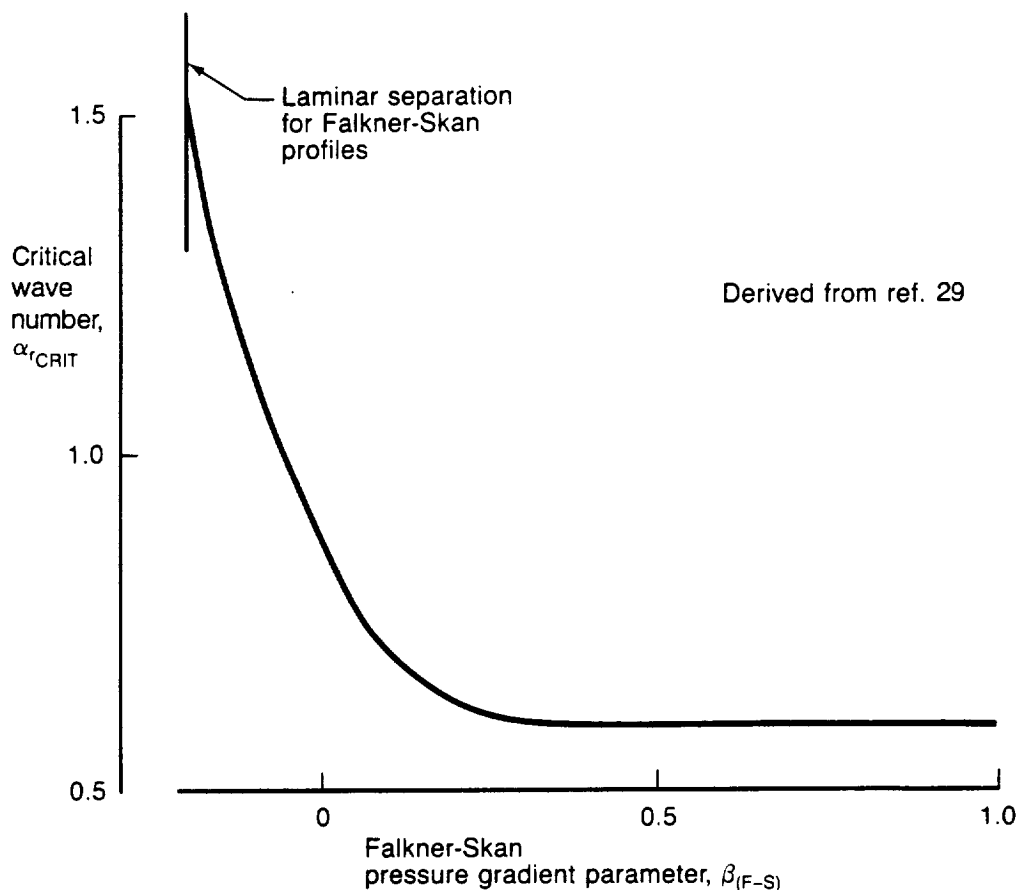
Figure 6. — Nondimensional Wave Number at Critical Frequency and $Re_{\delta^* CRIT}$

The initial guess for α_i is less critical for convergence of the search procedure and is 0.005. As eigenvalues are found in these early stages of the calculations, their values are used to get guesses of α_r and α_i for calculations at different ω and ψ and downstream stations in the boundary layer. This logic obviously works best when the frequency and wave angle increments are small and when the boundary layer changes are small between stations.

The MKMOD5 program examines high wave angle (crossflow) stability. In this program, α_r and wave angle are chosen, the imaginary part of β is assumed to be zero, and the remaining eigenvalues to be found are ω and a_i. As with the low wave angle stability, a reference was helpful in determining when the boundary layer was likely to have crossflow instability (ref. 30). The relationship between H(crossflow) and a critical crossflow Reynolds number is shown in figure 8.

Stability calculations are done in MKMOD5 if R_{CF} is greater than $R_{CF_{CRIT}} + 10$ and continue until R_{CF} is less than $R_{CF_{CRIT}} - 15$. These ranges were determined from experience with the program. Additionally, plots of spatial amplification rate for stationary ($\omega = 0$) crossflow disturbances shown in reference 30 indicate that for low crossflow Reynolds numbers the most amplified wave numbers are near 1.4 for wave numbers nondimensionalized by δ_{10}. This observation is also used to start MKMOD5 stability calculations.
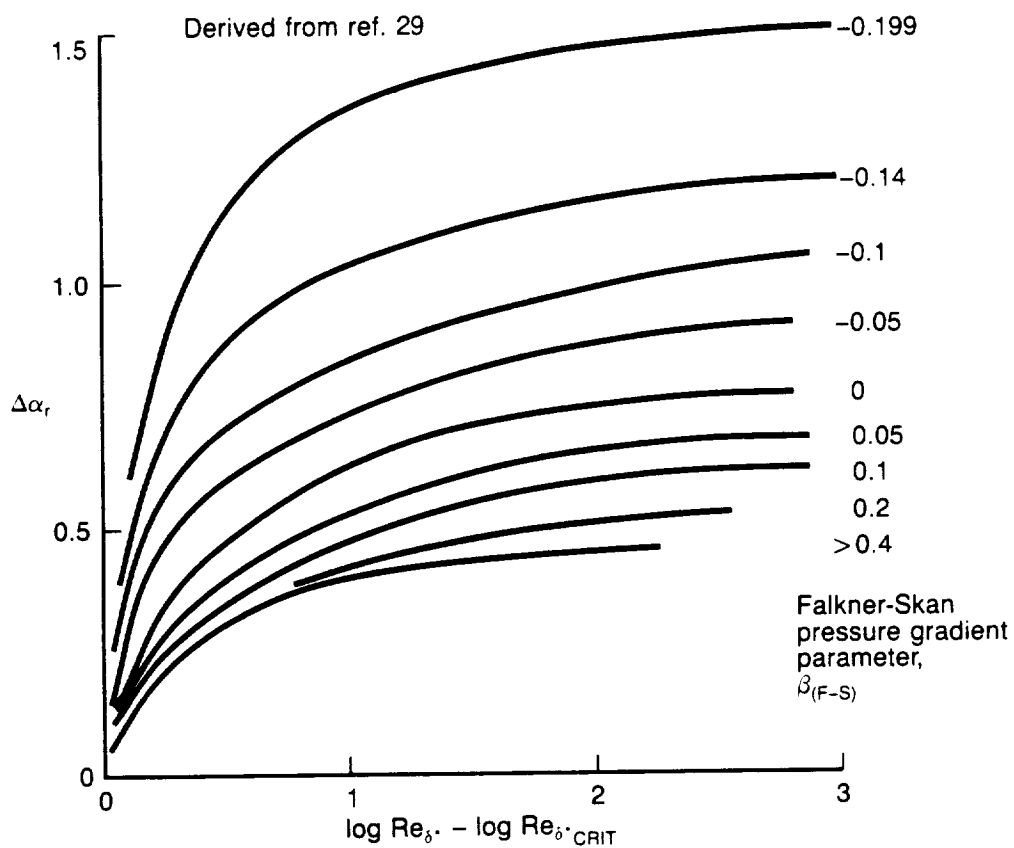
Figure 7. — $\Delta\alpha_r$ for Estimating Starting α_r in MKMOD3
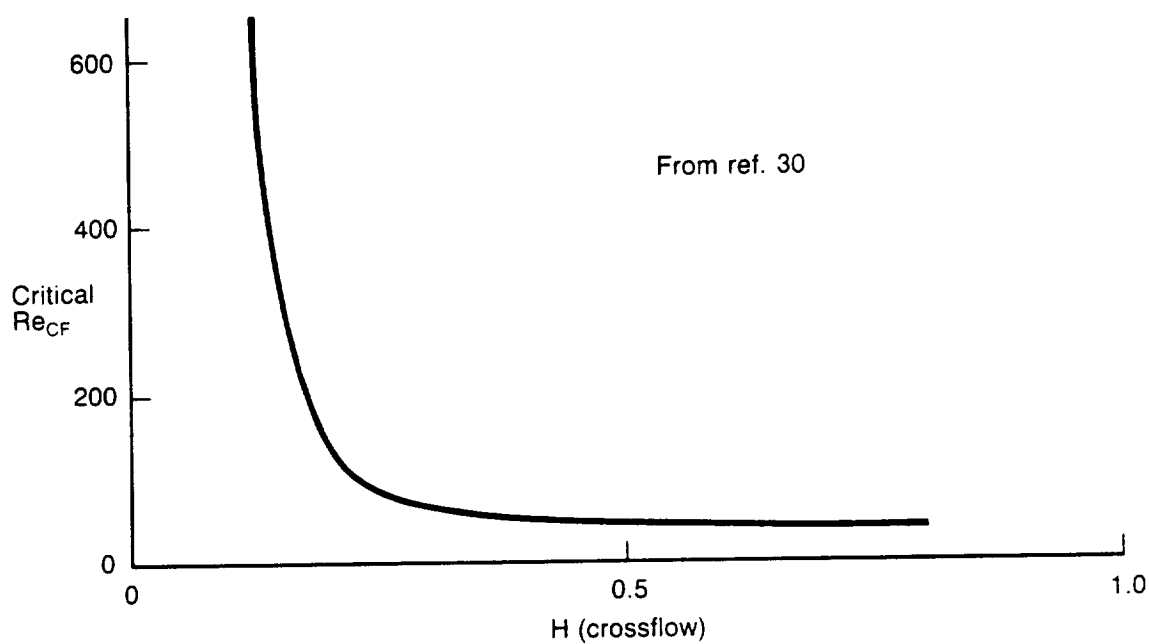
Figure 8. — Critical Crossflow Reynolds Number

When stability calculations begin in MKMOD5, the initial eigenvalue guesses are based on experience with the program as well as on published information. Experience has shown that when the calculations start at $(R_{CF} \approx R_{CF_{CRIT}} + 10)$ and $\alpha_r = 1.4$, that a good guess for ω is 10^{-5} and for α_i is 0.02 when the wave angle is slightly less (~ 1.0 degrees) than a critical angle that is determined from the boundary layer crossflow profile. This critical angle is defined as the direction for which the crossflow velocity profile has its inflection point at the point where the crossflow velocity is zero. In many cases these conditions of α_r, ψ, and ω give nearly the most unstable disturbance in the crossflow ($\psi \sim 90$ deg) region. When the initial eigenvalue search is successful, the MKMOD5 program works its way to other wave angles and values of α_r in order to outline the unstable crossflow region. Further details of this are given in section 7.0 under the paragraphs that describe the MKMOD5 output on the OPXQQYZ file. When the first boundary layer station has been analyzed, MKMOD5 follows a path similar to that of MKMOD3 in guessing at eigenvalues at following stations based on eigenvalues found at the previous station.

**Sixth-Order System.** Equations (11) can be solved by numerical techniques, but the fact that there are 16 real equations (one each for real and imaginary terms) and four independent solutions means that the computer time required to calculate an eigenvalue can be substantial. It is therefore important to know if it is possible to make use of a system of lesser order. We note that for a 2D wave in a 2D boundary layer, the system already is of only sixth order, as there can be no velocity component, either mean or fluctuating, in the z direction. Is there an exact reduction available from eighth to sixth order? The answer, unfortunately, as mentioned by Dunn and Lin (ref. 31) and explicitly demonstrated by Reshotko (ref. 32), is no.

We may observe from the coefficient matrix of equation (11) that the only term that couples the first six equations to the last two is the coefficient that comes from the last term of the energy equation (9e) and is one of four dissipation terms. It is the product of the gradient of the mean velocity normal to $\bar{k}$ and the gradient of the fluctuation velocity in the same direction. It was proposed by Mack (ref. 33) to simply set this term equal to zero and use the resultant sixth-order system for the calculation of eigenvalues. The numerical evidence is that except near the critical Reynolds number this approximation gives amplification rates within a few percent of those obtained from the full eighth-order system and is most accurate at higher Mach numbers.

Wave Propagation in a Growing Boundary Layer. We have already discussed some aspects of this problem earlier in this section, and we have chosen to use the quasi-parallel rather than the non-parallel theory. In the quasi-parallel theory, the normal-mode solutions are of the form

$$u(x, y, z, t) = A_0 \hat{u}(y; x) \exp\left[i\Theta(x, y, z, t)\right] , \qquad (21)$$

with similar expressions for the other flow variables. The slowly varying amplitude A(x) of the non-parallel solution has been set equal to the constant A_0, and

$$\Theta(x, z, t) = \int^x \alpha(x)dx + \beta(x_1)z - \omega(x_1)t . \qquad (22)$$

We have left β and ω as functions of the slow scale x_1 to make it clear that $\partial\Theta/\partial x = \alpha$, just as for strictly parallel flow. The eigenvalues α, β, and ω are locally related in what is called the dispersion relation and the eigenfunction $\hat{u}(y; x)$ is also a slowly varying function of x. Consequently, at each x a different eigenvalue problem has to be solved because of the change in the boundary layer thickness, or velocity profiles, or, as is usually the case, both. The problem we must resolve is how

to "connect" the possible eigenvalues at each x so that they represent a continuous wave train propagating through the growing boundary layer.

In a steady boundary layer, which is the only kind that we shall consider, the dimensional frequency of a normal mode is constant. For a 2D wave in a 2D boundary layer, $\beta = 0$, and the complex wavenumber a in the spatial theory is obtained as an eigenvalue for the local boundary layer profiles. The only problem here is the relatively minor one of calculating the wave amplitude as a function of x from the amplification rate, and we will discuss this in section 4.3.

"Irrotational" Wave Propagation.   When the wave is oblique, $\beta \neq 0$, and it is not obvious how to proceed, since a is a function of β, as well as of x. How do we choose β at each x? The answer is provided by the same procedure as used in conservative wave theory. When we differentiate equation (22) with respect to x (not x_1) and z, we obtain

$$\partial\Theta/\partial x = a, \partial\Theta/\partial z = \beta \ , \tag{23a}$$

or

$$grad \ \Theta = \vec{k_c} \ , \tag{23b}$$

where $\vec{k_c}$ is the complex wavenumber vector. Thus it follows directly that

$$curl \ \vec{k_c} = 0, \tag{23c}$$

and $\vec{k_c}$ is irrotational. This condition is a generalization to a nonconservative system of the well-known result for the real wavenumber vector in conservative kinematic wave theory.

In the boundary layers on an untapered wing, the mean flow is independent of z. Consequently, if we restrict ourselves to spatial waves of constant β at the initial x, they can be represented by a single normal mode, because the eigenvalue a will also be independent of z. Therefore, according to equation (23c) the sought after downstream condition on β is

$$\beta = const. \tag{24}$$

One caution is that if the reference length L^* is itself a function of x, as it will be if $L^* = \delta^*$ for example, the argument has to be slightly modified and equation (24) refers to β^* rather than to β. The untapered assumption is used in the disturbance growth calculations of the USS for the "irrotational" method, even though the boundary layer has been calculated using "infinite taper" assumptions.

It still remains to specify the initial value of β. Naturally occurring instability waves in a boundary layer will be a superposition of normal modes with a spectrum over both ω and β that will depend on the particular origin of the waves. It is probably only in a controlled experiment with a suitable wavemaker that a single normal mode can be excited. For example, the vibrating ribbon first used by Schubauer and Skramstad (ref. 34) in their celebrated experiment excites a spatial 2D normal mode with the frequency of the ribbon. It is also possible to conceive of wavemakers that excite single oblique normal modes in boundary layers that are independent of z. Such normal modes will have an initial β_r, which matches that of the wavemaker, and, because the wave can grow only in x, the initial β_i must be zero. These normal modes are well suited for use in stability calculations for the estimation of the location of transition. In the calculations, β_r is assigned as a parameter, β_i is zero, and equation (24) controls the downstream values of β_r. Not only do these normal modes

28

represent physical waves that can be produced by a suitable wavemaker, but they are also convenient to use in all calculations of normal modes, such as transition prediction where we are interested in the largest possible growth of any normal mode. In earlier work on 2D planar boundary layers, the angle ψ was chosen as the parameter to hold constant, rather than β_r, as the wave propagates downstream. Although α_r is nearly constant in such boundary layers, it changes enough so that the assumption of constant ψ is not equivalent to equation (24). In the work on 3D boundary layers, equation (24) is applied to the spanwise wavenumbers, but the direction of the spatial amplification rate is nearly parallel to the local potential flow, or more accurately, in the direction of the real part of the group-velocity angle.

This was identified in reference 35 by an argument based on the Nayfeh-Padhye amplitude propagation equation. For spatial waves the real part of the complex group velocity has x and z components $\dfrac{\partial \omega}{\partial \alpha_r}$, $\dfrac{\partial \omega}{\partial \beta_r}$ respectively. The direction of the real part of the group velocity, $\overline{\psi}$, with respect to the local potential flow is therefore

$$\tan^{-1}\left[\frac{\partial \omega}{\partial \beta_r}\bigg/\frac{\partial \omega}{\partial \alpha_r}\right]$$

In practice, this can be done using the finite differences

$$\frac{\partial \omega}{\partial \beta_r} \approx \frac{\Delta \omega}{\Delta \beta_r}\bigg)_{\alpha_r \text{ held constant}} \qquad \frac{\partial \omega}{\partial \alpha_r} \approx \frac{\Delta \omega}{\Delta \alpha_r}\bigg)_{\beta_r \text{ held constant}}$$

if there is adequate knowledge of the stability characteristics at this point in the boundary layer. This is exactly what the USS is intended to do, so the finite difference calculations necessary to find group velocity angles are done after the arrays of ω, α_r, and β_r are found for a point in the boundary layer. This procedure loses accuracy if the arrays of ω, α_r, and β_r are not defined by a dense number of points, but the arrays generally requested by the USS user are acceptable to define the group velocity angle, which is usually less than 10 deg.

4.3 DISTURBANCE GROWTH CALCULATION

The two programs of the USS that integrate disturbance amplification rate, dN/ds, along the wing surface to find the N-factors use similar mathematical techniques. They differ mainly in the integration philosophy, which determines the disturbance frequency, ω, and orientation, ψ, at which to pick the growth rate. The important mathematical properties of the programs will be described first.

The N-factors are calculated by numerically integrating the following equation using the trapezoidal rule.

$$N = \int_{S_o}^{S} \frac{dN}{ds}\,ds$$

S_o is the point at which a given disturbance begins to amplify. Although the path that is followed may be considered as lying along the surface of a streamwise section of a wing, because the ampli-

fication rates have been calculated along a streamwise section, the integration distance, Δs, is influenced by geometry, local velocity, and the disturbance group velocity. The following sketch illustrates this characteristic of the USS.
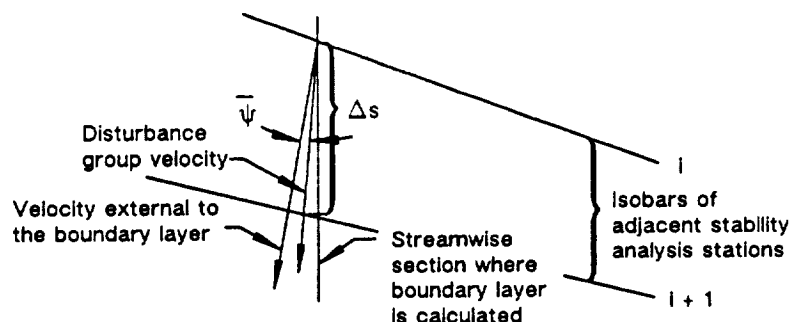
5-U80106-6

The direction used to determine Δs in the integration involves the average of group velocity angles and external streamline directions at points i and i + 1. This simplified method is a compromise between calculating stability and integrating along the disturbance growth direction, which is not known a priori, and the simplest approach of integrating strictly along the streamwise section surface. For many sweptwing analyses the streamlines do not depart significantly from the stream-wise direction, and the group velocity is generally within 10 deg of the local velocity direction.

The integration process uses a straight line interpolation (extrapolation if necessary) to locate the point at which a disturbance first begins to grow. If a disturbance goes into a stable region after experiencing growth, the integration continues until the N-factor becomes negative. It then stops until there is again amplification of the disturbance.

The amplification rate, dN/ds, used in the integration, is found from the tables of dN/ds created by the stability analysis programs. These tables represent discrete points on the stability surface

$$\frac{dN}{ds} = f(\psi, \omega)$$

calculated for each station on the section. The ω and ψ are determined by the integration philosophy described later, and the resulting dN/ds is found from interpolation of the tables. Various interpolations are necessary and for most of these a second-order Lagrangian technique is used. In certain situations, however, the stability surface may not be adequately defined to allow a second-order interpolation so first order is used for interpolating some of the variables. Limited extrapolation may be useful and is allowed in certain situations, but because it may give unrealistic results, a warning message is printed with the integration results if extrapolation was involved in that result.

The purpose of integrating disturbance growth rates along the wing surface is to find the total disturbance growth that can be correlated with boundary-layer transition. However, there are an infinite number of different disturbances that may be present in the boundary layer so some rationale must be reached as to which are to be used in the integration. As this document is written, no universally accepted philosophy is available regarding the disturbance integration so two commonly used philosophies are included in N-factor integration by the USS.

The first philosophy investigates two classes of disturbances: those more or less aligned with the local external flow (these are the classical TS waves) and those nearly perpendicular to the local external flow (called crossflow disturbances). The growth of TS disturbances is calculated for

30

different frequencies, all of which have the same wave angle, ψ. For each frequency and wave angle there is an associated, unique wavelength at each point of the wing surface, see figure 1. The growth is calculated for several wave angles, and the maximum growth for the frequency/wave angle combinations is considered to be representative of the physical situation. Unfortunately, for some boundary layers the wave angle that gives maximum growth does not occur at a wave angle that is low enough to be considered in the TS regime. For those cases the investigator must set some rather arbitrary maximum limit on the wave angles of disturbances that will be considered TS. For the crossflow class of disturbances, growth rates for different frequencies are again integrated as they proceed downstream. For the crossflow, however, disturbances at a constant wave angle are not followed. Instead, an "irrotational" consideration described in section 4.2 is used, which results in following disturbances that have a constant spanwise component of wave number, a_r^* . This rationale comes from a physical consideration of the disturbance's movement downstream and is explained in more detail in reference 6. Of the infinite number of frequencies that are present, any one or several can be considered in the integration. Many investigators consider the zero frequency (stationary) disturbance to be the one critical for transition, but this point is still debated.

The second disturbance growth philosophy can be called the maximum amplification approach. There is no distinction between TS and CF disturbances in this approach. In it, a disturbance of a given frequency is followed downstream using the maximum amplification rate for that frequency, considering the complete range of wave angles at each streamwise station on the wing. This integration is repeated for several different frequencies. A weakness of this approach lies in whether it is physically reasonable to follow a disturbance whose wave angle may change drastically as it moves downstream.

The two integration philosophies are pictured graphically in figure 1. N-factors using each of these philosophies are calculated by the USS codes INTTS2 and INTCF2. For the maximum amplification method, results from INTCF2 should be used for cases with moderate crossflow. INTCF2 has the ability to search through both crossflow and TS disturbances, if both are available, in its determination of maximum growth rate, whereas the INTTS2 code can only search the low-wave angle (TS) disturbances.

31

5.0 USS PROGRAMS AND FILES

Numerous files are created by the Unified Stability System (USS). The file names are determined by the user-specified case identification code, the wing surface analyzed, which program the job execution begins with, and a run version identifier. In naming the files, the following convention is used:

X   can be either "U" or "L" depending on whether the run involves an upper or lower wing surface analysis.

Y   the program step (1, 2, 3, 4, 5, 6 or 7) where job execution begins for this run.

STEP	EXECUTION BEGINS WITH PROGRAM
1	BLGL.
2	A411.
3	LAMSD.
4	MKMOD3 (TS disturbance analyses).
5	MKMOD5 (CF disturbance analyses).
6	INTTS2.
7	INTCF2.

Z   A version number (0, 1, ..., 9) assigned to certain files.

QQ   Case identification code.

Program RDECK

Purpose: This code creates a job deck for a USS run.

Input: RDECK is run interactively. The name of its input file is at the user's discretion. This input file contains seven blocked record sets, which are inputs to the seven programs in the system. The first record of this file contains input for RDECK.

Output: When RDECK is run, it prints a message to the screen informing the user that a "local" job file has been created, which can be submitted as a batch job. The name of the local file is JSXQQYZ, where the letters X, QQ, Y, and Z are as described above.

Program BLGL

Purpose: This program sets up the input for the boundary layer calculation by A411. This includes curve fitting the input C_p - x/c distribution, locating the attachment line, defining the boundary layer grid, and calculating appropriate velocity components at the edge of the boundary layer.

Input: File IBLGL (tape 1). This file is the second record of the user's input file (see the input description section).

Output: File I411UQQ (tape 2) or I411LQQ (tape 3). Input decks for the boundary layer code A411, upper and lower surfaces, respectively.

File CREFUQQ (tape 22) or CREFLQQ (tape 23). These files contain geometry information relating the A411 solution stations to streamwise x/c positions on the upper and lower surfaces.

File OPXQQYZ (tape 6). Printed output from BLGL and other programs.

Program A411

Purpose: This is the finite element boundary layer analysis code. For this system it is restricted to laminar boundary layers but can analyze both standard and inverse wing taper.

Input: File I411XQQ (tape 5). Inputs for A411 created by BLGL previously.

Output: File BLXQQ (tape 4). The BL-file is a binary file containing boundary layer solution parameters.

           File VPXQQ (tape 10). This is a binary file containing detailed velocity and temperature profile data through the boundary layer at each A411 solution station.

           File OPXQQYZ (tape 6). Printed output from A411 is also placed on the OP-file as noted previously.

Program LAMSD

Purpose: This interface program reads A411 boundary layer solution files and then generates input decks for the stability calculations. In addition, LAMSD can create plotting files containing boundary layer information.

Input: File IBLGL (tape 1). This file is used as input for LAMSD as well as BLGL.

           File CREFXQQ (tape 2). This is the geometry reference file created by BLGL.

           File BLXQQ (tape 4). One of the binary files created by A411.

           File ILAMSD (tape 5). This file contains the first and third blocked record sets of the user's input file. The primary use of this file is to supply the interface code with the locations at which boundary layer information is to be passed to the stability codes.

           File VPXQQ (tape 10). The binary file generated by A411 containing boundary layer profile data.

Output: File VPGPXQQ (tape 3). If desired, this file can be created, and it contains boundary layer profiles in plotting format at user-specified locations.

           File SIXQQ (tape 7). This file contains boundary layer parameters and profiles in binary form for use by the stability codes. The boundary layer information is at user specified locations.

33

File BLGPXQQ (tape 8). This file contains a condensed set of boundary layer parameters at each chordwise station analyzed by A411. The information is in plotting format.

File OPXQQYZ (tape 6). Printed output from LAMSD is also placed on the OP-file.

Program MKMOD3

Purpose: This is the modified MACK code, which calculates eigenvalues defining the boundary layer stability at wave angles less than 70 deg.

Input: File IMACKTS (tape 3). This is record set 4 of the user's input file.

File SIXQQ (tape 12). This is the binary file containing the boundary layer information required for the stability calculations.

Output: File OTSXQQZ (tape 4). One of the two files from MKMOD3 containing information regarding the calculation of each eigenvalue. The OTS-file is the longer of the two files and is useful for diagnosing program failures.

File OPXQQYZ (tape 6). The more brief of the two printed files from MKMOD3 is put onto the OP-file.

File TSIXQQZ (tape 8). The TSI-file contains stability information needed to calculate the TS N-factors.

Program MKMOD5

Purpose: This is also a modified MACK code that calculates the boundary layer stability in the 72- to 90-deg wave angle range.

Input: File IMACKCF (tape 3). This file contains record set 5 of the user's input file.

File SIXQQ (tape 12). As with the MKMOD3 code, this file contains the boundary layer parameters and profile information.

Output: File OCFXQQZ (tape 4). One of the two files from MKMOD5 containing information regarding the calculation of each eigenvalue. The OCF-file is the longer of the two files, and is useful for diagnosing program failures.

File OPXQQYZ (tape 6). The more brief of the two printed files from MKMOD3 is put onto the OP-file.

File CFIXQQZ (tape 8). The CFI-file contains stability information needed to calculate the CF N-factors.

Program INTTS2

Purpose: This code uses the stability information from MKMOD3, and calculates the N-factors at lower wave angles (Tollmien-Schlichting) using both constant wave angle and maximum amplification methods.

Input: File ITSI (tape 5). This file contains the sixth record set of the user's input file.

File TSIXQQZ (tape 8). This file contains the stability information calculated by the MKMOD3 code.

Output: File OTSIXQQ (tape 6). Printed output from INTTS2 is put only on this file, not on the OP-file.

File GTSIXQQ (tape 10). Output in plotting format for plotting N_{TS} versus x/c.

Program INTCF2

Purpose: This code uses the stability information from MKMOD5 and if necessary from MKMOD3 to compute the crossflow N-factors (irrotational method) and N-factors using the maximum amplification method.

Input: File ICFI (tape 5). This file contains the seventh record set of the user's input file.

File TSIXQQZ (tape 8). This file is used in this program as well as INTTS2, because the maximum amplification method may require stability information at low wave angles.

File CFIXQQZ (tape 9). This file contains the stability information calculated by the MKMOD5 code.

Output: File OCFIXQQ (tape 6). Printed output from the INTCF2 code is put on the OCFI-file, not on the OP-file.

File GCFIXQQ (tape 10). Output in plotting format for plotting N_{CF} versus x/c.

At the end of a run, two additional files are saved on the user's account: one is the dayfile from the run, named LSXQQYZ, and the second is the output file OSXQQYZ. The output file OS-contains a copy of the job cards used to control this run and the user's input file. In addition, if an abnormal termination occurs, then the contents of the OP-file will also appear on the OS-file.

The following table summarizes the information in this section.

Program	Input files required	Output files generated
RDECK	User input file (record 1).	JSXQQYZ ("local submit" file)
BLGL	IBLGL user input file (record 2). This file is not made permanent on the user's account.	I411XQQ CREFXQQ OPXQQYZ
A411	I411XQQ	BLXQQ (binary) VPXQQ (binary) OPXQQYZ
LAMSD	IBLGL (same as used for BLGL). ILAMSD (user input file records 1 and 3). This file is not made permanent on the user's account. CREFXQQ BLXQQ VPXQQ	SIXQQ (binary) BLGPXQQ OPXQQYZ VPGPXQQ (optional)
MKMOD3	IMACKTS (user input file record 4). This file is not made permanent on the user's account. SIXQQ	OTSXQQZ OPXQQYZ TSIXQQZ
MKMOD5	IMACKCF (user input file record 5). This file is not made permanent on the user's account. SIXQQ	OCFXQQZ OPXQQYZ CFIXQQZ
INTTS2	ITSI (user input file record 6). This file is not made permanent on the user's account. TSIXQQZ	OTSIXQQ GTSIXQQ
INTCF2	ICFI (user input file record 7). This file is not made permanent on the user's account. TSIXQQZ (if available). CFIXQQZ	OCFIXQQ GCFIXQQ
JSXQQYZ (batch job submittal file)		LSXQQYZ OSXQQYZ

6.0 USS INPUT DESCRIPTION

The input deck to the Unified Stability System (USS) is divided into seven separate records. If a certain case does not require the input in one or more records, the end-of-record marks are still required.

The first record of input is primarily used to set up the job control deck for the run.

Card 1   A descriptive card that tells the user what is input on the next card.

Card 2   (format A7, 3X, A7, 3X, A6, 4X, A7).

    USERN: User number.
    PASSWRD: Password.
    CHARGE: Charge number.
    LIB: Account where the USS codes are stored.
    Example:

```
 1 2 3 4 5 6 7 8 9 10 11 12 13 14 15 16 17 18 19 20 21 22 23 24 25 26 27 28 29 30 31 32 33 34 35 36 37 38 39 40 ... 56
 1 2 3 1 2 3 B       P  A  S  S  W  O  R  D        1  0  1  0  1  0            2  5  1  6  7  8
```
8-U80106-101

Card 3   A descriptive card that tells the user what is input on the next card.

Card 4   (format A40).

    USER: Mailing information for the job.
    Example:

```
 1 2 3 4 5 6 7 8 9 10 11 12 13 14 15 16 17 18 19 20 21 22 23 24 25 26 27 28 29 30
 B I N X X   H  O  L  D     F  O  R     R  O  Z  E  N  D  A  A  L
```
8-U80106-102

Card 5   A descriptive card that tells the user what is input on the next card.

Card 6   (format A2, 8X, 3F10.0).

    ID: Two characters identifying the case.
    PRI: Priority to give to this run. Not used for NASA.
    VERSION: A version number assigned to the output files generated by the stability codes. Valid entries are 0., 1., 2., ...,9.
    TIME: The CPU time limit for this run in seconds.
    Example:

```
 1 2 3 4 5 6 7 8 9 10 11 12 13 14 15 16 17 18 19 20 21 22 23 24 25 26 27 28 29 30 31 32 33 34 35 36 37 38 39 40
 A A                                        1  .                 1  5  0  0  .
```
8-U80106-103

Card 7   A descriptive card that tells the user what is input on the next card.

Card 8   (format 6F10.0).

    FIRST: The number of the first code in the USS to be executed first for this run.
            1. BLGL.
            2. A411.

3. LAMSD.

0. None of the first three codes need to be run.

END:	The number of the last (of the first three codes) code to be executed for this run.
TS:	Number to determine whether or not the MKMOD3 code will be run during this run. (1. for yes, 0. for no).
CF:	Number to determine whether or not the MKMOD5 code will be run during this run. (1. means yes, 0. means no).
TSI:	Number to determine whether or not the TS integrator code, INTTS2, will be run during this run. (1. for yes, 0. for no).
CFI:	Number to determine whether or not the crossflow integrator code, INTCF2, will be run during this run. (1. for yes, 0. for no).

Examples:

```
| 1|2|3|4|5|6|7|8|9|10|11|12|13|14|15|16|17|18|19|20|21|22|23|24|25|26|27|28|29|30|31|32|33|34|35|36|37|38|39|40|41|42|43|44|45|46|47|48|49|50|51|52|53|54|55|
|   1|.|               |3|.|                   |1|.|                       |1|.|                   |1|.|                   |1|.|
```

The above example is a full run of all codes in the system.

```
| 1|2|3|4|5|6|7|8|9|10|11|12|13|14|15|16|17|18|19|20|21|22|23|24|25|26|27|28|29|30|31|32|33|34|35|36|37|38|39|40|41|42|43|44|45|46|47|48|49|50|51|52|53|54|55|56|
|   0|.|               |0|.|                   |1|.|                       |0|.|                   |1|.|                       |0|.|
```

8-U80106-104

The above example is a run of only the MKMOD3 and INTTS2 codes. The first three codes must have been run previously to create the necessary input files for MKMOD3.

Card 9:	A description card that tells the user what is input on the next card.
Card 10:	(format A7, 3X, A7, 3X, F10.0).

DFILE:	The name of this input file.
GP:	The name of the A488 GP-file if C_p- x/c input will come from an A488 run. If the C_p's are input in this file, put the word "NOTHING" in this space.
SURF:	Number to determine which wing surface is to be analyzed in this run. (1. for lower, 0. for upper).

Example:

```
| 1|2|3|4|5|6|7|8|9|10|11|12|13|14|15|16|17|18|19|20|21|22|23|24|25|26|27|28|29|30|
|   T|E|S|T|A|A|     |N|O|T|H|I|N|G|       |0|.|
```

8-U80106-105

The second record of the input file is used by the BLGL code to set up inputs for the boundary layer calculation.

Card 1:	A descriptive card that tells the user what is input on the next card.
Card 2:	(format A80).

TITLE:	The title associated with this run.

Example:

```
| 1|2|3|4|5|6|7|8|9|10|11|12|13|14|15|16|17|18|19|20|21|22|23|24|25|26|27|28|29|30|
|   U|S|S| |C|O|D|E|   |T|E|S|T| |C|A|S|E|
```

8-U80106-106

Card 3:   A descriptive card outlining the input on the next card.

Card 4:   (format 4F10.0).

        EMINF: Freestream mach number.
        RBINF: Chord Reynolds number in the freestream direction.
        TINFK: Freestream static temperature in degrees Kelvin.
        ALPHA: Angle of attack. This parameter is not presently used.
        Example:

```
 1 2 3 4 5 6 7 8 9 10 11 12 13 14 15 16 17 18 19 20 21 22 23 24 25 26 27 28 29 30
  0 . 8              1 0 5 0 0 0 0 0 .       2 1 8 .
```

8-U80106-107

Card 5:   A descriptive card outlining the input on the next card.

Card 6:   (format 5F10.0).

        SWP1:   Sweep at the forward part of the wing in degrees. Must be greater than 0.
        XC1:   x/c at which the above sweep is applicable.
        SWP2:   Sweep at the rear part of the wing in degrees. Cannot be exactly equal to SWP1 but may be greater than SWP1, which indicates "inverse" taper (forward sweep).
        XC2:   x/c at which the above sweep is applicable.
        XCHORD: Chord length in feet in the streamwise direction.
        Example:

```
 1 2 3 4 5 6 7 8 9 10 11 12 13 14 15 16 17 18 19 20 21 22 23 24 25 26 27 28 29 30 31 32 33 34 35 36 37 38 39 40 41 42 43 44 45 46 47 48
  2 3 .            0 .                2 2 . 5              1 .                    7 . 0 7
```

8-U80106-108

Card 7:   A descriptive card.

Card 8:   (format 4F10.0).

        ETA2:   A boundary layer grid parameter. This is the grid spacing at the wall in decimal fraction of displacement thickness. The value 0.012 is recommended.
        ETAMAX: A boundary layer grid parameter. This value is the maximum distance from the wall to which the boundary layer will be calculated in units of displacement thickness. A value of 8.0 is recommended.
        FETA: The number of points defining the boundary layer profiles. A value of 70. is recommended. Maximum value is 100.
        FSUC: The number of points that will be used to define the suction distribution. The value 0. implies no suction. Less than or equal to 300.
        Example:

```
 1 2 3 4 5 6 7 8 9 10 11 12 13 14 15 16 17 18 19 20 21 22 23 24 25 26 27 28 29 30 31 32 33 34 35 36 37 38 39 40
  0 . 0 1 2              8 . 0                  7 0 .                        7 .
```

8-U80106-109

If there is suction, the next set of cards are input.

Card 8A: A descriptive card.

Card 8B: (format 2F10.0).

39

SSUC: s/c points defining the suction distribution on the wing. These values should start at s/c = 0. and end with a value greater than the s/c expected at the trailing edge. This distribution is fit with straight lines between defining points.

VSUC: Nondimensional suction rate, $(\rho v)_{wall}/(\rho U)_\infty$. A negative value denotes suction.

Example:

1	2	3	4	5	6	7	8	9	10	11	12	13	14	15	16	17	18	19	20	21	22	23	24	25	26	27	28	29	30
	0	.									0	.																	
	0	.	0	3	8	3	8				0	.																	
	0	.	0	4	1	5	7				-	0	.	0	0	0	2												
	0	.	6	8	8	3					-	0	.	0	0	0	2												
	0	.	7	2	2	1					-	0	.	0	0	1	2												
	0	.	7	5	5	4					-	0	.	0	0	1	8												
	1	.	0	3							-	0	.	0	0	1	8												

8-U80106-110

Card 9:   A descriptive card.

Card 10:   (format F10.0).

Put the value 2.1 on this card.

Card 11:   A descriptive card.

Card 12:   (format 4F10.0).

FNPTI: The number of points that will be used to describe the C_p - x/c distribution. Should be less than 250.

SWPCPI: The correction factor sweep in degrees that will be applied to the C_p and z/c input. This is used to apply simple sweep theory (i.e., if a "normal" pressure distribution is available) the BLGL program can do the adjusting of C_p by $\cos^2 \Lambda$ and z/c by $\cos \Lambda$.

FINPTC: Number indicating where the C_p information will come from.
0. - C_p - x/c input follows.
1. - C_p - x/c are input from an A488 GP-file. (Not available)

FNSEC: Number indicating the A488 wing section to be used if the C_p - x/c input is to come from an A488 GP-file. (Not available)

Example:

1	2	3	4	5	6	7	8	9	10	11	12	13	14	15	16	17	18	19	20	21	22	23	24	25	26	27	28	29	30	31	32	33	34	35	36	37	38	39	40
	7	0	.								2	3	.									0	.									1	.							

8-U80106-111

Card 13:   This is a descriptive card required if C_p - x/c are input in this file.

Card 14:   (format A40).

FORM: The format that will be used to read in the x/c, z/c, and C_p values. The format is enclosed in parentheses.

1	2	3	4	5	6	7	8	9	10	11	12	13	14	15	16	17	18	19
	(	3	F	1	0	.	5	)										

8-U80106-112

Card 15: This is a descriptive card, required if the C_p's are input in this file.

Card 16: (format as specified on card 14).

XCI: x/c, z/c, C_p input as sets on the streamwise airfoil. This set must start
ZCI: at the trailing edge lower surface and go completely around the section
CPI: to the trailing edge upper surface. Maximum of 250 sets of values.

Example:

1	2	3	4	5	6	7	8	9	10	11	12	13	14	15	16	17	18	19	20	21	22	23	24	25	26	27	28	29	30	31	32	33	34	35	36	37	38	39	40
	1	.	0								-	0	.	0	0	3					0	.	3	9	0	3													
	0	.	0									0	.	0							1	.	0	7	6	6													
	1	.	0									0	.	0	0	3					0	.	3	9	0	3														

8-U80106-113

The third record of the user input file contains information used by the interface program, LAMSD, to provide boundary layer information to the stability programs at the wing stations designated by the user.

Card 1: A descriptive card outlining what is input on the following card.

Card 2: (format 3F10.0).

FLAG: A number that determines how the boundary layer profiles from A411 will be chosen for input to the stability codes.
     0.   Choose the first N stations. N is specified in the following field.
     1.   Choose all stations generated by A411.
     2.   Choose N profiles from stations that are closest to the s/c values specified by the user later in this record. This is the recommended method.
     3.   Choose N stations selected by a geometric spacing criterion that is denser near the leading edge.

FSAV: The number of stations for which boundary layer profiles will be saved. If FLAG = 0. and FSAV = 0., the first 50 stations generated by A411 will be saved. However, only 40 stations can be calculated in one run of the stability codes.

FGGP: The number of stations where profiles will be saved on a plotting file. A value of 0. means no profiles are saved. The maximum number of stations that can be saved are all those generated by A411.

41

1	2	3	4	5	6	7	8	9	10	11	12	13	14	15	16	17	18	19	20	21	22	23	24	25	26	27	28	29	30	31	32	33	34	35	36	37	38	39	40
2	.										2	1	.									4	.																

8-U80106-114

Card 3:   A descriptive card required if the first number on the previous card was 2.

Card 4:   (format A40).

    FORM: The format used to read in the s/c values where boundary layer profiles will be saved for the stability codes. The format is enclosed in parentheses. This card is required only if the first number on card 2 is 2.

Example:

1	2	3	4	5	6	7	8	9	10	11	12	13	14	15	16	17	18
(	F	1	0	.	5	)											

8-U80106-115

Card 5:   A description card required if the first number on card 2 was 2.

Card 6:   (format as specified on card 4).

    SCPUT: s/c values where boundary layer profiles and other parameters will be saved for use by the stability codes.

Example:

1	2	3	4	5	6	7	8	9	10	11	12	13	14	15	16	17	18	19	20
0	.	0	0	5															
0	.	0	1																
0	.	6	5																

8-U80106-116

Card 7:   A descriptive card required if the number in field three of card 2 is not zero.

Card 8:   (format A40).

    FORM: The format that will be used to read in the locations whose boundary layer profiles are to be put onto a plotting file. The format is enclosed in parentheses.

Example:

1	2	3	4	5	6	7	8	9	10	11	12	13	14	15	16	17	18	19	20
(	F	1	0	.	5	)													

8-U80106-117

Card 9:   A descriptive card required if the number in field three of card 2 is not zero.

Card 10:   (format as prescribed on card 8).

    FGGPL: The numbers of the A411 spanlines (chordwise locations) at which the boundary layer profiles will be put into a plotting file.

1	2	3	4	5	6	7	8	9	10	11	12	13	14	15	16	17	18	19	20
	1	.																	
	5	.																	
	1	0	.																
	1	1	8	.															

8-U80106-118

The fourth record of the user input file contains the input for the MKMOD3 code.

Card 1:   (format 4I5, F10.0).

LFRST: A number that is the wing station to start checking the local $Re_{\delta*}$, and if it is beyond some threshold (which is a function of Falkner-Skan β) the MKMOD3 code starts calculating stability information. This station number is referenced to those that were put on the SI-file, not all those produced by the A411 program.

LLAST: The number of the station to stop doing stability calculations. This station number is also referenced to those put in the SI-file. There can be no more than 40 stations analyzed by the stability codes in one run.

NPSI: The number of wave angles to calculate stability for at each station 4 < NPSI < 8.

NFR: The number of frequencies, ω, to calculate stability for at each station. 4 < NFR < 10.

DELPSI: The wave angle increment in deg. Recommended values are between about 12 deg to 20 deg. This may have to be reduced for difficult cases such as adverse pressure gradients.

1	2	3	4	5	6	7	8	9	10	11	12	13	14	15	16	17	18	19	20	21	22	23	24	25	26	27	28	29	30	31	32	33	34	35	36	37	38	39	40
				1					2	2				5					7		1	5	.																

8-U80106-119

The rest of this record is made up of namelist input for MKMOD3.

Namelist $TDAT:

PSIB3D: Group velocity angle with respect to the local external flow. This effects the stability results only slightly and is usually near 0. The recommended input value is 0. and the default value is 0.

NUNIT: Tape unit on which the longer portion of printed output and optional output will be placed. Use 4 only.

NPR3D: Optional printing during eigenvalue iteration.
    0   Minimum print (default).
    1   First level of extra printing.
    2   Second level of extra printing.

NTABPR: Optional printing of the boundary layer profiles.
    0   No profile printing. This is the default and recommended value.
    1   Print profiles in F-format.
    2   Print profiles in E-format.

CKOUT: More optional printing.
    0   None. This is the default and recommended value.

43

| 1 | Level 1 extra printing. |
| 2 | Level 2 extra printing. |

Example:

1	2	3	4	5	6	7	8	9	10	11	12	13	14	15	16	17	18	19	20	21	22	23	24	25	26	27	28	29	30	31	32	33	34	35	36	37	38	39	40
	$	T	D	A	T			P	S	I	B	3	D	=	0	.	.		N	U	N	I	T	=	4			$											

8-U80106-120

Namelist $ADAT:

NI: The maximum number of iterations allowed in the eigenvalue searches. The default and recommended value is 9.

NSOL: This variable controls whether the dissipation terms are included in the solution. A value of 3 is recommended and results in the dissipation terms being ignored. If NSOL is not input, dissipation will be included.

Example:

1	2	3	4	5	6	7	8	9	10	11	12	13	14	15	16	17	18	19	20	21	22	23	24	25	26	27	28	29	30	31	32	33	34	35	36	37	38	39	40
	$	A	D	A	T			N	I	=	9	,		N	S	O	L	=	3		$																		

8-U80106-121

Namelist $TAB:

N1: The number of evenly spaced intervals into which the boundary layer profiles are divided for integration in the MKMOD3 code. The default value is 100. The minimum number of steps that does not significantly effect the accuracy of the results is about 80. The maximum allowed is 200. However, the user is cautioned that a case that involves difficult eigenvalue convergence may be assisted somewhat by using more integration steps (i.e., increasing N1). This is the only variable in TAB that may require changing at present.

Example:

1	2	3	4	5	6	7	8	9	10	11	12	13	14	15	16	17	18	19	20
	$		T	A	B		N	1	=	8	0		$						

8-U80106-122

The fifth record of the user input file has the input for the MKMOD5 program.

All the namelist input described for the MKMOD3 input is identical for MKMOD5. However, the first card is different.

Card 1: (format 4I5, 3F10.0).

LFRST: A number that is the station to start checking the local crossflow Reynolds number. If it is greater than some threshold (which is a function of the crossflow H parameter), the MKMOD5 code starts calculating stability information. This station number is referenced to those put on the SI-file.

LLAST: These three quantities are defined in the MKMOD3 input.
NPSI:
NFR:

ALPHAI: This is the guessed value for the nondimensional disturbance growth rate eigenvalue to be used in starting the stability calculations. For a run starting from the leading edge, the recommended value is 0.02. If the case being run might start at a station that is only slightly unstable, a smaller value will be required. For many cases the accuracy of this guess is not critical.

44

FRINP: This is the guessed value for the nondimensional disturbance frequency eigenvalue to be used in starting the stability calculations. This value is related to the following input parameter, DPSIST. For cases that start at the leading edge, a value of 0.00001 is recommended when DPSIST is near 2. If DPSIST is smaller, FRINP should be proportionally smaller, too. For cases that start at downstream locations, a smaller value of FRINP is appropriate.

DPSIST: This is the incremental wave angle in degrees that is subtracted from the critical wave angle to define the wave angle at which stability calculations will start. It is desirable to have a small ($< 2.$) value for DPSIST, and its value influences what is to be used for FRINP, as mentioned above. 1. to 2. is usually a good range of values to use for DPSIST.

Example:

1	2	3	4	5	6	7	8	9	10	11	12	13	14	15	16	17	18	19	20	21	22	23	24	25	26	27	28	29	30	31	32	33	34	35	36	37	38	39	40	41	42	43	44	45	46	47	48	49	50
			1					2	2						6					6	0	.	0	2							0	.	0	0	0	0	1				2	.	0						

8-U80106-123

The sixth record of the user input file has input for the INTTS2 program.

Card 1: (format I5).

ITYPE: A number that determines the integration philosophy to be used to find the N-factors.

1 Integrate disturbances of different frequencies at the wave angle for maximum growth rate.

0 Integrate disturbances of different frequencies at a user input wave angle.

Card 2: (format I5, 9F10.0).

If card 1 has a 0, then this card is required. Otherwise, it isn't.

NIPSI NIPSI's the number of different wave angles for which N-factors will
PSII: be calculated. The PSII are each of the wave angles in degrees. A maximum of nine wave angles can be used.

This record is set up to do two integrations of N-factors; one with the maximum growth rate method and one with the constant wave angle method.

Example:

1	2	3	4	5	6	7	8	9	10	11	12	13	14	15	16	17	18	19	20	21	22	23	24	25	26	27	28	29	30	31	32	33	34	35	36	37	38	39	40
				1																																			
				0																																			
				3		2	5	.							3	5	.							4	5	.													

8-U80106-124

The seventh record of the user input file has input for the INTCF2 program.

Card 1: (format I5).

METHOD: The first field contains a number that determines the integration philosophy to be used to find the N-factors.

1 Integrate disturbances of different frequencies at the wave angle for maximum growth rate.

0   Integrate disturbances of constant dimensional spanwise component of wave number and of a user-specified frequency (the "irrotational" method).

Card 2:   (format I5, 9F10.0, /, 5X, 9F10.0).

If card 1 has a 0, then this card is not required.

NIFR: The number of different frequencies for which N-factors will be calculated.

FRI: Each of the different frequencies in Hertz. A maximum of 18 frequencies can be used.

This record is set up to do two integrations of N-factors; one for the maximum amplification method and one with the irrotational method.

Example:

1	2	3	4	5	6	7	8	9	10	11	12	13	14	15	16	17	18	19	20
				1															
				0															
				1		0	.	0											

7.0 USS OUTPUT DESCRIPTION

This section describes the output of the various Unified Stability System (USS) programs. The file naming convention is defined in the Programs and Files section.

RDECK Output File JSXQQYZ

This file is made up of CDC job control statements for this particular run of the USS. The combination of programs to run and files to use and create are reflected in this job stream.

BLGL Output Files I411UQQ or I411LQQ

One of these two files is created when the BLGL program is run, depending on whether the upper or lower surface of a wing is being analyzed.

The first line on the I411-file is the run title, and the second has flag settings for A411 which are fixed for the USS applications. The third line has these parameters, in order:

1. The negative of the freestream Mach number.

2. Chord Reynolds number.

3. Freestream static temperature in degrees Kelvin.

4. This fourth number does not apply to laminar boundary layer calculations.

5. Prandtl number.

6. This sixth number does not apply to laminar boundary layer calculations.

7. The last two parameters are internal A411 flags and are not changed in the USS application.

The fourth line has the following parameters, in order:

1. ETA2 from the user input file.

2. ETAMAX from the user input file.

3. The rest of these parameters are fixed for the USS application.

Line five has a fixed output control flag, and line six has the number of wing sections and number of chordwise divisions to be analyzed. There is only one section for the USS application, but the chordwise stations to be analyzed varies around 220.

Line seven always has a 0. for the USS application, and line eight starts a set of input that gives the ZI coordinates of the chordwise stations to be analyzed. These values always start at zero. ZI is defined in figure 3.

After the ZI input are two lines that have values not applicable for the USS.

47

The file is completed by a set of lines that are in groups of three. The values on the first two lines of these three are fixed for the present application. On the third line the first, second, sixth, and seventh parameters are variable. The first is the local external velocity component parallel to the sweep nondimensionalized by freestream velocity. The definition of the velocity components is illustrated in figure 3. The second number is the local external velocity component perpendicular to the sweep. The sixth value on this line is the curvature of the chordline used for the A411 analysis. It would be zero for a nontapered case. The seventh value is surface suction defined as $(\rho v)_{wall}/(\rho Q)_e$. Note that the definition of this parameter is different from the user input suction parameter, VSUC.

This three-line group of input is repeated for each chordwise station to be analyzed by A411.

BLGL Output Files CREFUQQ or CREFLQQ

One of these two files is created when the BLGL program is run, depending on whether the upper or lower surface of a wing is being analyzed. The first line has (in order)—

1. The total number of stations on the chord at which A411 may compute the boundary layer.

2. The sweep in degrees at the wing trailing edge. If the case has inverse taper, this will be the conventional definition of wing sweep minus 180 deg.

3. The last two numbers are not important for this program application.

Following the first line are columns of information for each A411 solution station. The first column is the number of the station. The second is the ZI coordinate as defined in figure 3. The third column is x/c, and the fourth is z/c. The next two columns are geometric information. Column five is the negative of the sine of local sweep and column six is the direction cosine in the planform plane of the surface direction vector along the section used by A411; see figure 3. Column seven is the ratio of local streamwise chord to the user-specified streamwise chord; see figure 3. Column eight is the local sweep in degrees. If the case has inverse taper, this will be the conventional wing sweep −180 deg. The last column is s/c of each solution station but on the user-specified streamwise section.

BLGL Output on the OPXQQYZ File

There are several groups of output from BLGL on the OP-file. Several are of minimal use and will not be explained here. The case title starts the output. The next important group has column headings that start with I, ZI, XC, etc. This group contains information on the upper surface of the user-supplied section. The "I" column contains the numbers of the A411 analysis stations. ZI is defined in figure 3 and is nondimensionalized by the chord of the user-supplied streamwise section. XC is x/c. XB, YB, and ZB are A411 coordinates defined in figure 3, nondimensionalized like ZI. XLAM and ZLAM are angles in the A411 coordinate system as shown in figure 3. Note how these values are affected by inverse sweep. CAOCB is the ratio of "local" streamwise chord to the chord at the user-defined section. QQQ is the magnitude of the local external velocity nondimensionalized by the freestream velocity and CPQQQ is local C_p. The CPQQQ values are the result of curve-fitting done by BLGL of C_p versus s/c, so this dense array of points in this output group can be very useful for confirming the accuracy of the curve fit by plotting CPQQQ versus XC and spotting the user-supplied input points on the plot. The total number of stations input to A411 is around 220, and the density of them is greatest at the leading edge and at sudden

changes in C_p. This output group is followed by several unimportant ones. The next useful one is the lower surface station information. Both upper and lower surface station information are output, even though only one of the surfaces will be analyzed per run by A411.

The lower surface station output is followed again by some groups of unimportant output. The next noteworthy output is a repeat of the I411-file output, explained above. The last output from BLGL placed on the OP-file is a repeat of the CREF-file that was explained previously.

A411 Output Files BLXQQ and VPXQQ

These two files are in binary format and are only used to transfer information to the next program in the USS.

A411 Output to the OPXQQYZ File

The A411 program prints details of the boundary layer solution at each station, starting at the attachment line. It is important to note that the "UNIT RE" referred to in the output is actually chord Reynolds number. Most of the numerous other parameters whose values are printed are defined in reference 10. The exceptions are defined below:

For the attachment line output only, spanline 1, there are several special parameters printed. They are:

DSTR3Z	The partial derivative of DSTR3, with respect to the surface coordinate perpendicular to the attachment line, ZI.
HSSS	The ratio DSTRS/THSS.
TH13Z	The partial derivative of TH13, with respect to ZI.
CSTAR	$[(H3)\ (UEB)^2]/[(\text{kinematic viscosity at the edge of the boundary layer})\ (WEBZ)]$.
WEZBX	$\partial(\partial(WEB)/\partial(ZI))/\partial XI$, XI is along the attachment line.
CPZZ	$\partial^2\ (\text{pressure coefficient})/\partial ZI^2$.
K13Z	The rate of change of spanline curvature. For the USS application, this is 0.

For all spanlines (actually chordwise stations) after the attachment line, the additional parameters printed that are not defined in reference 10 are defined here.

BETASMAX	The maximum crossflow angle in the boundary layer. The definition for BETAS is not conventional. See reference 10.
BETASMIN	The minimum crossflow angle in the boundary layer.
DSTTOT	Displacement thickness based on the local total velocity in the boundary layer.

THTOT	Momentum thickness based on the local total velocity in the boundary layer.
OMEGABY, OMBSQRX, OMBSQRZ	These parameters only apply to applications that use a rotating reference frame, and therefore are 0.0 for the USS application.

When A411 reaches laminar separation, a note will be printed at each station saying: SOLUTION FORBIDDEN AT THIS STATION. KFORB(I) = the station number at which separation occurred. This concludes the pertinent A411 output to the OP-file.

LAMSD Output File VPGPXQQ

This is an optional file that can be created if the user desires. The file is formatted to plot velocity profiles calculated by A411. The profile information from any of the A411 chordwise stations can be written onto this file as chosen by the user-supplied input to LAMSD. The profile parameters written onto the VPGP-file are—

ETA	Distance above the wing surface nondimensionalized by δ of the velocity profile in the vertical plane which contains the external velocity vector.
U	Velocity profile in the vertical plane which contains the external velocity vector, nondimensionalized by the magnitude of external velocity.
UP	$d(U)/d(ETA)$.
UPP	$d^2(U)/d(ETA)^2$.
W	Velocity profile in the vertical plane perpendicular to the external velocity vector. Positive is outboard and the magnitude is nondimensionalized by the magnitude of the external velocity.
WP	$d(W)/d(ETA)$.
WPP	$d^2(W)/d(ETA)^2$.
T	Static temperature nondimensionalized by boundary layer edge temperature.
TP	$d(T)/d(ETA)$.
TPP	$d^2(T)/d(ETA)^2$.

The profiles at each station make up one set of output on the VPGP-file, and the number just after the KI printed at the beginning of each set is the A411 chordwise station number.

LAMSD Output File SIXQQ

This file is in binary format and is used to transfer the boundary layer parameters and profiles to the MKMOD3 and MKMOD5 programs. User-specified input to LAMSD determines which stations from A411 have information passed on to the stability programs.

LAMSD Output File BLGPXQQ

This is another file formatted for plotting, and it contains several of the more important boundary layer parameters for each station analyzed by A411. The information extends from the first station behind the attachment line to the location where A411 experienced laminar separation or to the trailing edge.

The parameters printed to this file are defined below:

ZI	The chordwise surface coordinate in the A411 coordinate system, see figure 3.
XOC	x/c of the station.
QEB, BETA1E, DSTR1, DSTR3, TH11, TH33	These parameters are all defined in reference 10 or have been defined earlier in this section.
RXFLO	Local crossflow Reynolds number. The length used is the greatest height in the boundary layer at which the crossflow velocity is $\frac{1}{10}$ of its maximum value. The velocity value used is the magnitude of the maximum crossflow velocity.
HI33	This is the incompressible boundary layer shape factor for the profile in the A411 "chordwise" direction.
HCF	Crossflow shape factor. The height in the boundary layer where the crossflow velocity is greatest divided by the greatest height where the crossflow velocity is $\frac{1}{10}$ its maximum value.
REDSTRZ	Boundary layer Reynolds number based on displacement thickness. The profile used is the A411 "chordwise" one.
BETAF	Falkner-Skan beta parameter, calculated using the velocity profile in the A411 "chordwise" direction.
CROSSM	Maximum crossflow velocity in the vertical plane perpendicular to the external velocity vector. Positive is outboard. This is nondimensionalized by the magnitude of the external velocity vector.

LAMSD Output Placed on the OPXQQYZ-File

The first printing that LAMSD does to the OP-file tells the user where A411 stopped its boundary layer calculations because of laminar separation. The second set of output starts with the user-specified title for this run and whether the upper or lower surface is being analyzed. Following this, there is a summary of parameters supplied to the stability analysis programs. They are defined below.

CHORD	XCHORD from input.
SWEEP 1 (DEG)	SWP1 from input.
SWEEP 2 (DEG)	SWP2 from input.
RADIUS	Radius in the A411 coordinate system; see figure 3.
FREESTREAM MACH	EMINF from input
FREESTREAM CHORD RE	RBINF from input.
STATION	The number of the station, as picked by LAMSD from A411 results to be transferred to the stability codes, is given here and also the total number of those stations.
A411 STATION	The number of this A411 station picked by LAMSD.
XOC	x/c of this station.
ZOC	z/c of this station.
SOC CHORDWISE	The s/c of this station measured from the attachment line on the user-input streamwise section.
CHORD CORRECTION	This is CA/CB; see figure 3.
DEL THETA (RAD)	This is an incremental sweep angle in radians and referenced to the leading edge sweep. A negative number is given when inverse taper is input.
LOCAL SWEEP(DEG)	Sweep at this station.
POINTS IN PROFILE	This is FETA from the user-supplied A411 input.
DISPL THICKNESS (DSTRZ)	Displacement thickness, in feet, of the velocity profile in the vertical plane perpendicular to local sweep.
B.L. THICKNESS (DELTA)	Boundary layer thickness, in feet, to where the velocity is 99% of the edge velocity. It is calculated using the profile in the vertical plane which is perpendicular to local sweep.

52

DELTA/DSTRZ	Ratio of the above two parameters.
DELTA/CHORD	Boundary layer thickness divided by airfoil chord.
SHAPE FACTOR	Boundary layer shape factor, δ^*/θ. It is calculated using the profile in the vertical plane which is perpendicular to local sweep.
FALKNER-SKAN BETA	This is calculated using the shape factor just above.
A411 TURBULENCE FLAG	0. for the USS application.
FLOW ANGLE (DEG)	The angle in degrees of the local edge flow measured from the local chordwise direction, positive outboard.
PHI CRIT (DEG)	This is the so-called critical angle, the angle at which the second derivative of crossflow velocity with respect to the "vertical" coordinate is zero at the same vertical distance as the crossflow velocity itself is zero. It is referenced to the plane perpendicular to local sweep and is positive outboard.
ETA OF CROSS-FLOW MAX	Height in the boundary layer in DSTRZ units at which the crossflow velocity, in the plane perpendicular to the edge velocity, has its maximum absolute value.
ETA WHERE CROSS FLOW IS 0.1 OF MAX	Height in the boundary layer in DSTRZ units at which the crossflow velocity is $\frac{1}{10}$ of its maximum absolute value. When there are several points in the boundary layer where this is true, the largest height is printed here.
CROSSFLOW REY	Crossflow Reynolds number. The length unit is the height in boundary layer where the crossflow velocity is $\frac{1}{10}$ of the maximum, and the velocity unit is the maximum crossflow velocity.
REY DSTRZ	Boundary layer Reynolds number based on DSTRZ and edge velocity perpendicular to local sweep.
MACK REY	Reynolds number used in the stability codes. This is local boundary layer Reynolds number based on the local external velocity and height in the boundary layer to 99% of the external velocity.
EDGE VEL (UE)	This is the magnitude of the local edge velocity in feet per second.
EDGE TEMP (DEG R)	Local static temperature at the edge of the boundary layer in degrees Rankine.

MACK STAG TEMP
(TSTAG39 DEG K)

Local stagnation temperature at the edge of the boundary
layer in degrees Kelvin.

LOCAL EDGE MACH
ZME39)

Mach number of the local edge flow.

The next group of output contains the velocity and temperature profiles at this station and their
first and second derivatives with respect to the local nondimensionalized "vertical" coordinate.
ETA is the "vertical" distance nondimensionalized by the displacement thickness determined
from the velocity profile in the vertical plane perpendicular to local sweep. U is the velocity com-
ponent in this direction, and W is the component perpendicular to U. T is static temperature
nondimensionalized by the edge static temperature. CROSS is the crossflow velocity determined
in the plane perpendicular to the local edge velocity.

The two groups of output described above are repeated for each station on the wing at which
boundary layer information is transferred from the A411 code to the stability codes.

The last set of output from LAMSD placed on the OP-file is nearly a repeat of what is on the
BLGP-file that was explained earlier. However, the format is different and the CROSSM parame-
ter that is placed onto the BLGP-file is omitted here.

MKMOD3 Output on the OTSXQQZ File

This file contains an expanded form of the output associated with the eigenvalue search for distur-
bance wave angles less than 70 deg. The more brief form is on the OP-file. If a run fails in the
MKMOD3 program, this output may be useful for finding and working around the problem.

The first output on the OTS-file is a line with four numbers on it. This line is printed every time the
program changes frequency in its solution process (i.e., NFR times per station). The first number
is FR, the nondimensional frequency. The second number is PSI, the wave angle in degrees. The
third number is the eigenvalue a_r guess supplied to the solution process, and the fourth number is
the a_i guess.

The next set of output is repeated for each of the NPSI wave angles analyzed at the frequency
printed on the preceding line. The words SPATIAL and COMPRESSIBLE remind the user of the
type of solution process being used. In MKMOD3, only the SPATIAL COMPRESSIBLE equa-
tions are allowed. The words NO DISSIPATION will appear next if the user has chosen to use the
faster sixth-order equation set. ICNTRL and KMUL are two internal flags that the user need not
be concerned about. ALPHA, DEL are the real and imaginary parts of the eigenvalue followed by
a convergence parameter, and they are printed for each iteration in the solution process. The

convergence parameter, DEL, in MKMOD3 is defined as $\sqrt{\dfrac{(\Delta a_r)^2 + (\Delta a_i)^2}{a_r{}^2 + a_i^2}}$. $\Delta\alpha_r$ and $\Delta\alpha_i$ are

the predicted changes to α_r and α_i for the next iteration in the Newton-Raphson search proce-
dure; see section 4.2. The solution is considered converged in MKMOD3 when DEL is 0.005 or
less. If the solution converges, the next set of output contains the following variables:

XQC	x/c at this station.
ALPHARC	$a^*_r \cdot c$, this is the dimensional wave number in the unrotated coordinate system (see fig. 9) multiplied by the streamwise chord.
ALPHAIC	$a^*_i \cdot c$, dimensional spatial amplification rate in the unrotated coord. system (see fig. 9) multiplied by chord. This equals $-(dN/ds) \cdot c$.
FR	Nondimensional disturbance frequency, $\omega^* \nu^*_e / U^{*2}_e$.
PSI3D	Disturbance wave angle in degrees, ψ.
PSIB3D	User-specified group velocity angle in degrees $\bar{\psi}$.
INTEGRAL	Not used in MKMOD3.
BETARC, BETAIC	These are similar to ALPHARC and ALPHAIC but are in the "Z" direction in the unrotated coord. system. BETAIC will be 0. by definition if $\bar{\psi}$ is input as 0.
UNROTATED ALPHA, BETA	These are a_r, a_i, β_r, and β_i in the unrotated coord. system. β_i is 0. by definition if $\bar{\psi}$ is input as 0.
ALPHAR	a_r, nondimensional wave number in the rotated coord. system (see fig. 9).
ALPHAI	a_i, nondimensional spatial amplification rate in the rotated coord. system.
R	Re_δ, Reynolds number based on δ.
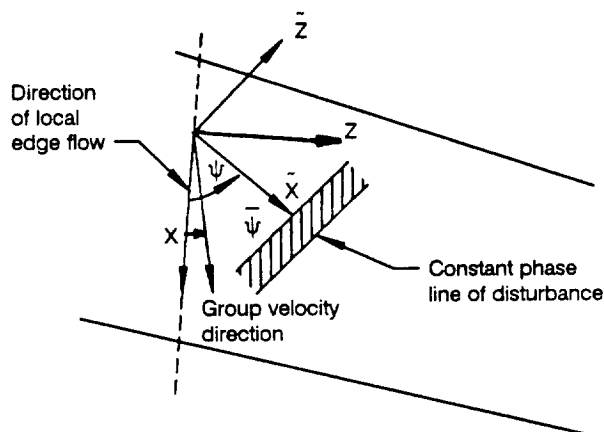
Legend:
X, Z Define the unrotated coordinate system.
$\bar{X}$, $\bar{Z}$ Define the rotated coordinate system.
α Component of the wave number in the $\bar{X}$ or X direction.
It has real and imaginary parts.
β Component of the wave number in the $\bar{Z}$ or Z direction.
It has real and imaginary parts.

Figure 9. Coordinate Systems for Stability Analysis

6-U90150-0

CR	Real part of the phase velocity.
CI	Imaginary part of the phase velocity.
FR	Explained above.
FI	Imaginary part of complex frequency. This is 0. for this application of MKMOD3.
FREQ	FR times R.
FREQI	0. for this application.
PHASE VEL	Dimensional phase velocity, $FREQ/a_r$.
PSI3D	Explained above.
BETAR	β_r in the rotated coordinate system, 0. by definition.
BETAI	β_i in the rotated coordinate system.

If the solution process does not converge, a message "MAXIMUM NUMBER OF ITERATIONS. CONVERGENCE NOT ACHIEVED" may be printed. If it is, the program will continue to run and may be able to successfully calculate eigenvalues at the conditions that follow. A more serious consequence of the solution not converging is an "arithmetic error" failure, which will stop MKMOD3 calculations altogether.

MKMOD3 Section of the OP-File

A loadmap of the MKMOD3 program is the first output to be put on the OP-file having to do with the MKMOD3 program. This can be useful for locating serious errors that terminate the program during execution.

The next group of output from MKMOD3, which appears on the OP-file, consists of two lines. It gives the wing station number (referenced to the stations picked by the LAMSD program), the station x/c location, the critical Reynolds number at this station (based on δ^*), the actual Reynolds number at this station (also based on δ^*), and the Falkner-Skan β at this station. The velocity profile used to calculate δ^* and the Falkner-Skan β is the one in the plane containing the velocity vector outside the boundary layer and perpendicular to the surface.

If the program determines that this station may have disturbance growth, the next group of output gives the following information. The eigenvalue guess (a_r, a_i) for the first wave angle at this frequency is given first. This guess for the first eigenvalue is calculated by the main program and is determined by empirical knowledge and/or converged results at other frequencies or stations during this run. Guesses for the eigenvalues at the second and higher wave angles at this frequency are determined by logic in parts of the MKMOD3 code not modified under this contract. The next output is a_r, a_i, and a convergence parameter called DEL and is printed for each iteration in the solution for this particular eigenvalue. If convergence is achieved, a message to that effect is printed next. If the solution does not converge, the program may terminate because of a numerical error or a message will be printed that says "MAXIMUM NUMBER OF ITERATIONS, CON-

VERGENCE NOT ACHIEVED." If this message appears, the program will at least try to continue the calculation process. Convergence is considered to take place when DEL is less than 0.005.

When eigenvalues for each of the NPSI wave angles are calculated at the first frequency, a summary is printed next which contains:

R Re_δ at this station.

ALPHAR a_r.

ALPHAI a_i.

PHVEL   This is zero for the mode being used in MKMOD3.

FREQR   Nondimensional frequency, FR times R.

FR   Nondimensional frequency.

The program then increments the frequency and repeats the eigenvalue search through the wave angles again.

After NFR frequencies are completed, the stability work at this station is complete and a summary table for this station is printed. The station number, x/c location, and angle of the local edge flow with respect to the freestream are printed first. The edge flow angle is in degrees and positive is a flow outboard with respect to the freestream. In the summary table the columns are at constant frequencies, which are in Hertz and are printed at the top of each column. The next row of printing gives the wave angle in degrees (referenced to the local edge flow direction, positive outboard) and then the disturbance growth rate, dN/ds, for this wave angle at each of the frequencies. The units for dN/ds are 1/ft. The third row of printing is the group velocity direction for the wave angle-frequency combinations. It is in degrees, referenced to the local edge flow direction and positive outboard. The above summary output continues until results for each of the NPSI wave angles are printed. The program then continues to the next station and the cycle of printing described above repeats until the run is complete.

MKMOD3 Output on the TSIXQQZ File

The TSI-file is used by the INTTS2 program to integrate the disturbance growth rates according to user-specified rules to get the N-factors at the various wing stations. The information on this file is a series of tables summarizing the MKMOD3 program results and is very similar to the tables that the program prints on the OP-file.

The first line of output on the TSI-file contains, in order; NPSI, the number of different wave angles analyzed for each station; NFR, the number of different frequencies analyzed for each station; and the chord length in feet. The second line contains the x/c value of the station immediately ahead of the first station at which the program starts calculations. If the program started stability calculations at the first station, then this value would be 0.0.

The third line starts a set of output that is repeated for each station. This line contains, in order, the number of this station, the x/c value of this station, the s/c value of this station measured from the attachment line, the local sweep in degrees defined conventionally, and the angle in degrees between the local external velocity and a line perpendicular to the local sweep, defined as positive

for flow toward the wingtip. The second line of output in this set contains the values of the frequencies analyzed at this station. These are in Hertz and start with the lowest value at the left. After this line there are four lines, repeated for each wave angle. The first of these four lines starts with the disturbance wave angle in degrees and then has the disturbance growth rates, dN/ds, for that wave angle and the disturbance frequencies printed above it. The second of the four lines contains the nondimensional wave number, a_r, which the program converged to for this wave angle and frequency. The third line contains the spanwise component of wave number in dimensional units of one per foot. Neither the dimensional nor non dimensional wave numbers in the TSI-file are presently used in the N-factor integration, but they are included for possible future use. The last of the four lines has the group velocity angle of this disturbance in degrees, measured relative to the local external velocity and positive outboard. After these four lines are repeated NPSI times, the summary information at this station is complete. The summary information for the next station is printed next and this continues for each station until the run is complete.

MKMOD5 Output on the OCFXQQZ File

This file contains an expanded form of the output associated with the eigenvalue search for disturbance wave angles greater than 72 deg. The shorter form of this output is on the OP-file. If a run fails in the MKMOD5 program, this output may be useful for finding and working around the problem.

The output on the OCF-file is similar to that on the OTS-file, which was explained earlier; therefore, only the differences will be detailed here. For the MKMOD5 program the first line of output, which contains FR, PSI, the a_r guess, and the a_i guess, is printed for each eigenvalue solution, instead of only once for each different frequency, as was the case with the MKMOD3 program. After the ICNTRL, KMUL line there is a message printed: VARYING BETAI — NOT ALPHAI. This tells the user that the program is operating at high-disturbance wave angles, greater than 72 degrees. Before the ALPHA, DEL line of output, the OCF-file has a line containing DELT1, DELT2, and AMPAZT. DELT1 is the change in nondimensional frequency predicted by the program for the next iteration. DELT2 is the change predicted for β_i, which is the nondimensional dN/ds for MKMOD5. It is important to note here that the eigenvalues solved for by MKMOD5 during the iteration process are frequency and β_i, with wave angle, ψ, and wave number, a_r, held fixed. In the MKMOD3 program, a_r and a_i are the eigenvalues solved for, with frequency and wave angle held fixed. The AMPAZT parameter gives the user some idea of how well the solution process is matching the boundary conditions at the wing surface. The reader will recall that the basis for this stability method is an integration of the disturbance equations through the boundary layer from top to bottom, changing the eigenvalues until the wall boundary conditions are adequately met. The magnitude of AMPAZT is not of much concern to the user, but it should decrease as the iteration process converges. When the solution is converged, AMPAZT will generally be 10 or less, but for some very difficult velocity profiles, AMPAZT may be a very strong function of frequency and β_i. In these cases AMPAZT may still be in the order of 1000 when sufficient eigenvalue accuracy has been achieved.

Following the line described above is the ALPHA, DEL line. As mentioned before, the real part of ALPHA is held fixed in this program, although the imaginary part varies. In MKMOD5, DEL is defined as

$$\sqrt{\left(\frac{\omega}{1 \times 10^{-6}}\right)^2 + \left(\frac{\text{DELT2 in dimensional units}}{5.}\right)^2}$$

For convergence DEL must be less than or equal to 0.01. When convergence occurs, the output that starts with the "XQC, ALPHARC ---" line and ends with the "CONVERGENCE ACHIEVED" line is printed and is the same as was explained for the MKMOD3 program.

The output explained above is repeated for each eigenvalue that the MKMOD5 program finds or attempts to find.

MKMOD5 Output on the OPXQQYZ File

As with the MKMOD3 program, a loadmap of MKMOD5 is the first output that is printed on the OP-file.

The next set of output from the MKMOD5 program that appears on the OP-file has two lines. Station number and x/c are given on the first line. The station refers here to the stations picked by the LAMSD program. The second line contains the critical crossflow Reynolds number, the actual crossflow Reynolds number at this station, and the value of the crossflow H parameter. The critical crossflow Reynolds number is a function of crossflow H and is determined from an empirical table lookup from reference 30 (see fig. 8). Only if the crossflow Reynolds number is 10 or more units greater than the critical crossflow Reynolds number will the eigenvalue calculations begin.

If eigenvalue calculations start at this station, the next output is the eigenvalue guesses at the first wave number/wave angle calculation point. The wave number is chosen from expirical information by the program. The wave angle is the so-called "critical angle" minus a user-supplied increment, DPSIST, generally between 1 and 3 deg. The ALPHAR printed right after EIGENVALUE GUESS is the fixed wave number to be used at this condition and the BETAI and FR are the guesses for the two eigenvalues. At the first conditions these are the user-supplied inputs called ALPHAI and FRINP, respectively (see sec. 6.0). Results of the iteration process are printed next. The first number to the right of ALPHA, DEL is a_r. This remains fixed in the MKMOD5 iteration process. The next number is a_i, and it changes as β_i is changed during the iteration. DEL is the measure of the change in the eigenvalues requested by the program for the next iteration. When DEL is 0.01 or less, the solution is considered converged. If the solution converges, a message to that effect is printed as well as the final values of the eigenvalues. The program then goes to the next wave angle/wave number condition, calculates the eigenvalue guesses for that condition, and repeats the solution process. For this first series of solutions the program is finding the lower limit on the wave angle range to use for this first station. It does this by fixing the wave number and finding solutions at different wave angles, starting at the first angle and working down in 0.5-deg increments. This series continues until either the wave angle is less than 73 deg or a converged BETAI is found that is less than 30% of the first BETAI. If the eigenvalue iteration process does not converge, the eigenvalues that are returned from it will be much in error and the wave angle ranging logic will probably fail. An improved user-input guess may solve this problem. If the wave angle range is calculated normally, this series of solutions will be terminated with a printout saying, "•••••• WAVE ANG. RANGE FOR FIRST STA. IS _ TO _." The maximum value for the wave angle is always the "critical angle" plus 0.6 deg.

Once the wave angle range for the first station is determined, the wave number range is found. This is done by going back to the first wave angle and decreasing the wave number by 0.1 for a series of conditions that end when 10 different wave numbers have been analyzed at this wave angle or until a converged BETAI is found that is less than 20% of the first BETAI found. The program then switches from decreasing the wave number to increasing it from the very first condition. The results of this series of wave number calculations are curve fit, and the wave numbers to

analyze for the first station are determined from it. A message is printed giving the wave number range. The range printed here applies to the (NPSI-1) wave angle only, because the wave number range changes with wave angle. Experience with MKMOD5 has shown that the unstable region of wave angle/wave number conditions can best be covered for a wide variety of boundary layer profiles if the lower limit for wave number is held fixed for the different wave angles, but the upper limit is a function of wave angle to the 1.6 power.

After the ranges of wave angles and wave numbers to analyze are found for the first station, the standard order of calculating eigenvalues for these ranges is worked through. The program starts at the lowest wave angle and wave number and proceeds from there to higher wave numbers. When all the NFR wave numbers are analyzed at the first wave angle, the calculation goes to the next higher wave angle and starts again at the lowest wave number, working to higher ones. The output seen by the user on the OP-file during this process is a set of EIGENVALUE GUESS —, ALPHA, DEL, and RESULTS FROM MACK, for each converged solution. If the solution does not converge during this part of the analyses, it will trigger internal recovery logic which will either change the eigenvalue guess (this is the approach used for the first four wave angle and wave number combinations) or break up the step from a previous converged solution into 8 small steps so the eigenvalue guess can be improved. This recovery procedure is explained more fully in figure 10.

Figure 10. — Estimating the Next Eigenvalue and Recovering From Divergence—MKMOD5
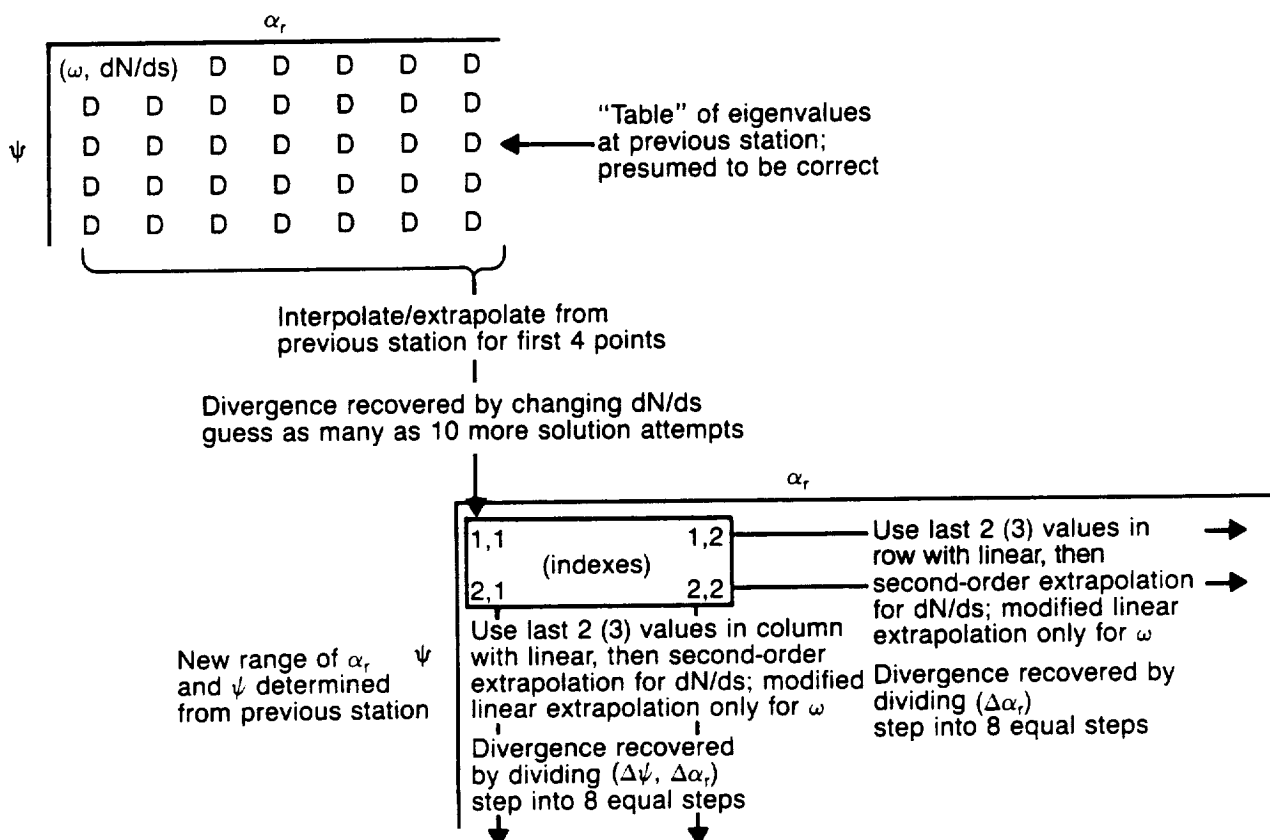
When eigenvalues for all the wave angle/wave number combinations for this station have been calculated, a summary of the results is printed. The summary contains the station number and x/c, the critical angle in degrees as well as the angle of the local edge velocity with respect to the freestream, also in degrees and positive outboard. The next five lines give calculation results at the lowest wave angle. Included here are wave angle in degrees, frequencies in Hertz, nondimensional wave numbers, the dimensional wave number components perpendicular to the local edge velocity; the disturbance growth rates per foot, dN/ds; and the group velocity angles of these disturbances in degrees, referenced to the local edge velocity and positive outboard. This set of five lines is repeated for each of the wave angles analyzed.

The output for this station is completed with the printing of the wave angle ranges to be used for the next station. These are calculated by curve-fitting with parabolas the dN/ds versus wave number, a_r, at the first and next-to-highest (NPSI-1) wave angles. If the maximum value of dN/ds of this parabola is greater than 1.0, the wave number range for the next station is determined to be from the wave number where dN/ds = 0 on the lower branch of the parabola to the wave number where dN/ds a negative ⅓ of the maximum value on the upper branch. If the maximum value of dN/ds of the parabola is less than 1.0, the wave number range is from the wave number on the lower branch at which dN/ds equals the maximum value of dN/ds on the parabola minus 1.0 to the wave number on the upper branch at which dN/ds is the maximum value minus 1.5. In addition, the lower end of the range of wave number must be greater than or equal to 0.3. In this way the wave number ranges for all stations after the first one analyzed are determined by the eigenvalue results from the previous station.

As with the wave number range determination, the lower limit on the wave angle range for all stations after the first is calculated using results from the previous station. Again a curve-fit is used. In this case dN/ds versus wave angle results for the (NFR+1)/2 wave numbers are used. In the summary table described earlier, this is the middle column for odd NFR or the column just to the left of center for an NFR that is even. The lower range of wave angle is then determined to be at the angle where dN/ds is ⅙ of the maximum value from the parabolic curve-fit, or 72 deg, whichever is larger. The largest wave angle to be considered at the next station is again the critical angle for that station plus 0.6 deg. The wave angle range for all stations after the first one analyzed is printed after the first two lines of output for that station.

The output described above that did not have to do with finding the wave angle and number ranges for the first station analyzed is repeated in sets for the rest of a MKMOD5 run.

MKMOD5 Output on the CFIXQQZ File

The CFI-file is similar to the TSI-file in that it summarizes the MKMOD5 program results and is used by an integration program, INTCF2, to calculate N-factors. The series of tables printed on the CFI-file are similar to those that MKMOD5 prints on the OP-file.

The first line of output on the CFI-file contains, in order; NPSI, the number of different wave angles analyzed during this run; NFR, the number of different wave numbers analyzed during this run; and the chord length in feet. The second line contains the x/c value of the station immediately ahead of the first station at which the program starts calculation. If the program started stability calculations at the first station, then this value would be equal to x/c)$_1$ - [x/c)$_2$ - x/c)$_1$] or 0., whichever is greater.

The third line starts a set of output that is repeated for each station. This line contains, in order, the number of the station, the x/c value of this station, the s/c value of this station measured from the attachment line, the local sweep in degrees defined conventionally, and the angle in degrees between the local external velocity and a line perpendicular to the local sweep, defined as positive for flow toward the wingtip. The fourth card is the beginning of a set of five cards that summarize the MKMOD5 results for the first wave angle examined at this station. This line contains first the wave angle in degrees and then all the disturbance frequencies for each of the wave numbers examined at this wave angle. The frequencies are in Hertz and correspond with the nondimensional wave numbers that are printed on the line immediately following them. The third line in this set is the component of the wave numbers perpendicular to the local edge velocity in dimensions of one per foot. The fourth line contains the disturbance growth rates in dimensions of one per foot for each wave number printed immediately above. The fifth line gives the corresponding group velocity angles in degrees, measured with respect to the local edge velocity and positive outboard. The output then proceeds to the next wave angle and repeats the above set for it, continuing through all the wave angles examined at this station. The same information is then printed for following stations until the run is complete.

INTTS2 Output on the OTSIXQQ File

The INTTS2 program creates two output files: one is readable and the other is for machine plotting. Both files contain N-factors as a function of x/c for different frequencies. The INTTS2 program presently calculates N-factors by both the maximum amplification method and the method used by Boeing (constant wave angle method). Results from both these methods are printed on the OTSI-file, starting with the maximum amplification method. The frequency in Hertz for the first N-factor integration is printed first. Following that, four columns are printed that are headed with their descriptions: x/c, dN/ds, wave angle, and N-factor. The program searches the table of dN/ds versus frequency and wave angle for each station (TSI-file) to find the wave angle for maximum growth rate at the desired frequency. This procedure is allowed to extrapolate outside the table but the resulting value of dN/ds found from extrapolation may not be reasonable. Therefore, if extrapolation occurs, a message to that effect is printed and the user should closely examine the associated N-factors. The next set of output is for the next frequency analyzed. Note that the program searches all the tables contained in the TSI-file to find the frequency range over which to calculate the N-factors, and then goes back and calculates N-factors for 36 different frequencies in this range. This range of frequencies has always proven to be more than adequate to define the envelope of most amplified disturbances.

After N-factor results for the 36 frequencies using the maximum amplification method are printed, the program repeats the process for the same frequencies, using the first of the user-specified wave angles. This is the method used by Boeing. Several different wave angles can be specified, and N-factors for each are printed as a set in the order in which they are input (see sec. 6.0).

INTTS2 Output to the GTSIXQQ File

The GTSI-file contains N-factor information from the INTTS2 program in plotting format. The first set of output before an end-of-file mark are the results from the N-factor calculations using the maximum amplification method. The first line contains the format of each dataset. The second line is a graph title. The third line is a note placed on the graph which tells the reader that the NTS - x/c plot was calculated using dN/ds at the wave angle that gave maximum growth. Lines four through seven give first the independent variable name, XOC, and then the parameter names associated with each of the N-factor versus x/c plots that can be made. These parameter names

are "F" followed by the frequency in Hertz rounded to the nearest whole number. There is one parameter name for each of the 36 frequencies at which the INTTS2 program calculated N-factors. What follows this line of output are sets of numbers, one for each station at which MKMOD3 analyzed the boundary layer stability, starting at the first station. The first number in each of these sets is the x/c of the station. The numbers that follow are the N-factor information for the NASA calculation method.

For N-factor calculations using the constant wave angle method, a set of output almost identical to that described above is created for each wave angle specified by the user. The graph title changes appropriately, as does the "note" given on line three. Each set ends with an end-of-file mark.

INTCF2 Output on the OCFIXQQ File

The INTCF2 program creates two output files: one for reading and the other for machine plotting. Both contain N-factors as a function of the x/c for (1) different frequencies, in the case of the maximum amplification method, (2) different values of dimensional components of wave number in the spanwise (perpendicular to local edge flow) direction, in the case of the irrotational integration method. Results from both these methods are printed on the OCFI-file, starting with the maximum amplification method. The frequency in Hertz for the first N-factor integration in printed first. Following that, four columns are printed that are headed with their descriptions; x/c, dN/ds, wave angle, and N-factor. The program searches the table of dN/ds versus frequency (which varies with wave number) and wave angle for each station to find the wave angle for maximum growth rate at the desired frequency. If the program determines that the wave angle for maximum growth rate at this frequency is at a wave angle that is lower than that available in the CFI-file, it includes information from the lower angle analyses on the TSI-file, providing that file is in existence and has information on it at the desired station. The maximum amplification integration method is allowed to extrapolate beyond its tables in some limited ways. If it does extrapolate or pick growth rate values at the edge of the tables, it prints a message that warns the user that the associated N-factors may not be accurate. The next set of output is for the next frequency. The program searches all the tables contained in the CFI-file, but not the TSI-file, to determine the frequency range over which to calculate the N-factors. It then calculates N-factors for 25 different frequencies in this range, which usually is adequate to define the envelope of most amplified disturbances. Since this integration program can use disturbance growth rates from wave angles calculated by both of the stability programs, the N-factors calculated by the maximum amplification method from this program are probably more accurate than those calculated by the INTTS2 program.

After N-factor results for the maximum amplification method are printed, the program switches to the irrotational method. After the printed message to this effect, the frequency in Hertz and spanwise wave number in units of 1 per foot are printed. Following this, the four columns of x/c, dN/ds, wave angle, and NCF are printed for this wave number. Extrapolation beyond the wave angle and frequency tables provided by the CFI-file is also permitted for this integration method, and a message warning the user is printed if extrapolation is done. This set of output is repeated for each of 26 different wave numbers chosen automatically by the program. If the user has specified by input to the INTCF2 that N-factors for more than one frequency are to be calculated with the irrotational method, the above output is repeated in turn for each frequency.

INTCF2 Output to the GCFIXQQ File

The GCFI-file contains N-factor information from the INTCF2 program in plotting format. The first set of output before an end-of-file mark are the results from the N-factor calculations using the maximum amplification method. The first line contains the format of each dataset. The second line is a graph title. The third line is a note placed on the graph that tells the reader the N - x/c plot was calculated using dN/ds at the wave angle that gave maximum growth. Lines four through six give first the independent variable name, XOC, and then the parameter names associated with each of the N-factor versus x/c plots that can be made. These parameter names are "F" followed by the frequency in Hertz rounded to the nearest whole number. There is one parameter name for each of the 25 frequencies at which the INTCF2 program calculated N-factors. What follows this line of output are sets of numbers, one for each station at which MKMOD5 analyzed the boundary layer stability, starting at the first station. The first number in each of these sets is the x/c of the station. The numbers that follow are the N-factors at this station for each of the frequencies, and in the same order as the parameter names on lines 4 through 6. The set of N-factor information for the maximum amplification calculation method ends with an end-of-file mark.

For crossflow N-factor calculations using the irrotational method a set of output very similar to that described above is created for each frequency specified by the user. The graph title changes appropriately, as does the "note" given on line three. The parameter names are "K" followed by the spanwise component of wave number rounded to the nearest whole number. The set of N-factor information for each frequency is separated by an end-of-file mark.

8.0 GUIDELINES FOR THE USS USER

8.1 PRERUN CONSIDERATIONS

Preparing to make a run on the Unified Stability System (USS) starts with gathering the information needed in the input deck. Of the information required, the accuracy of the C_p - x/c distribution is among the most critical. The more sparse the definition of the pressure distribution or questionable its accuracy, the more care will be required to ensure that the dense definition generated by the BLGL program for the boundary layer analysis is a "reasonable" one. Reasonable as used here means that aerodynamic judgment may be required. The user may be disappointed to see that the pressure distribution for the complete wing section is required as input. Although this is the case, the accuracy of the geometry and pressure outside the region of interest is not very important, except as it may affect the curve-fitting near the edges of the region of interest. This may be an important issue near the leading edge when pressure data are only available on one surface or the other.

Another important aerodynamic input is the taper (the actual input is local sweep at two different chordwise locations). If nothing is known about the isobar pattern in the area of interest, geometric taper can be used. However, the boundary layer really responds to aerodynamic taper, so if the aerodynamic taper changes with x/c in the region of interest, some average must be chosen. As a rough rule of thumb, the isobars that the USS assumes based on its two sweep inputs, should match the actual isobars most closely in regions of high chordwise pressure gradient.

8.2 CONSIDERATIONS FOR BOUNDARY LAYER CALCULATIONS

When a new USS run is started, the user can choose to run just the first program (BLGL) or as many as all seven of the programs in one job submittal. If there is a question concerning the curve-fitting of the pressure distribution by BLGL, only that program should be run and the dense array of C_p - x/c that it generates should be plotted. A distribution that results in a poor curve fit can be improved by adding additional input points. If the curve-fit of pressure seems adequate, the second program in the USS, the A411 boundary layer code, can be run. It is possible that A411 will predict laminar separation and stop calculations at a point on the wing section ahead of where the user knows transition took place. If this happens, all input that affects the boundary layer calculation should be checked first. If the input is correct and the pressure distribution curve-fit looked acceptable, the user has little recourse but to make small changes to the pressure coefficient input until the program runs at least to the point where the user knows transition took place.

After the boundary layer is calculated, appropriate stations need to be picked for input into the stability programs. This is done by the third code of the USS, LAMSD. As described in the input description, there are three options for choosing the stations for stability analyses from the many calculated by A411. Of these, the option in which the user specifies the s/c locations of the desired stations is recommended. The distribution and number of stations to be picked varies considerably with each case, but there are guidelines that can assist the choices. In general, pick stations about 0.5% chord apart for the first 5% chord, starting at 0.5% chord. For the next 5% to 10% chord, pick stations about 1% chord apart. For the rest of the distance, 2.5% to 5.0% chord spacing may be possible. Without knowing the boundary layer results, a priori, it is the pressure gradient and its variation that guides the user in determining the station distribution. Rapid changes in gradient call for closer spacing. Closer spacing also implies smaller changes in stability

characteristics between stations, which makes the eigenvalue "guessing" logic in the stability programs more accurate. The number of stations chosen is a compromise between wanting a detailed picture of the stability characteristics and the cost of the computation time. There is also a limit of 40 stations currently in the USS.

The LAMSD program can also create a file containing boundary layer profiles in a plottable format. These are generally not required, but some cases may exhibit such strange stability behavior that the user will want to go back and rerun LAMSD to see the profiles. The means of picking the stations for which profiles will be saved on the plotting file is cumbersome (see the input description), but does allow the user to plot the profiles of any station calculated by the boundary layer program. The correlation between A411 station number, x/c at the station, and s/c at the station can be found on the CREF-file created by the BLGL program.

8.3 SETTING UP THE MKMOD3 RUN

The MKMOD3 program calculates the boundary layer stability characteristics at wave angles below 65 deg. It develops sets of information that can be represented as tables as shown in table 1.

Table 1. — MKMOD3 Program Tables

Wave angle	Frequency, Hz		
	ω_1	$\cdots \omega_j \cdots$	ω_{NFR}
ψ_1	$\left.\dfrac{dN}{ds}\right)_{1,1}$ $\bar{\psi}_{1,1}$	Disturbance growth rate Group velocity angle, deg	$\left.\dfrac{dN}{ds}\right)_{NFR,1}$ $\bar{\psi}_{NFR,1}$
ψ_K			
ψ_{NPSI}			$dN/ds)_{NFR,NPSI}$ $\bar{\psi}_{NFR,NPSI}$

For the first stability analysis run of a given case, the user usually specifies that the program start at station 1 and continue to the last station. The program then determines from the boundary layer characteristics at which station there may be unstable disturbances and starts eigenvalue calculations there. This logic is based on comparing the displacement thickness Reynolds number of the boundary layer profile perpendicular to the local sweep with a "critical" Reynolds number from reference 29 (see fig. 4). Once the program is triggered to start eigenvalue calculations, it does not "turn off" at later stations that may have no disturbance growth.

The DELPSI input to MKMOD3 determines how much of the wave angle region is covered by this run. Internal limits constrain the minimum wave angle to be -50 deg and the maximum to be 65 deg. Picking DELPSI is a compromise between the desire to—

a. Establish the stability characteristics over a wide wave angle range. This is particularly important for using the "maximum amplification" N-factor calculation.

b. Limit cost by choosing fewer wave angles to analyze, and/or the desire to get a more dense definition of the stability with a given number of wave angles, and/or the desire to increase the odds for a successful run by making the increments between wave angles smaller.

66

The program tries to distribute the wave angles it analyzes around an empirical estimate of the most unstable wave angle, which is a function of local Mach number (see ref. 6). In practice this empirical estimate of the most unstable wave angle has not proven to be very accurate, but it is still worth including. As an example, if DELPSI = 20 and NPSI = 5, the wave angles of about -40, -20, 0, 20, and 40 would be analyzed for local Mach numbers below 0.7. For local Mach numbers in the 1.0 to 1.3 range, the upper limit on wave angle would come into play. The lowest angle would be near 0. deg. The resulting wave angles to be analyzed would then be approximately 0, 16, 33, 49, and 65 deg.

The frequency range to be analyzed by MKMOD3 is chosen by empirical logic in the program, developed from reference 29 (see sec. 4.2). For most cases this range adequately covers the region of instability, at least well enough to establish the envelope of disturbance growth. The empiricism is weakest for boundary layers that are near separation.

8.4 CHECKING FOR PROBLEMS AND RESTARTS WITH MKMOD3

The tables of disturbance growth generated by MKMOD3 are available on the OP-file or the TSI-file. It is advisable for the user to scan these tables to check for unusual results. The program may occasionally return incorrect results, even if the failure is not serious enough to stop the run. One possible failure is nonconvergence of an eigenvalue search that is not serious enough to stop the run. This can be spotted in the stability tables if dN/ds at two or more frequencies have identical values for the same wave angle or if the group velocity angles appear to be too high. The group velocity angles are calculated by an interpolation process. This is an efficient but not a highly accurate method, and the answers from it are sometimes suspicious; occasionally they are obviously wrong. This is not necessarily a cause for concern. Although the group velocity angle is used in the N-factor integrations, the integration programs limit the angle they use to be between ±10 deg. If the stability tables have strange-looking results, the user should look at the OP-file and perhaps the OTS-file to get more clues as to the validity of the results.

If the user wishes to start the MKMOD3 program at some station partly through the region of interest, this presents no particular problem. The start-up logic for guessing eigenvalues at the first station calculated in a run is sometimes even more robust than that which uses results at previous stations. This is an especially important point if the boundary layer changes are excessive between stations. On a run that continues calculations begun in a previous run, the user must change the version number or the OP-, OTS-, and TSI-files created by the second run will write over those created by the previous run. For a case that has been completed by several different runs, the user must combine the TSI-files from the runs in order for the integration programs to work properly. Additionally, NFR and NPSI for all these files must not change.

If the MKMOD3 program fails, consider the following:

a. Density of the stations with regard to the change in the boundary layer between adjacent stations.

b. Size of the wave angle increment.

c. Size of the frequency increment.

8.5 SETTING UP AND RESTARTING AN MKMOD5 RUN

The MKMOD5 program calculates the higher wave angle stability characteristics. It has a lower limit on wave angle of 72 deg and an upper limit of 0.6 deg above the "critical" angle of the boundary layer profile. This wave angle range does not necessarily cover all the unstable area but is intended to cover all the unstable area for positive frequencies. For most cases of interest to wing designers, the envelope of the most amplified disturbances will be defined by positive frequency disturbances.

Like the MKMOD3 program the MKMOD5 program develops "tables" of stability information at each wing station.

Table 2. — MKMOD5 Program Tables

Station $x/c)_i$	j-index		
Wave angle, ψ_1	$\omega_{1,1}$ $\alpha_{r_{1,1}}$ $\alpha^*_{r_{s_{1,1}}}$ $\dfrac{dN}{ds}\Big)_{1,1}$ $\bar{\psi}_{1,1}$	Disturbance frequency, Hz Nondimensional wave number Spanwise component of dimensional wave number, 1/ft Spatial disturbance growth rate, 1/ft Group velocity angle, deg	$\omega_{NFR,1}$ $\alpha_{r_{NFR,1}}$ $\alpha^*_{r_{s_{NFR,1}}}$ $\dfrac{dN}{ds}\Big)_{NFR,1}$ $\psi_{NFR,1}$
ψ_K			
ψ_{NPSI}			

The frequency in this program is not constant on a column of the table, as it was for the MKMOD3 program.

If the MKMOD5 program is started from station 1 for a stability analysis run, it parallels the MKMOD3 program in examining the boundary layer characteristics to determine which station probably contains disturbance growth. In MKMOD5 this logic compares the crossflow Reynolds number of the boundary layer profile to an empirically determined critical value of crossflow Reynolds number as given in reference 30. This program, unlike MKMOD3, does contain logic to skip stability analyses at stations if (1) the maximum dN/ds at the (NPSI-1) wave angle of the previous station was less than -2. and (2) the crossflow Reynolds number is 15 less than the empirical "critical" value. At the high wave angles the solution for the eigenvalues is more difficult than at lower wave angles, especially for conditions in which the disturbances are damped. This is why logic in the MKMOD5 program is tailored to prevent calculations at stations that are probably stable. A compromise on this issue is required; however, because an adequate definition of disturbance growth and damping is required to properly define the N-factor envelopes.

For cases showing a "reasonable" amount of crossflow instability near the leading edge, the suggested input values for ALPHAI, FRINP, and DPSIST will probably result in a normal program start. Cases that are only slightly unstable but do trigger the logic that starts eigenvalue calculations may require changes in ALPHAI and FRINP to obtain program convergence during the starting phase. This may also be true when starting the program at downstream stations. The starting phase

involves finding the wave angle and wave number ranges to cover in subsequent "table" calculations. After the first station these ranges are determined from results at the previous, upstream station. If the program does not get good converged eigenvalues during this starting phase, it does not necessarily fail, but the subsequent stability table results should be closely examined. The degree of instability at the starting station can be critical for getting a successful start; generally the more unstable the more likelihood of a successful start. Some measure of the instability at a station can be gained by comparing the crossflow Reynolds number to the "critical" crossflow Reynolds number. The former is located on LAMSD output to the OP- or BLGP-files, and the latter can be found from figure 8, knowing H(crossflow). H(crossflow) is also output by LAMSD. The user's desire to start the calculations at a station that is unstable enough to get a successful start must be tempered by remembering that N-factor accuracy is reduced when the chordwise increment between stations is increased.

The stability tables generated by MKMOD5 may be found on the OP- or CFI-files. It is advisable to scan these tables to check for unusual results. After a few successful runs users will get an idea of what constitutes an "unusual" result. The program can give incorrect results without actually stopping. One possible problem is the inability to converge during an eigenvalue solution. Because this is much more likely to happen at these high wave angles, MKMOD5 has logic for recovering from cases that do not converge. For the first four points in the stability table (two lowest wave angles and wave numbers), this logic involves changing the ALPHAI guess and trying the solution again, for a maximum of ten attempts. For the rest of the points in the table, the recovery logic involves taking a smaller step (⅛ the size) in wave angle or wave number from the previous point, at which it is assumed there is a converged solution. Figure 10 outlines this recovery procedure. The group velocity angles are calculated by MKMOD5 the same way as done by MKMOD3, so the shortcomings mentioned with regard to that program are also possible for this one. If the stability tables have strange-looking results, the user should look at the OP-file and perhaps the OCF-file to get clues as to the validity of the results and possible causes of problems.

Restarts of MKMOD5 are more common than with MKMOD3 because unusual program terminations are more common for it. Unfortunately, restarts are also more difficult with MKMOD5 because—

a. The logic affecting the start of calculations is less robust in MKMOD5 because the calculations are inherently more difficult at the high-wave angles.

b. The logic that allows the program to start calculations at a station based on crossflow Reynolds number may not allow a restart in an area that is only slightly unstable.

c. The initial eigenvalue guesses that the user must input may be more difficult to determine. If results at previous stations are available, they are usually helpful.

8.6 DISTURBANCE GROWTH CALCULATIONS

The two programs that use the stability tables to calculate N-factors are similar and will be discussed together. Both programs are presently set up to do two sets of calculations, one using the constant wave angle (for TS) or irrotational (for CF) approach and one using the maximum amplification approach. The maximum amplification approach may require stability information over a wide wave-angle range, so if both TSI- and CFI-files are available, the INTCF2 program uses them both. However, the other integration program, INTTS2, still does the maximum amplification integration as well because it is possible that the CFI-file might not have been calculated.

The user is reminded that if both files are available, the maximum amplification results from INTCF2 are probably more accurate. The following points should be remembered about the integration programs:

a. Accurate N-factor calculations require knowing the disturbance growth rates from the point on the wing where they first become unstable.

b. If the TSI- and CFI-files were generated by combining the results of several different runs of the stability codes, be sure there are no duplicate stations in the files.

c. A failure of the integration programs is unusual. If it happens, check the CFI- or TSI-file and the tape 5 input. If there is a suspicious station in the CFI- or TSI-file, it may be edited from the file if the user feels the integration without that station will still have enough accuracy.

d. The message printed by the integration programs concerning extrapolation is only informative. Extrapolation is permitted because in many cases, it improves the answer. However, whether it is reasonable or not in a particular instance has to be judged by the user.

e. The boundary layer and stability characteristics are calculated on a streamwise section of a wing. However, the integration of dN/ds over the wing does include the effect on Δ s of the disturbances growing in the direction of the group velocity (see fig. 11).
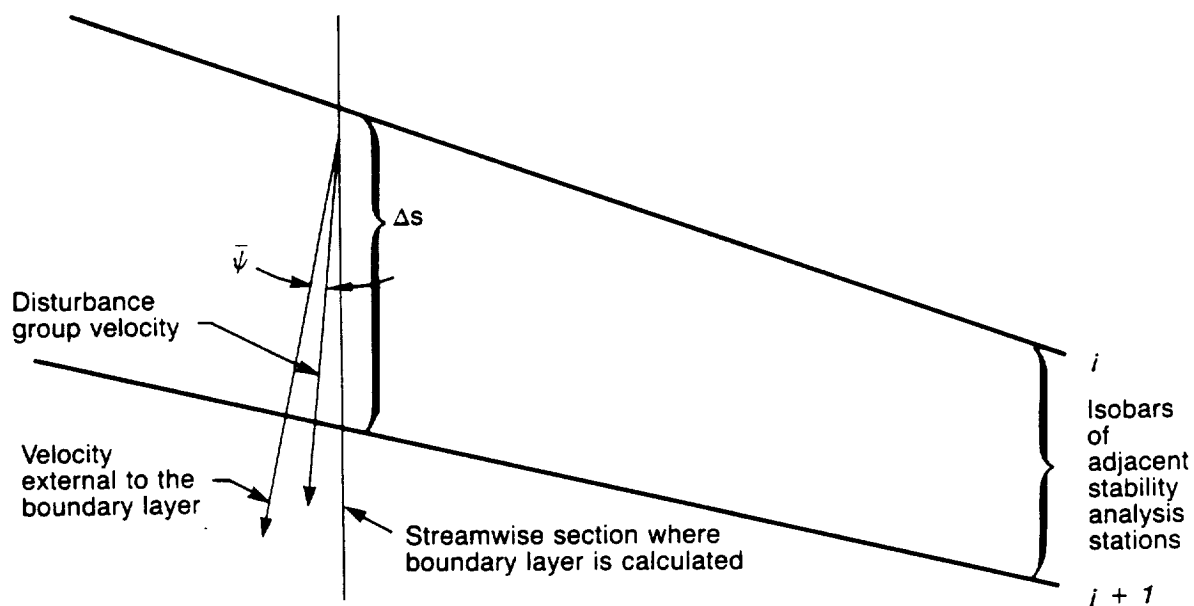
Figure 11. — Effect on Δs of the Disturbances Growing in the Direction of the Group Velocity

9.0 CONCLUSIONS AND RECOMMENDATIONS

The Unified Stability System (USS) was developed to provide a more versatile sweptwing laminar boundary layer stability analysis method and also one that was easier to use than previous methods. These two goals tend to be at odds with each other, and obviously, compromises had to be made. Most of the computer coding necessary for the system, the laminar boundary layer analysis and the stability analysis, was a modification of existing codes, which saved a great deal of effort. Additionally, results from previous authors were very helpful in setting up the initial eigenvalue "guessing" logic used in the stability codes of the USS.

The USS was thoroughly verified during its development. Some of this verification is described in reference 4 and some was a result of the F-111 reanalyses described in the appendix of this report.

The numerous files and large amount of output generated by the USS can be intimidating for the first-time user. Most of this information is never used, but it is still included for possible debugging of problems or for use by the analyst looking at details of the boundary layer or its stability characteristics. Therefore, the cost of running a case (one streamwise "cut" on a wing) will depend on the computer system and costing algorithm used, but the USS can be considered a moderately expensive system to use. The first-time user of the USS should either carefully read the sections of this report on the system's use or use the system under the direction of someone who is familiar with it.

Several files created by a USS run are information formatted for plotting on Boeing graphics facilities. It is hoped that these files will require little change to make them available for plotting by other computer systems.

Currently, the USS can be used for examining the stability characteristics of laminar boundary layers on sweptwings from incompressible speeds through transonic speeds. The extension of the USS to supersonic speeds is believed possible, but has not been verified at this time.

The N-factors at transition presented in the appendix for F-14 VSTFE, F-111, and 757 NLF flight data show considerable scatter. This indicates a need for further development of correlations of transition on sweptwings. The USS should be a valuable tool for this research, eliminating much of the handwork previously required.

It was shown in references 36 and 37 that the curvature of the path of the disturbance can introduce terms into the classical stability equations that noticeably affect the eigenvalues of these equations for the spinning disk and yawed cylinder cases respectively. Recently, the effect of these curvature terms has been examined for sweptwing boundary layers and has been found to have a substantial effect on stability there too, reference 38. It would be straightforward to add curvature terms arising from surface curvature and streamline curvature to the USS, but considering the curvature of the path of the disturbance followed by any particular growth philosophy would require an iterative process.

71

10.0 REFERENCES

1. Meyer, R. R., Trujillo, B. M., and Bartlett, D. W. "F-14 VSTFE and Results of the Cleanup Flight Test Program." Research in Natural Laminar Flow and Laminar Flow Control, Part 3, NASA CP 2487, Mar. 16-19, 1987.

2. Rozendaal, R. A., "Variable Sweep Transition Flight Experiment (VSTFE)—Parametric Pressure Distribution Boundary Layer Stability Study and Wing Glove Design Task," NASA CR 3992, June 1986.

3. Waggoner, E. G., Campbell, R. L., Phillips, P. S., and Hallissy, J. B. "Design and Test of an NLF Wing Glove for the Variable Sweep Transition Flight Experiment." Research in Natural Laminar Flow and Laminar Flow Control, Part 3, NASA CP 2487, Mar. 16-19, 1987.

4. Rozendaal, R. A. "Variable Sweep Transition Flight Experiment (VSTFE)—Stability Code Development and Cleanup Glove Data Analysis." Research in Natural Laminar Flow and Laminar Flow Control, Part 3, NASA CP 2487, Mar. 16-19, 1987.

5. Malik, M. R., "COSAL—A Black Box Compressible Stability Analysis Code for Transition Prediction in Three-Dimensional Boundary Layers," NASA CR-165925, May, 1982.

6. Mack, L. M., "On the Stability of Boundary Layer on a Transonic Swept Wing," AIAA 17th Aerospace Sciences Meeting Paper 79-0264, New Orleans, LA, January 15-17, 1979.

7. Mack, L. M., "Boundary-Layer Stability Theory," AGARD Report No. 709, 1984.

8. Runyon, L. J., Navran, B. H., and Rozendaal, R. A. "F-111 Natural Laminar Flow Glove Flight Test Data Analysis and Boundary Layer Stability Analysis," NASA CR-166051, January 1984.

9. New Product Development Organization, BCAC, "Flight Survey of the 757 Wing Noise Field and Its Effects on Laminar Boundary Layer Transition," NASA CR-178419, March 1988.

10. Randall, J. L., and McLean, J. D., "Computer Program To Calculate Three-Dimensional Boundary Layer Flows Over Wings With Wall Mass Transfer," Program User's Document, NASA CR-158967, December 1978.

11. Kaups, K., and Cebeci, T. "Compressible Laminar Boundary Layers With Suction on Swept and Tapered Wings." Journal of Aircraft, Vol. 14, No. 7, July 1977.

12. Gaster, M. "A Note on a Relation Between Temporally Increasing and Spatially Increasing Disturbances in Hydrodynamic Stability," J. Fluid Mech., Vol. 14, pp. 222-224, 1962.

13. Gaster, M. "On the Stability of Parallel Flows and the Behavior of Separation Bubbles," Ph.D. Thesis, Univ. of London, 1963.

14. Gaster, M. "On the Generation of Spatially Growing Waves in a Boundary Layer," J. Fluid Mech., Vol. 22, pp. 433-441, 1965.

15. Tollmien, W. "Uber die Entstehung der Turbulenz," Nachr. Ges. Wiss. Gottingen, Math.-phys. Klasse, pp. 21-44, 1929.

16. Lin, C. C. "On the Stability of Two-Dimensional Parallel Flows," Parts I, II, III, Quart. Appl. Math., Vol. 3, pp. 117-142, 218-234, 277-301, 1945.

17. Thomas, L. H. "The Stability of Plane Poiseuille Flow," Phys, Rev., Vol. 91, pp. 780-783, 1953.

18. Kurtz, E. F., Jr. "Study of the Stability of Parallel Flows," Ph.D. Thesis, Massachusetts Institute of Technology, Cambridge, MA, 1961.

19. Osborne, M. R. "Numerical Methods for Hydrodynamic Stability Problems," SIAM J. Appl. Math., pp. 539-557, 1967.

20. Jordinson, R. "The Flat Plate Boundary Layer, Part I, Numerical Integration of the Orr-Sommerfeld Equation," J. Fluid Mech., Vol. 43, pp. 801-811, 1970.

21. Gallagher, A. P., and Mercier, A. M. "On the Behavior of Small Disturbances in Plane Couette Flow, Part I," J. Fluid Mech., Vol. 13, pp. 91-100, 1962.

22. Orszag, S. A. "Accurate Solution of the Orr-Sommerfeld Stability Equation," J. Fluid Mech., Vol. 50, pp. 689-703, 1971.

23. Brown, W. B., and Sayre, P. H. "An Exact Solution of the Orr-Sommerfeld Stability Equation for Low Reynolds Numbers," Report No. BLC-43, Northrop Aircraft Inc., Hawthorne, CA, 1954.

24. Chai, A. S. "A Modified Runge-Kutta Method," Simulation, May 1968.

25. Kaplan, R. E., "The Stability of Laminar Incompressible Boundary Layers in the Presence of Compliant Boundaries," ScD. Thesis, MIT, 1964.

26. Godunov, S. K. "On the Numerical Solution of Boundary Value Problems for Systems of Ordinary Differential Equations," Uspekhi Mat. Nauk, Vol. 16, pp. 171-174, 1961.

27. Bellman, R. E., and Kalaba, R. E. "Quasilinearization and Boundary-Value Problems," American Elsevier, N. Y., 1965.

28. Radbill, J. R., and Van Driest, E. R. "A New Method for Prediction of Stability of Laminar Boundary Layers," AFOSR Report No. 66-0702, 1966.

29. Wazzan, A. R., Okamura, T. T., and Smith, A.M.O. "Spatial and Temporal Stability Charts for the Falkner-Skan Boundary-Layer Profiles." Douglas Aircraft Company Report DAC-67086, September 1968.

30. Dagenhart, J. R., "Amplified Crossflow Disturbances in the Laminar Boundary Layer on Swept Wings With Suction," NASA TP 1902, November 1981.

31. Dunn, D. W., and Lin, C. C. "On the Stability of the Laminar Boundary Layer in a Compressible Fluid," J. Aero. Sci., Vol. 22, pp. 455-477, 1955.

32. Reshotko, E. "Stability of Three-Dimensional Compressible Boundary Layers," NASA Tech. Note D-1220, 1962.

33. Mack, L. M. "Boundary-Layer Stability Theory, Jet Propulsion Laboratory," Pasadena, CA, Document No. 900-277, Rev. A., 1969.

34. Schubauer, G. B., and Skramstad, H. K. "Laminar Boundary Layer Oscillations and Transitions on a Flat Plate, " J. Aero. Sci., Vol. 14, pp. 69-76; also NACA Report 909, 1948.

35. Mack, L. M. "Three Dimensional Effects in Boundary-Layer Stability," Proceedings of Twelfth Symposium on Naval Hydrodynamics, pp. 63-70, National Academy of Sciences, Washington, D.C. ,1979.

36. Malik, M. R., Wilkinson, S. P., and Orszag, S. A., "Instability and Transition in Rotating Disk Flow," AIAA Journal, Vol. 19, No. 9, September 1981.

37. Malik, M. R. and Poll, D. I. A., "Effect of Curvature on Cross-Flow Instability," Laminar-Turbulent Transition IUTAM Symposium, Novosibirsk, 1984.

38. Collier, F. S. Jr., "Curvature Effects on the Stability of Three-Dimensional Boundary Layers," Ph.D. Thesis, Virginia Technical Inst., May 1988.

11.0 APPENDIX—STABILITY ANALYSES USING THE USS

Fifteen cases were selected from the Variable Sweep Transition Flight Experiment for boundary layer stability analysis. The measured data were obtained from the F-14 cleanup glove. The data for each case consisted of flight conditions, pressure distributions and hot-film traces on the upper surface. The results from these analyses provide further insight into how the crossflow (CF) and Tollmien-Schlichting (TS) disturbances interact during the boundary layer transition process, for a range of sweep angles. Table A-1 lists the features of the 15 cases.

Three separate rows of pressure taps were placed in the cleanup glove to measure the pressure distributions at wing-buttock-lines 200.8, 260, and 320 (defined with Λ_{LE} at 20 deg). Each row consisted of 19 ports on the upper surface and 2 ports on the lower surface. In addition, the state of the boundary layer was determined by surface hot-film sensors. These sensors were installed at every 10% chord location, staggered about 30 deg from the streamwise line. Only one row of hot-film sensors was used per case, placed between the first and the second or the second and third pressure orifice rows. Figure A1 shows a schematic planform of the test region.

For the selected cases, the three rows of pressure data were used to determine the pressure isobars. Knowing the leading edge sweep and isobars, an effective taper ratio for the laminar portion of the wing could be determined. The USS code has the capability to include the taper effect. The hot-film traces were used to locate the transitional region by locating the gauge that shows transitional traces or had just gone turbulent. The location of that gauge was then marked and an effective chord line was drawn through it. Figure A2 illustrates the definition of effective chord as opposed to chord at a nominal sweep angle. The pressures al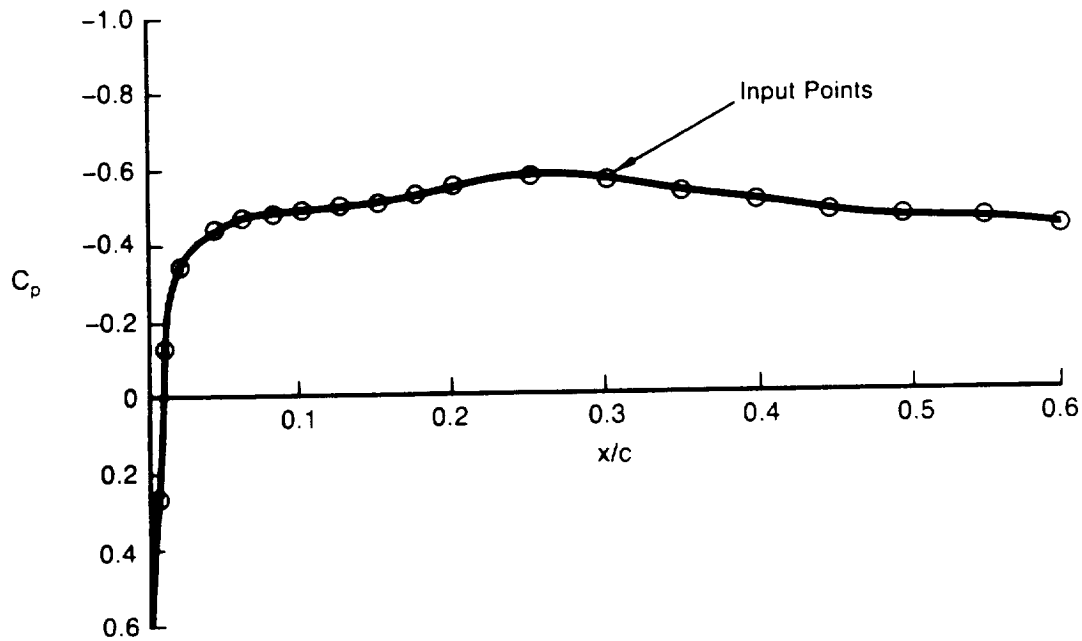ong the effective chord line were found by an interpolation between the three measured rows to the WBL of the measured transition point. This chordwise distribution was used for the boundary layer stability analysis.

Once all the data were reduced to the final form required by the USS, the code was run for all 15 cases. The compressible CF and TS disturbance growth envelopes, with the corresponding pressure distributions, are shown on figures A3 through A22. For TS disturbances, the solid line represents the envelope of growth of disturbances of different frequencies at a wave angle that gives the maximum growth. This is the "constant wave angle" approach described in the body of this report. However, if the growth envelope keeps increasing with wave angle, a limit of 55 deg is imposed. For many laminar boundary layers, there is no clear division between a region of TS disturbances and CF disturbances. For CF disturbances, the dashed line represents the envelope of crossflow disturbance growth at zero frequency and with a range of values of the spanwise component of the dimensional wavenumber, $a^*_{r_s}$ (this is the "irrotational" approach). For a few of these cases, the "maximum amplification" envelope is also shown in an additional figure. That envelope represents the maximum growth of disturbances of varying frequencies, with wave angle changing to give maximum growth rate for each frequency at each chordwise position as the disturbance moves aft on the wing. The transition location for each case, determined from hot-film traces, was used along with the CF and TS envelopes to determine the CF and TS amplification factors at transition. These amplification factors are summarized in table A-1, and figure A23 shows the traces of the amplification factors for a distance of 2.5% chord on either side of the experimentally determined transition location. These traces show the sensitivity of the correlation of experimental transition with analytically determined disturbance growth.

As a supplement to the F-14 VSTFE cases, a few cases from earlier NLF flight tests (F-111 (ref. 8) and 757 (ref. 9)) were reanalyzed by the USS. The reanalyses of these data were consid-

75

ered important because these two sets of data had been used previously to define a transition criterion, but the boundary layer analysis and stability analysis procedures of the USS represent an improvement over that used in those previous studies. The cases chosen tend to define the envelope of the F-111/757NLF transition data band. Pressure distributions and disturbance growth curves for those cases are shown in figures A24 through A41. Tables A-2 and A-3 summarize each case with their updated results. Figure A42 shows the movement of the transition point N-factors for the F-111 and 757 cases due to the change in analysis methods.

Transition N-factors from the present study and those recalculated from previous data are presented together in figure A43. The mean and estimate of standard deviation using $\sqrt{N_{CF}^2 + N_{TS}^2}$ are also shown in figure A43. The scatter in the transition N-factors is large, even for the VSTFE points, for which the experimental data are most complete and accurate, indicating the need for further improvement in transition correlation. The USS should be a useful tool for further research.

Table A-1. — Summary of F-14 VSTFE Cleanup Glove Cases

Case ID	Flight No.	Test point	Position of gages	Λ_{LE}, deg	M_∞	Re/ft x 10⁻⁶	x/c_{TR}	Local chord, ft	Re_{TR} x 10⁻⁶	N_{TS}	N_{CF}	α, deg
V1	13	1C	Outer	35	0.703	1.732	0.25	6.23	2.70	4.2	3.1	1.1
V2	17	46A3	Middle	24	0.603	3.423	0.25+	7.56	7.12	8.3	5.2	0.5
V3	17	31B	Middle	15	0.802	3.251	0.45+	7.62	11.76	0.1	9.4	0.2
V4	18	17B	Middle	20	0.806	2.843	0.40+	7.65	9.24	0.3	10.4	0.5
V5	12	22A	Outer	30	0.802	1.957	0.40+	6.25	5.20	3.1	7.5	0.8
V6	17	41B	Middle	15	0.702	4.095	0.40	7.53	12.33	9.9	6.2	0.2
V7	13	10A	Outer	31	0.802	1.964	0.35	6.18	4.25	4.2	6.0	2.4
V8	16	22A3	Middle	28	0.703	2.450	0.30	7.69	5.18	12.2	2.0	1.7
V9	13	2C	Outer	30	0.704	1.690	0.40	6.23	4.21	8.1	2.8	1.4
W1	13	12C	Outer	20	0.803	1.954	0.45+	6.00	5.57	0.3	6.5	-0.2
W2	17	32B	Middle	20	0.804	3.338	0.25+	7.47	6.58	0.1	8.6	0.4
W3	13	11C	Outer	25	0.801	1.967	0.45	6.13	5.43	1.5	8.2	1.4
W4	16	22A2	Middle	31	0.702	2.444	0.15	7.65	2.80	7.8	4.1	2.0
W5	18	18D	Middle	25	0.800	2.808	0.20	7.50	4.21	3.3	6.2	1.5
W6	13	16.1	Outer	22	0.804	2.836	0.30	5.86	4.98	0.2	9.0	0.5
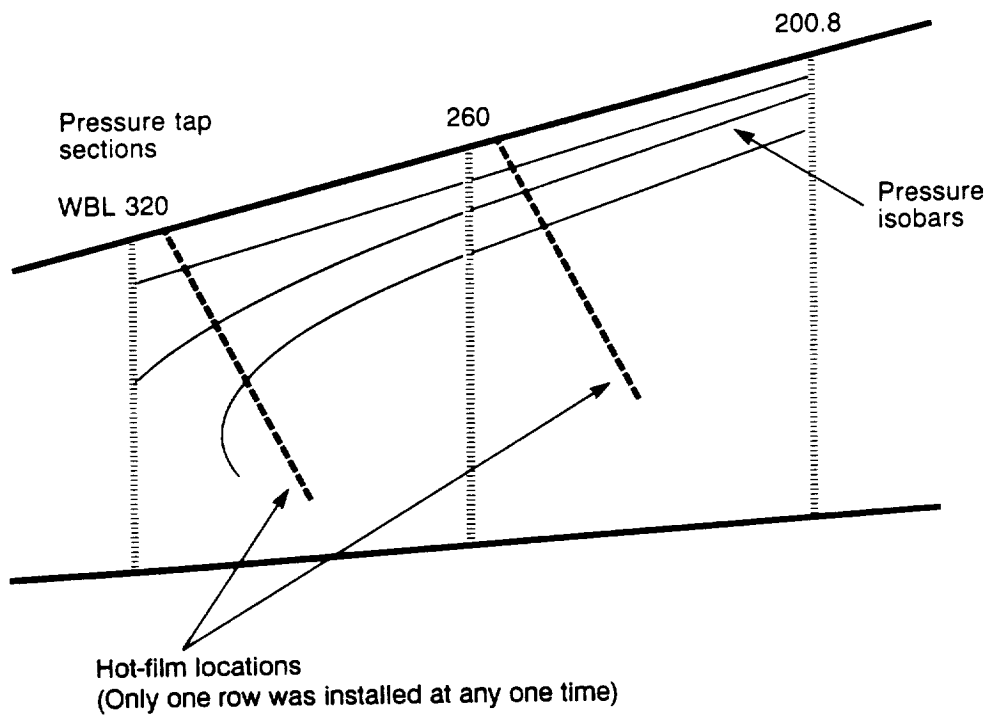
Figure A1. — Plan View of the Glove Showing Pressure Isobars, Hot Film Locations, and Static Pressure Geometry
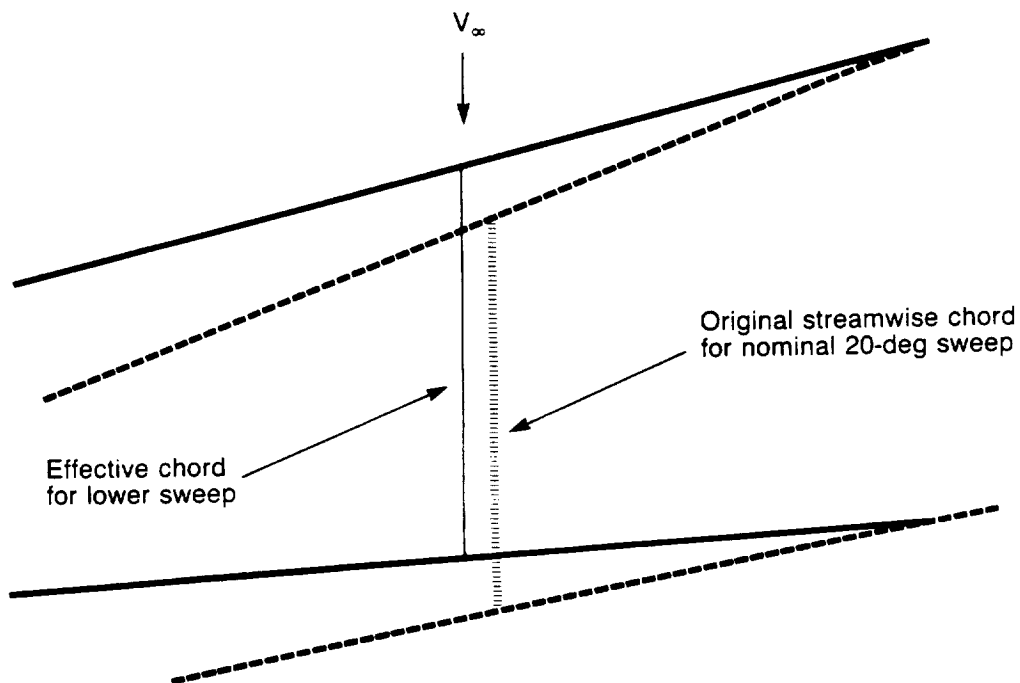
Figure A2. — Definition of Effective Chord as Opposed to a Chord at a Nominal Sweep Angle
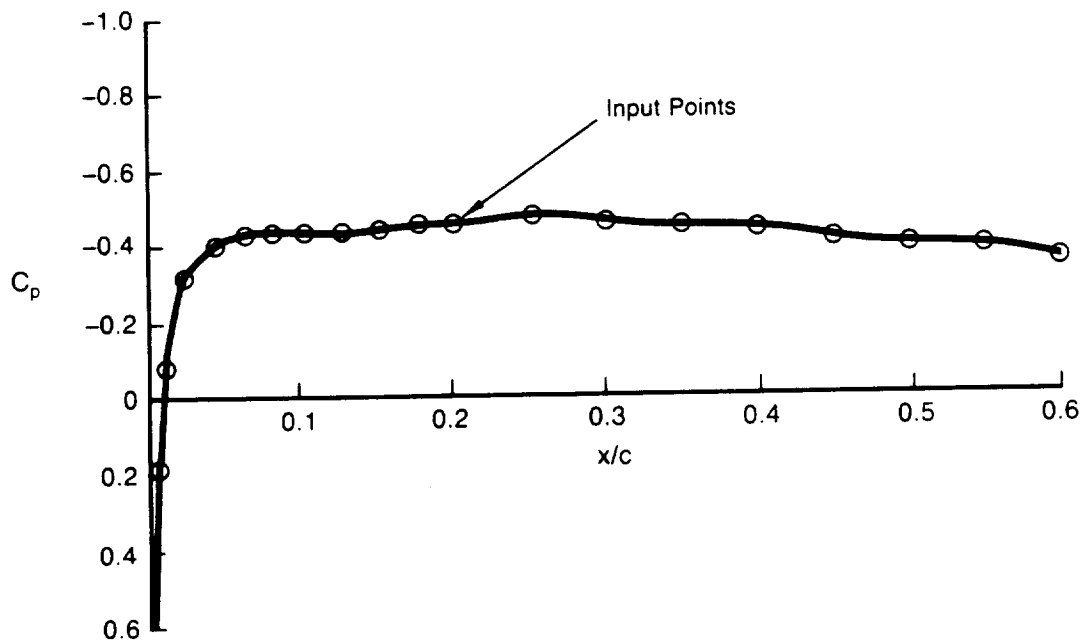
(a) Pressure Distribution
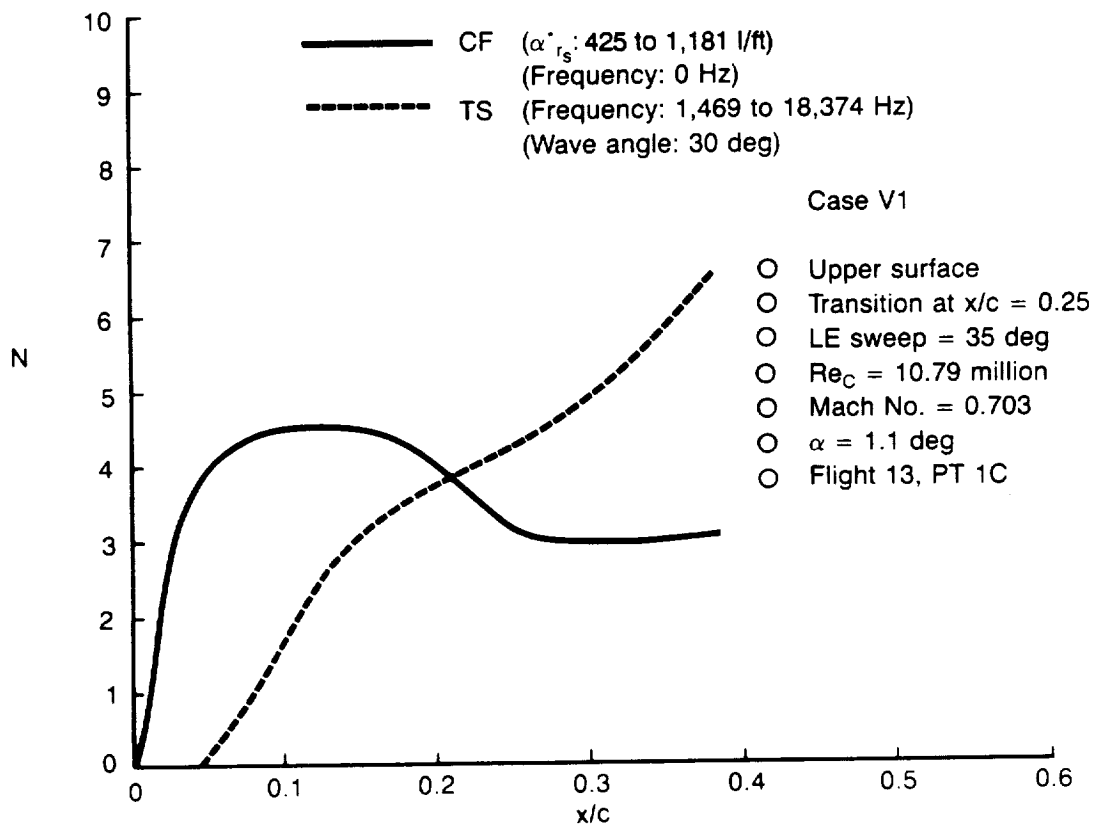
(b) Compressible Stability

Figure A3. — Pressure Distribution and Compressible Stability Results for Case V1
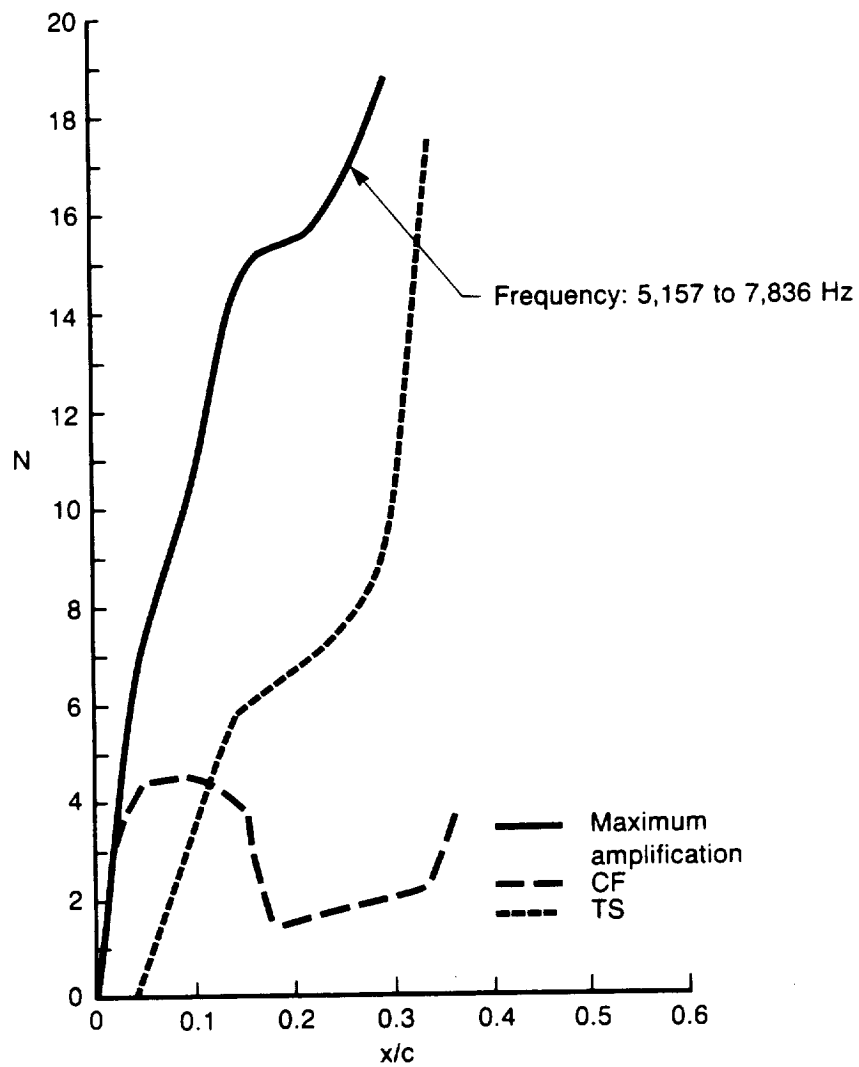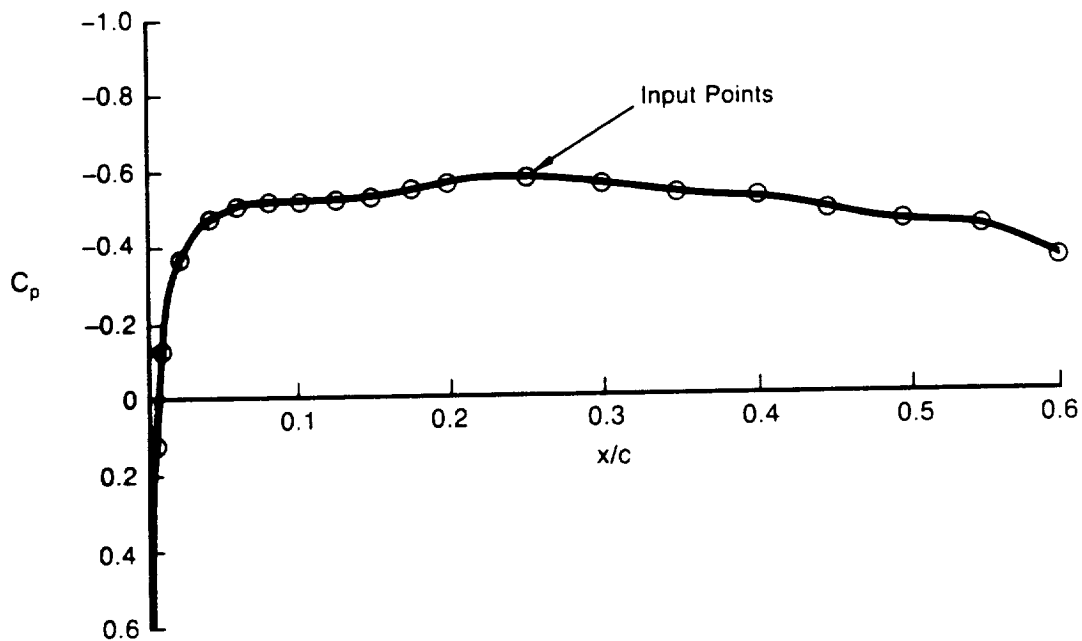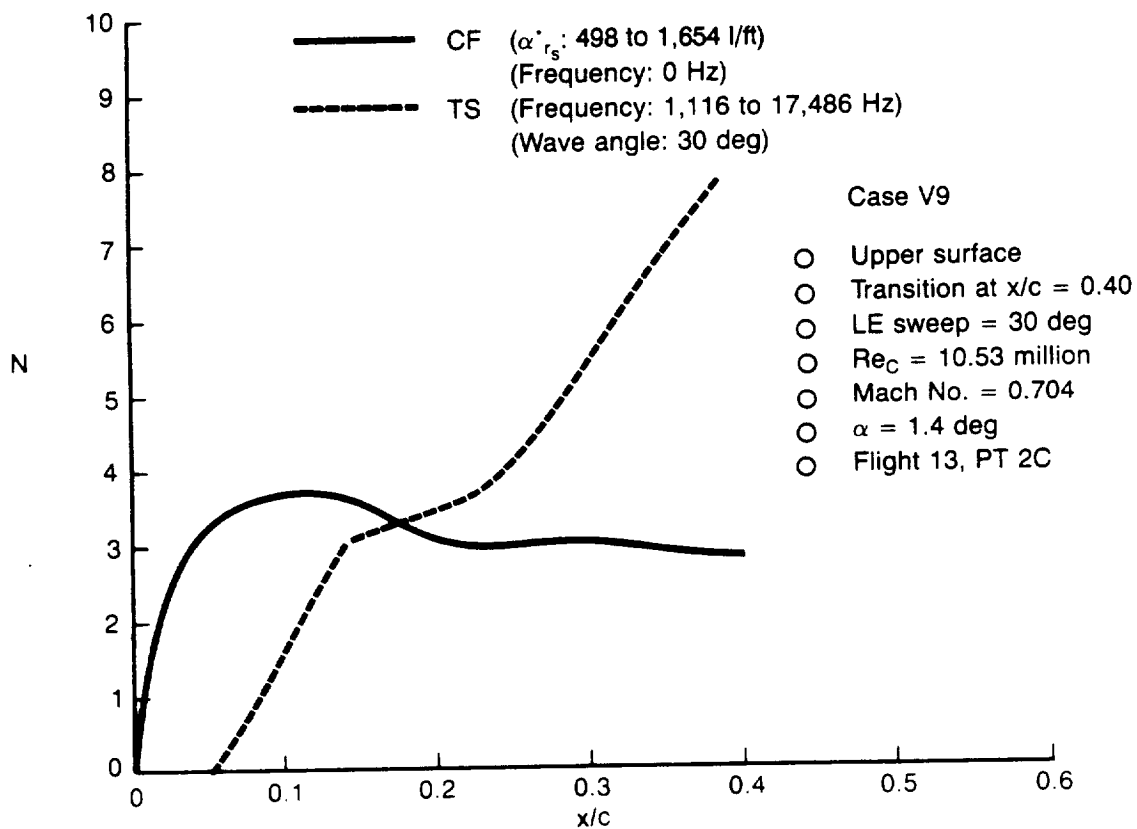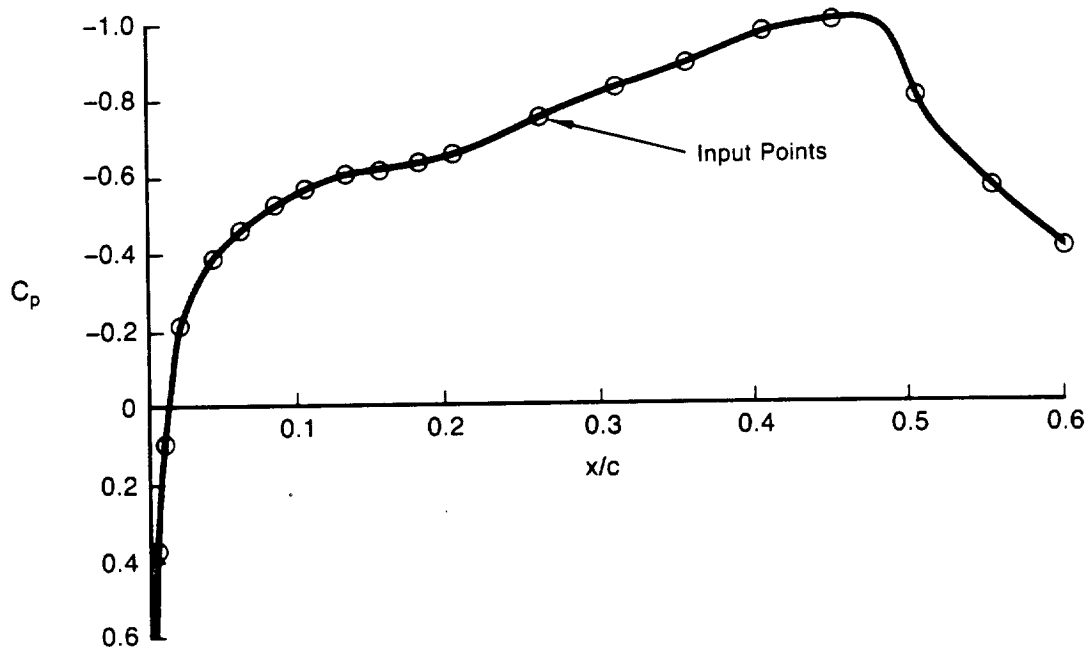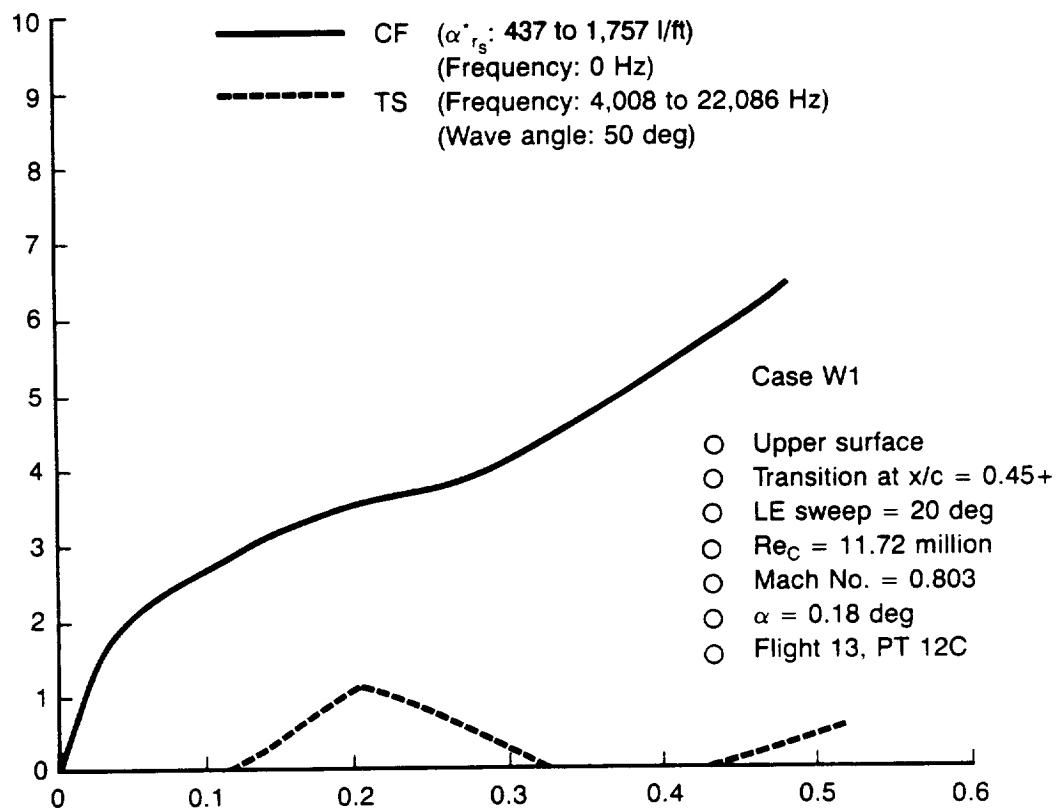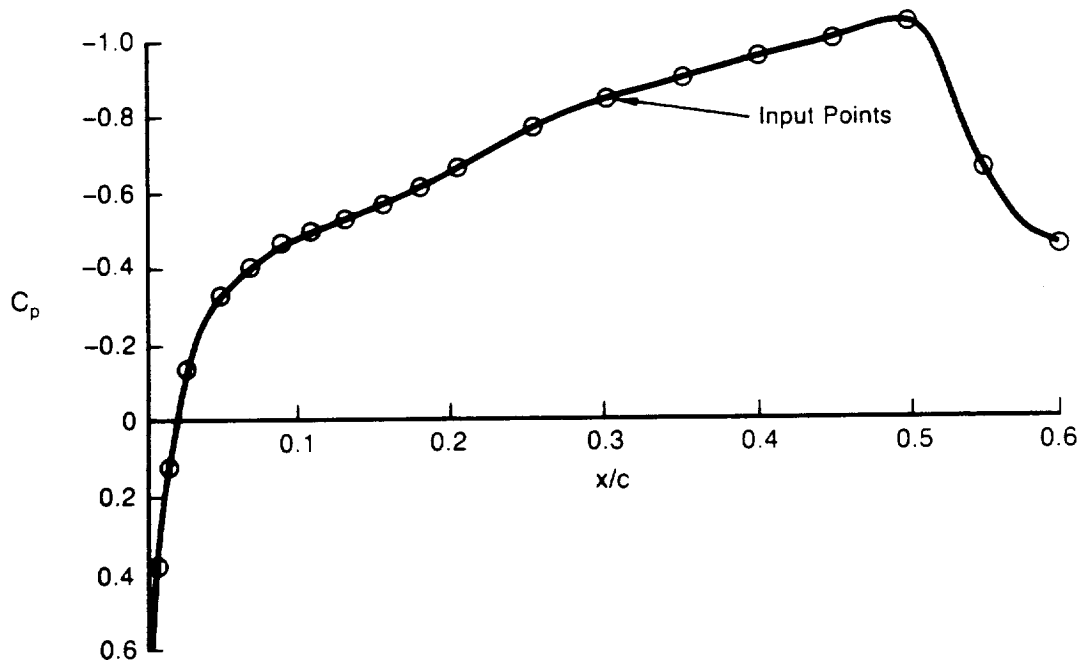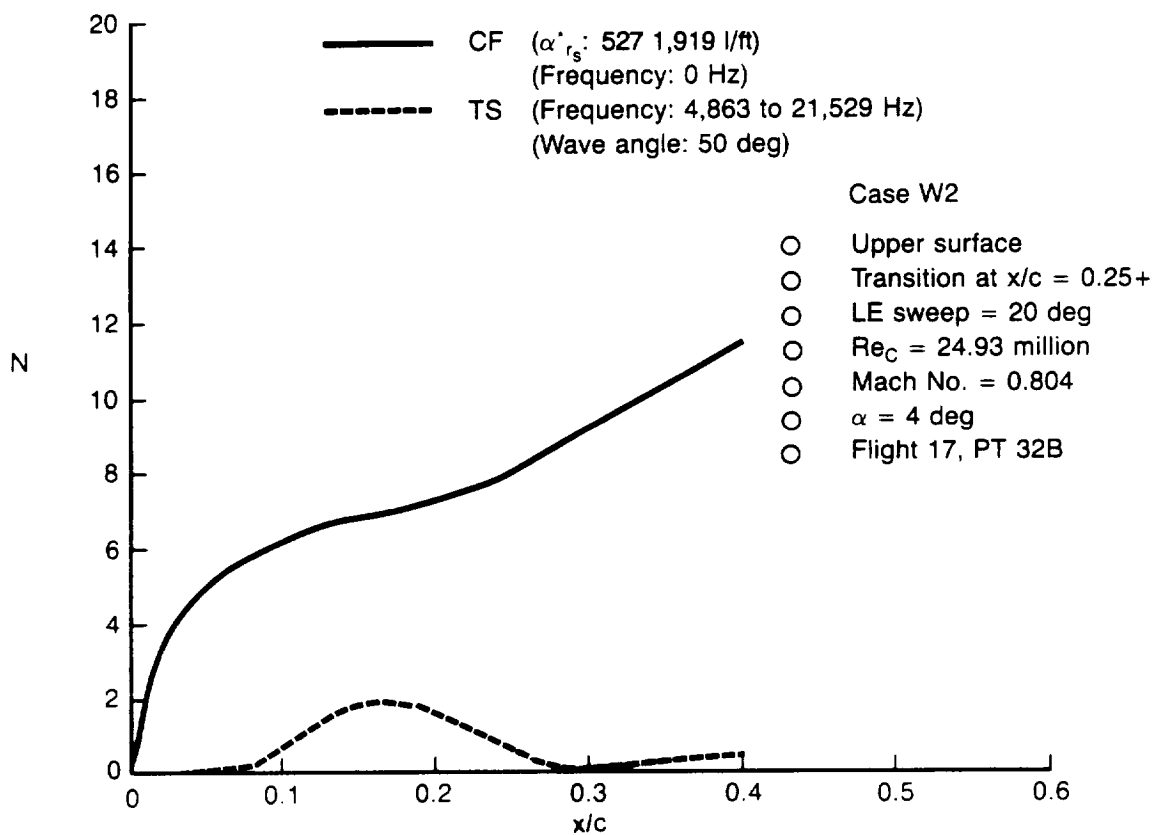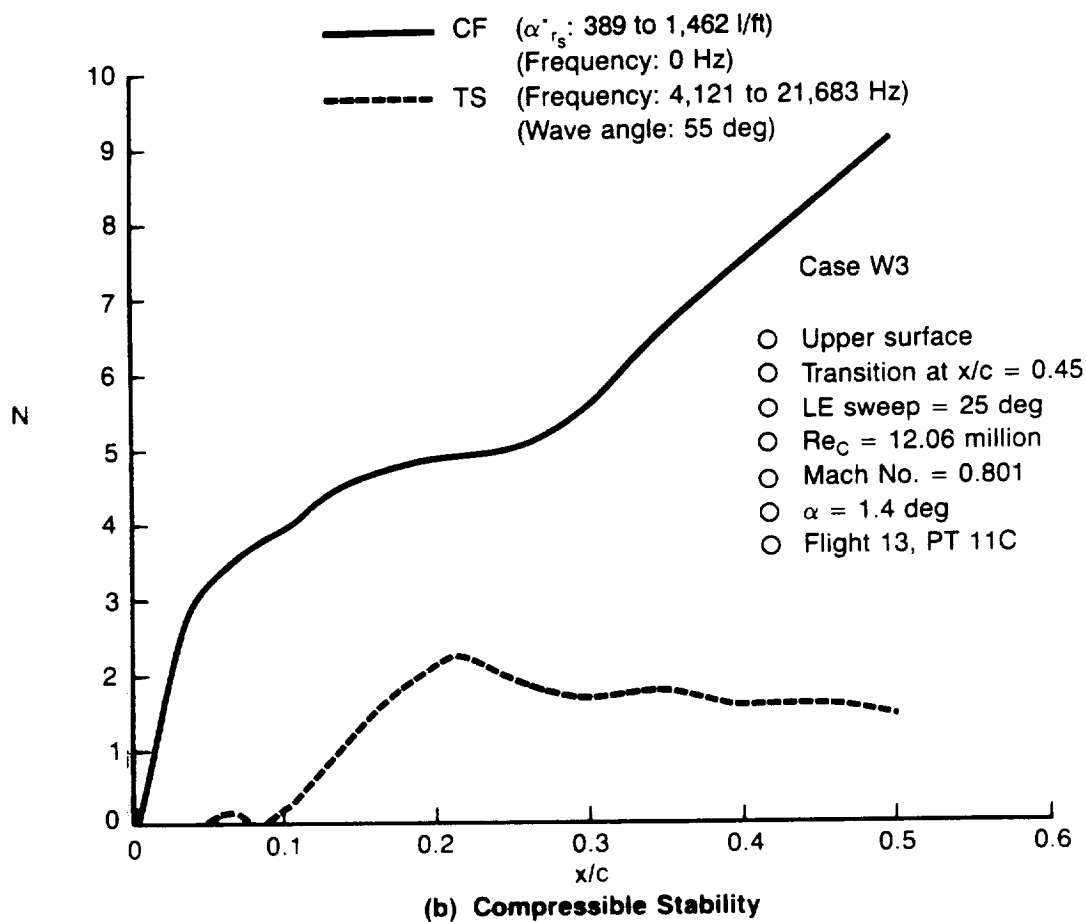
(a) Pressure Distribution

CF ($\alpha^{\cdot}_{r_s}$: 778 to 2,018 l/ft)
(Frequency: 0 Hz)
TS (Frequency: 4,504 to 31,212 Hz)
(Wave angle: 25 deg)

Case V2

O   Upper surface
O   Transition at x/c = 0.25+
O   LE sweep = 24 deg
O   Re$_C$ = 25.88 million
O   Mach No. = 0.603
O α = 0.5 deg
O   Flight 17, PT 46A3
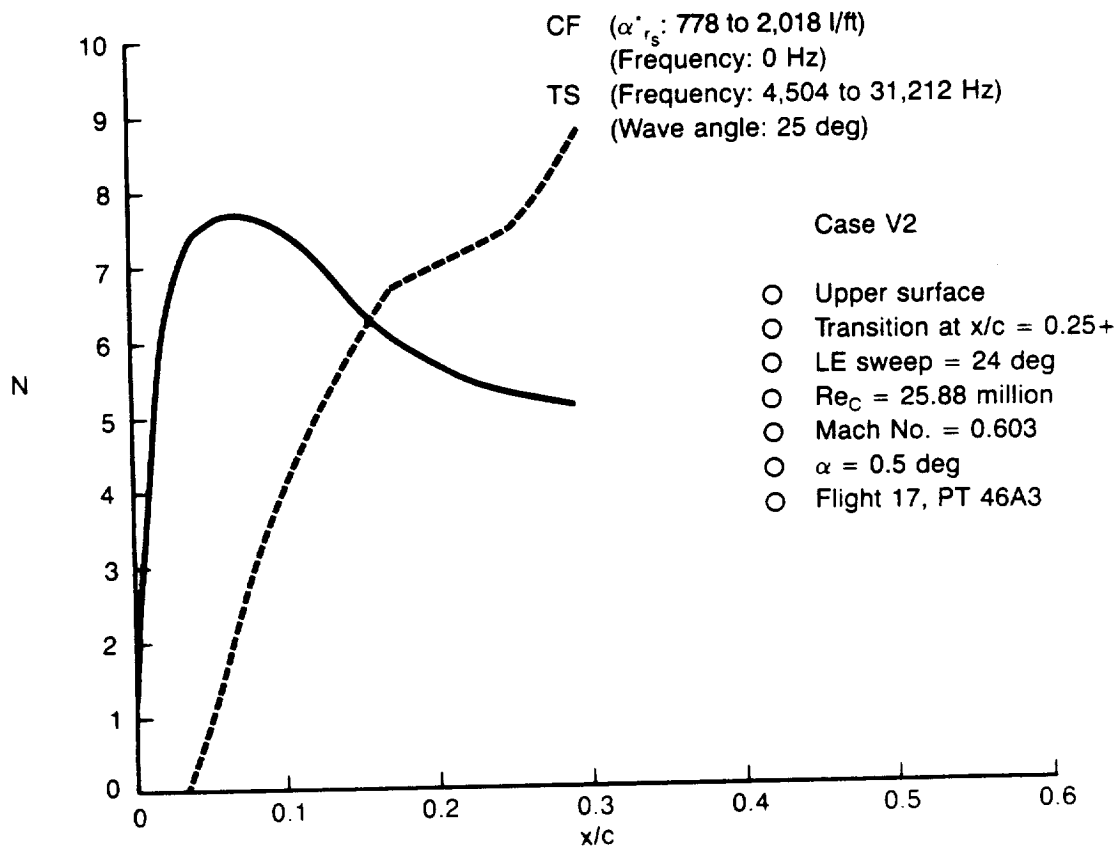
(b) Compressible Stability

Figure A4. — Pressure Distribution and Compressible Stability Results for Case V2
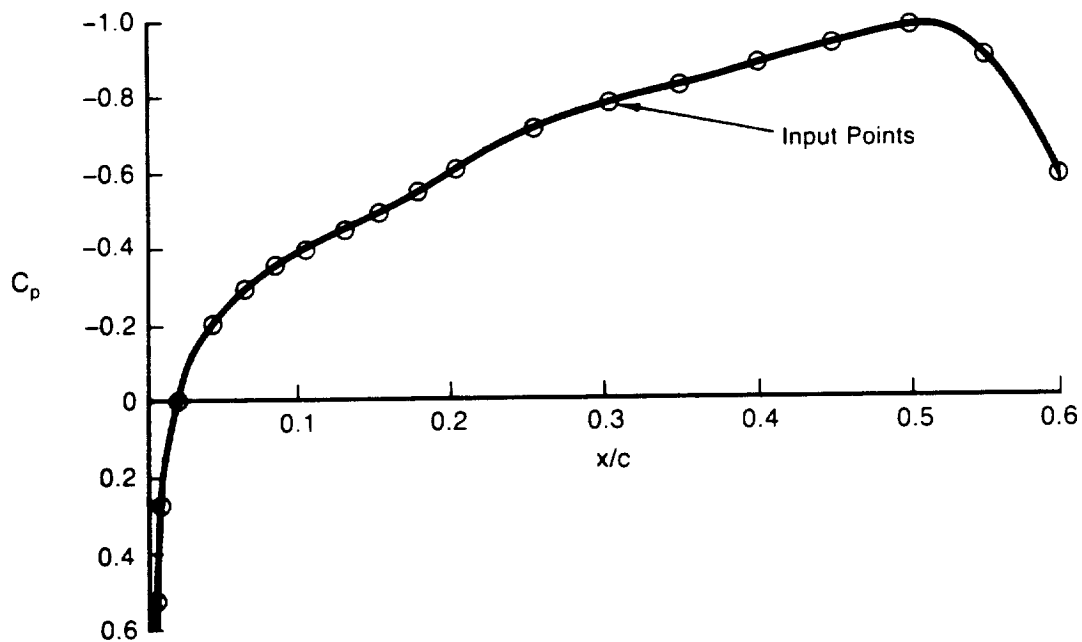
(a) Pressure Distribution
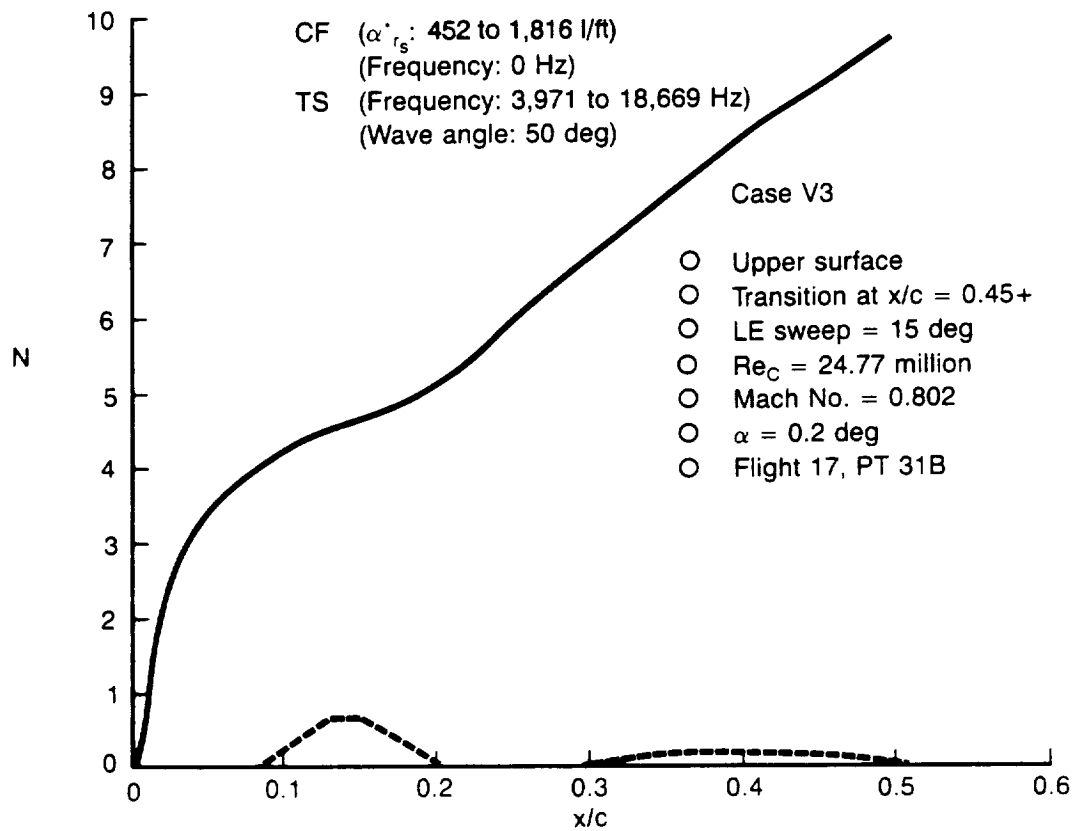
(b) Compressible Stability

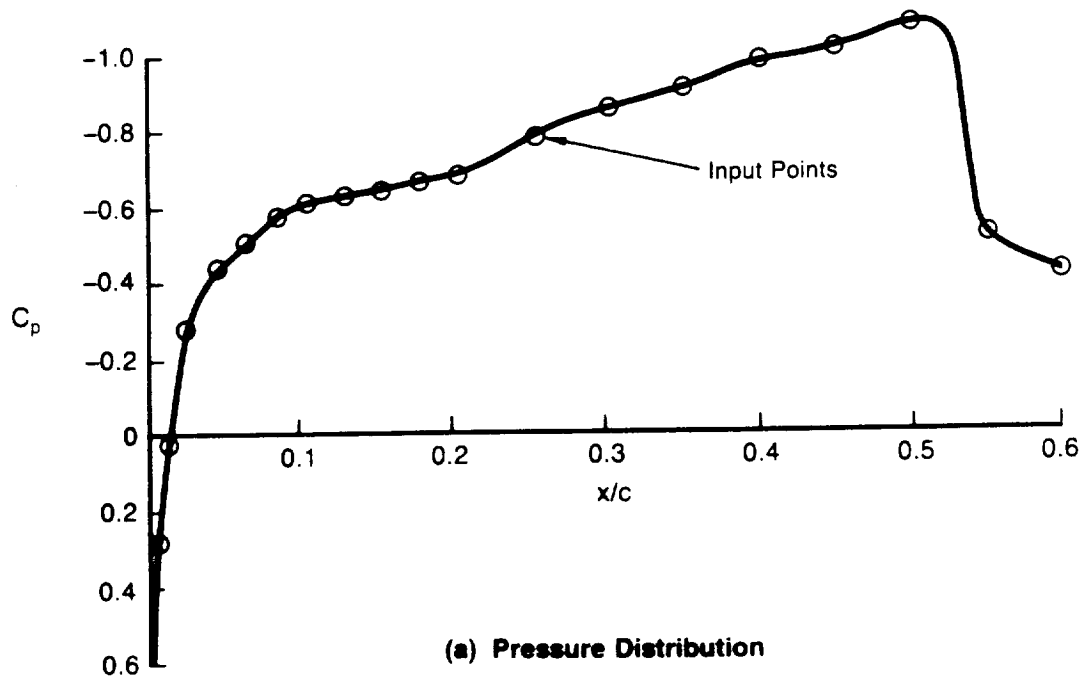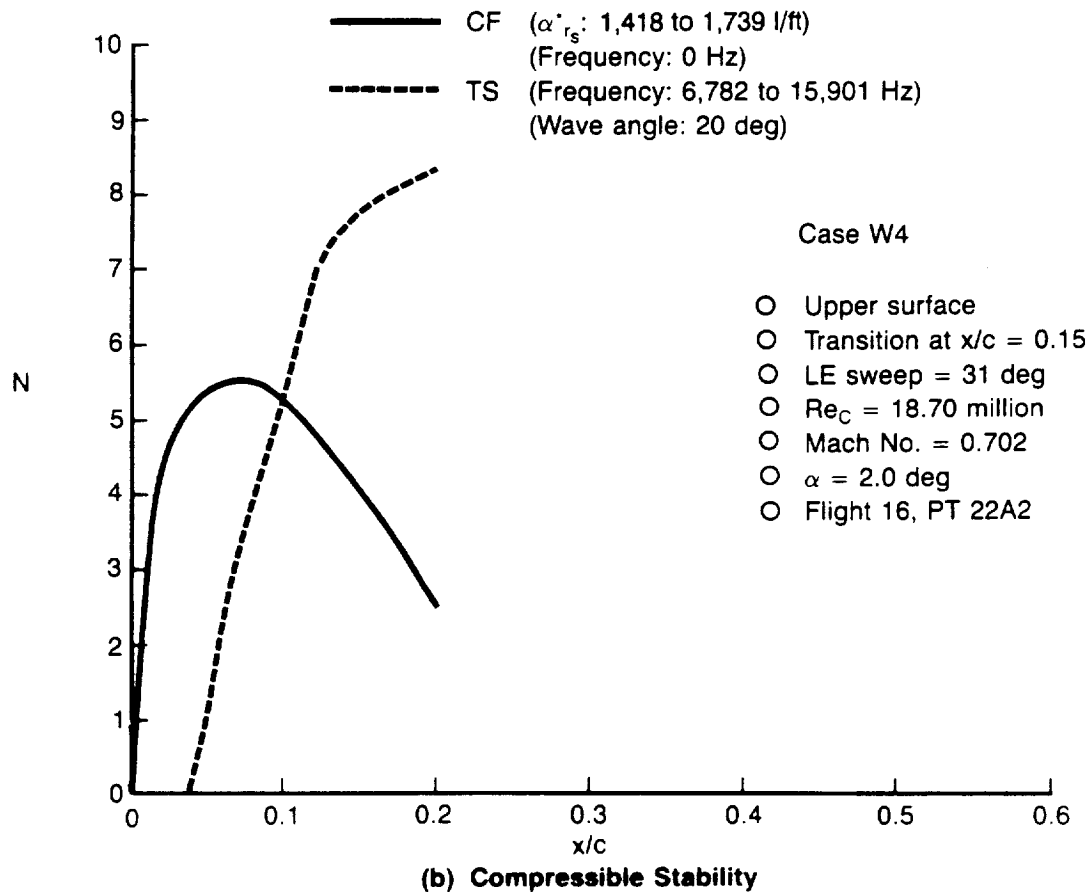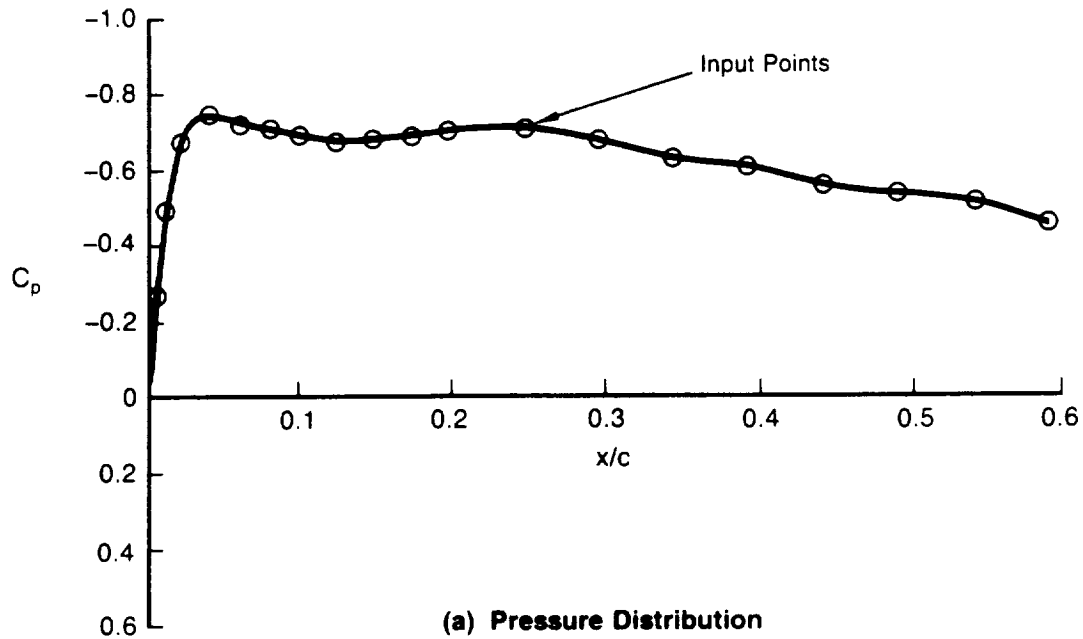*Figure A5. — Pressure Distribution and Compressible Stability Results for Case V3*
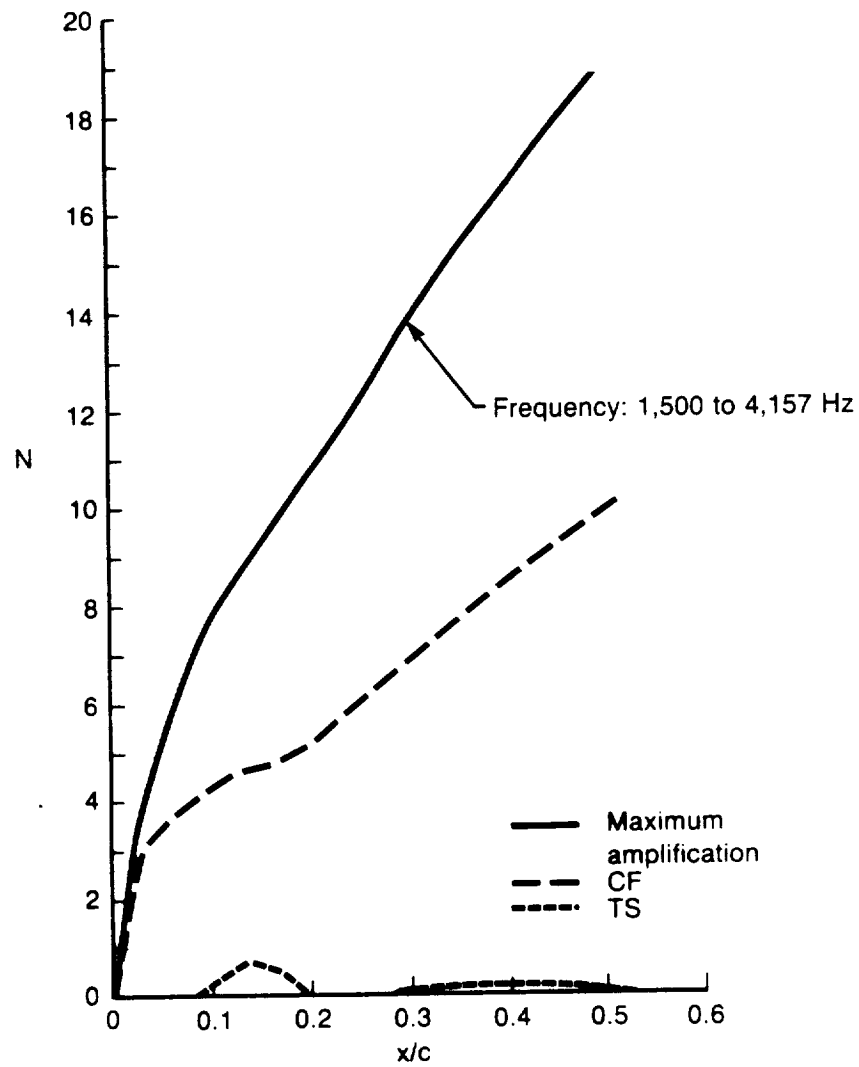
Figure A6. — Compressible Stability Results for Case V3 Including Maximum Amplification Method
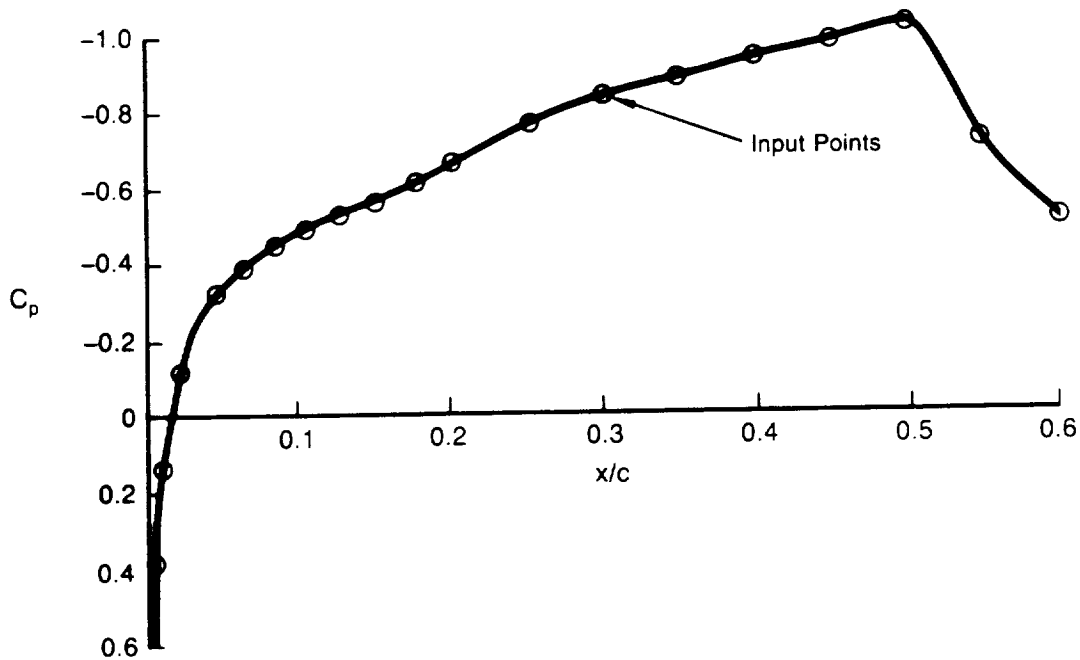
(a) Pressure Distribution
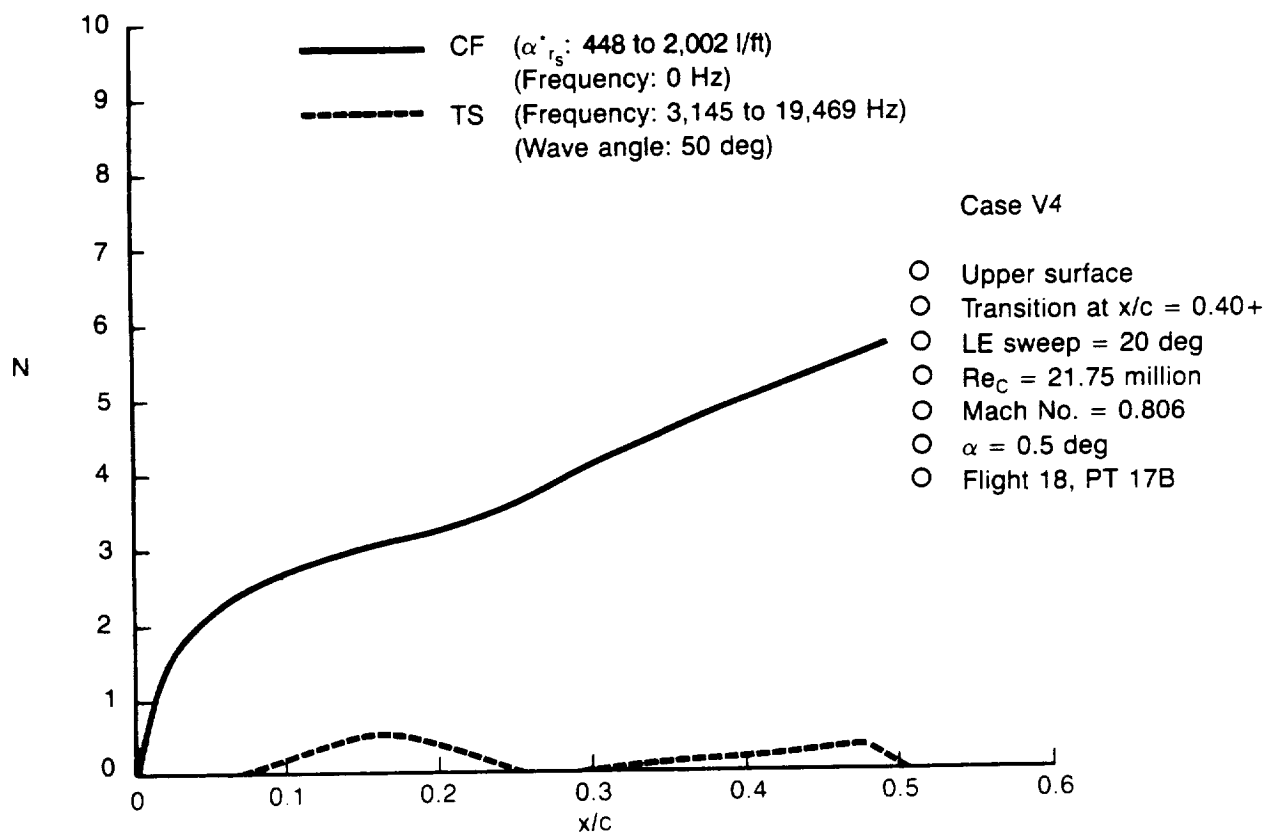
(b) Compressible Stability

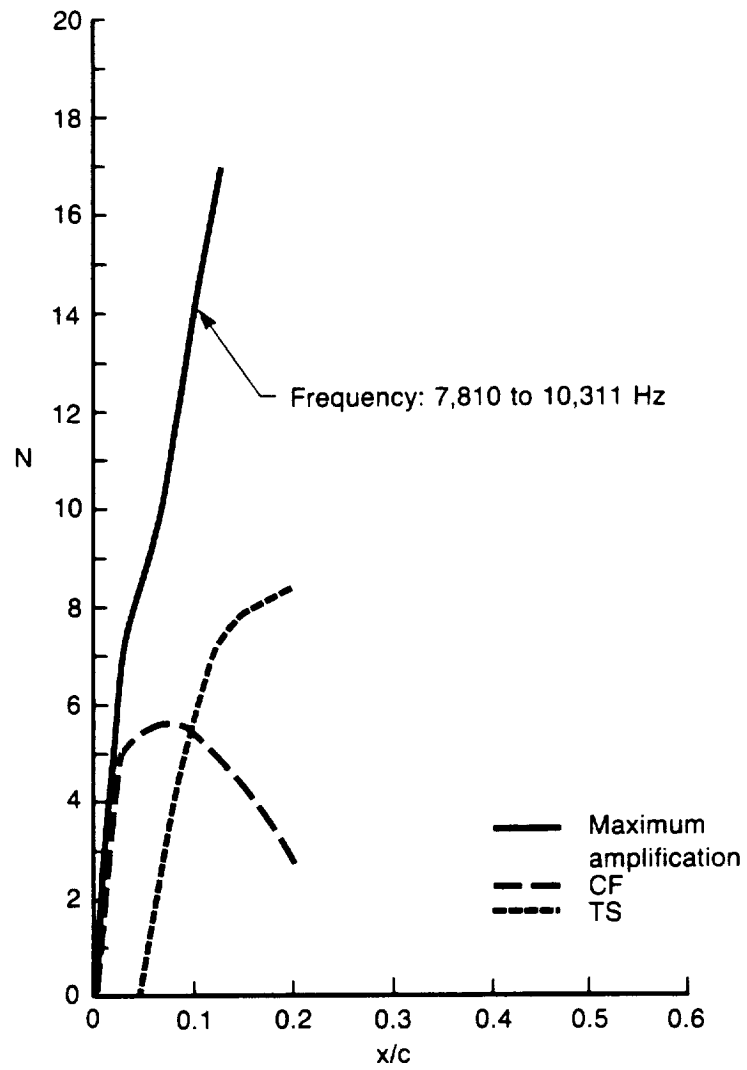Figure A7. — *Pressure Distribution and Compressible Stability Results for Case V4*

(a) **Pressure Distribution**

(b) **Compressible Stability**

CF (α'_{r_s}: 369 to 1,454 l/ft)
(Frequency: 0 Hz)

TS (Frequency: 3,781 to 21,652 Hz)
(Wave angle: 50 deg)

Case V5

O Upper surface
O Transition at x/c = 0.40+
O LE sweep = 30 deg
O Re_C = 12.23 million
O Mach No. = 0.802
O α = 0.81 deg
O Flight 12, PT 22A
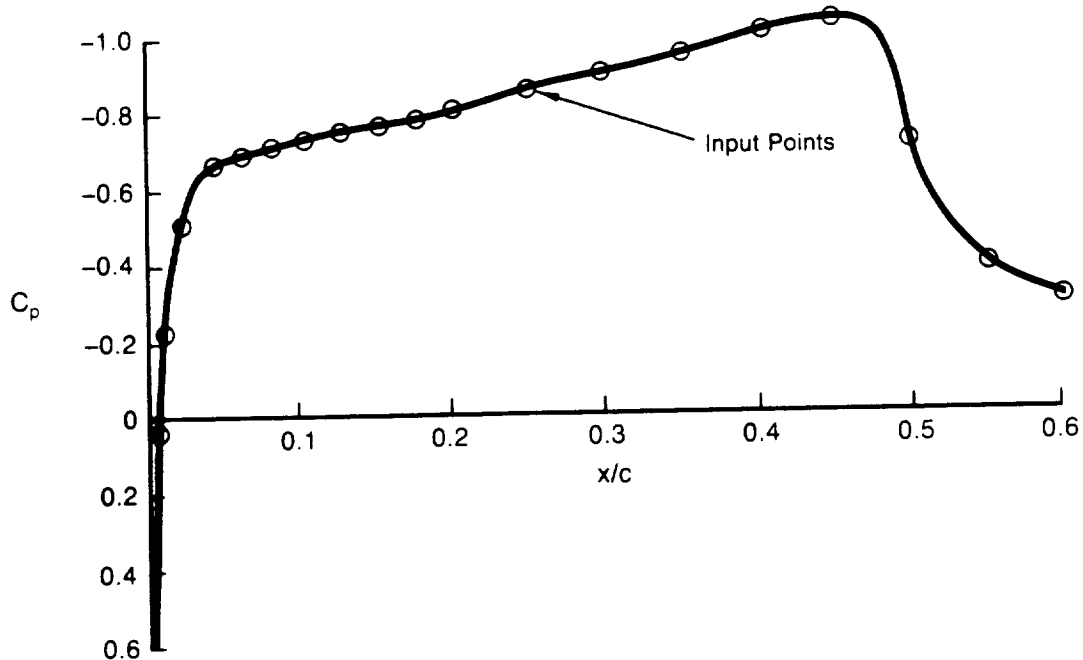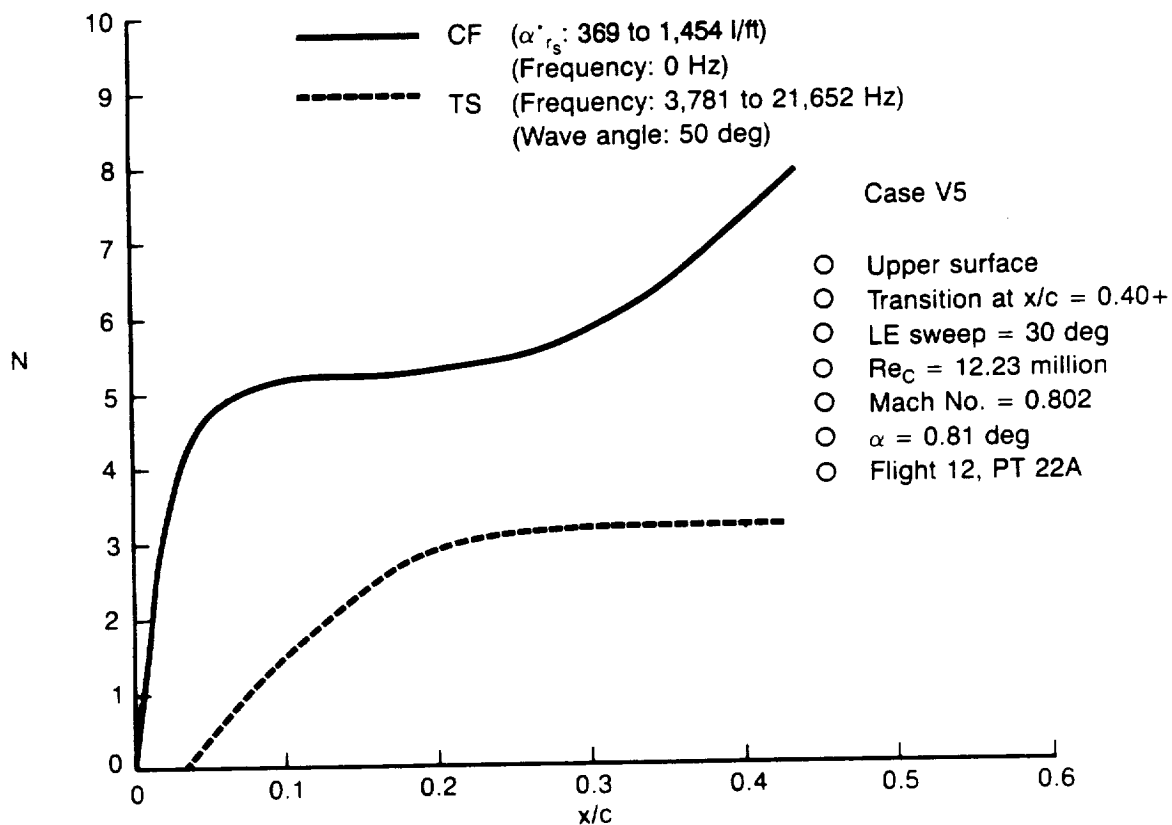
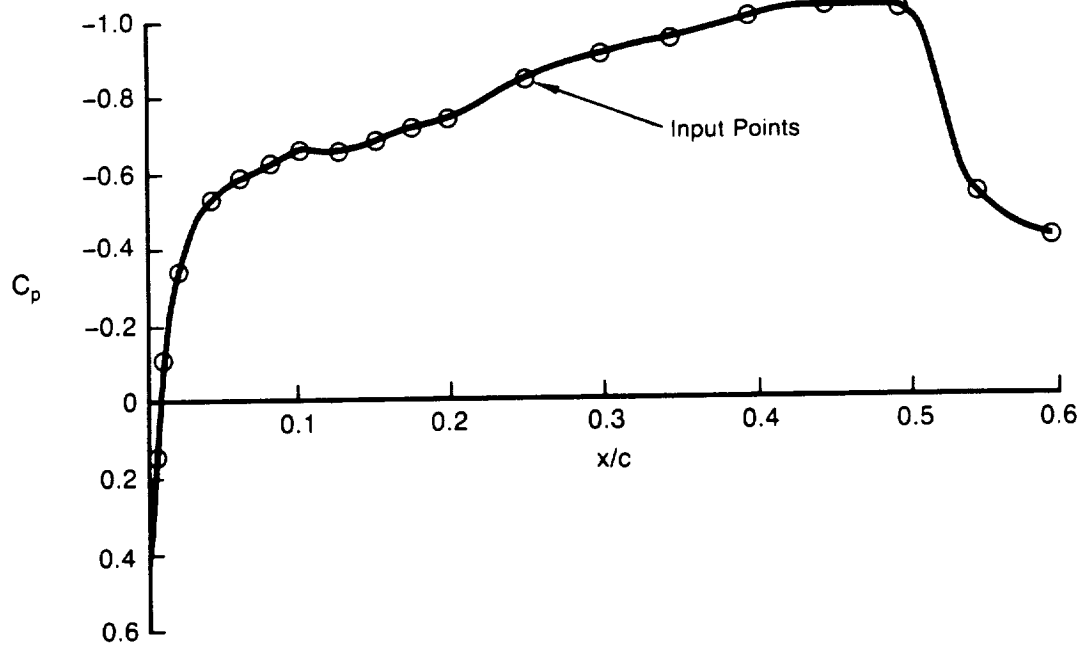*Figure A8. — Pressure Distribution and Compressible Stability Results for Case V5*

(a) **Pressure Distribution**

CF ($\alpha^*_{r_s}$: 638 to 2,350 l/ft)
    (Frequency: 0 Hz)

TS (Frequency: 4,502 to 23,270 Hz)
    (Wave angle: 40 deg)

Case V6

O Upper surface
O Transition at x/c = 0.40
O LE sweep = 15 deg
O Re_C = 30.84 million
O Mach No. = 0.702
O α = 0.2 deg
O Flight 17, PT 41B

(b) **Compressible Stability**
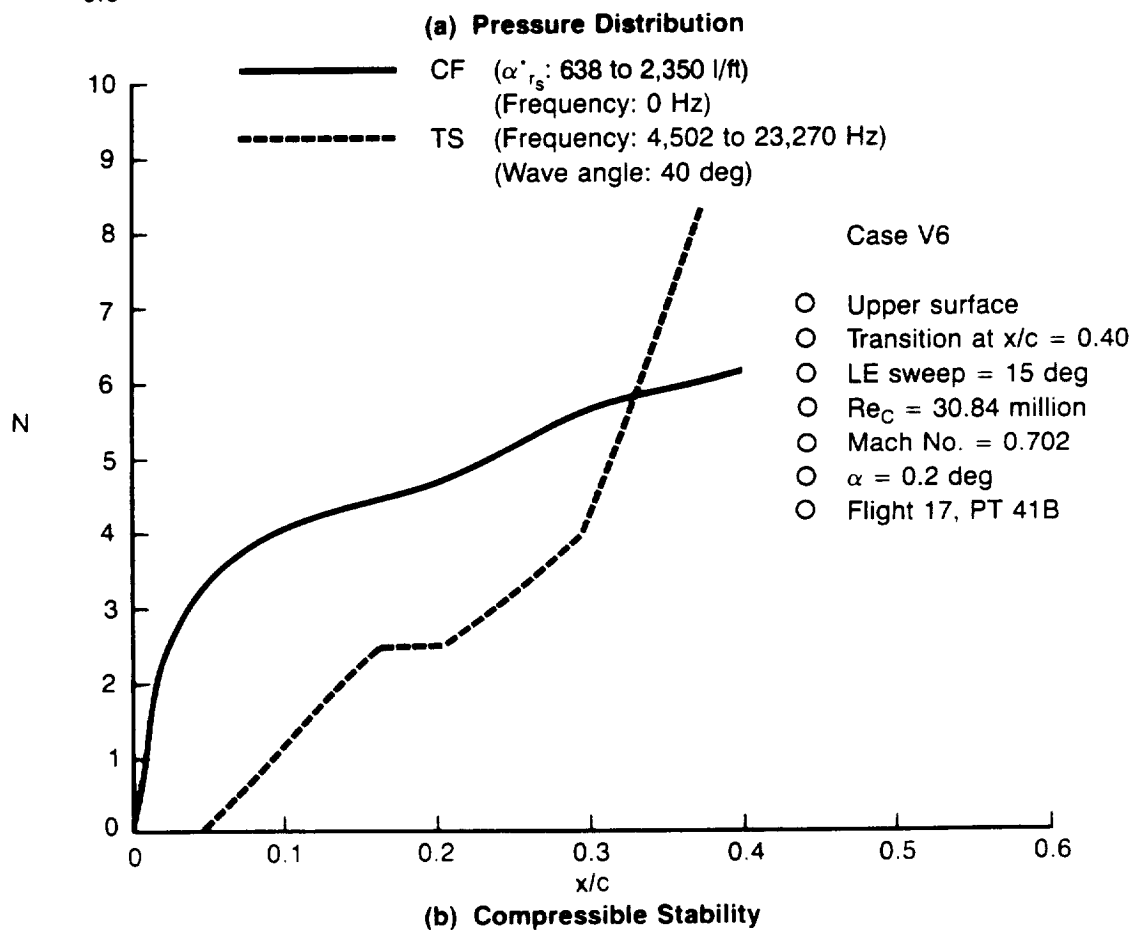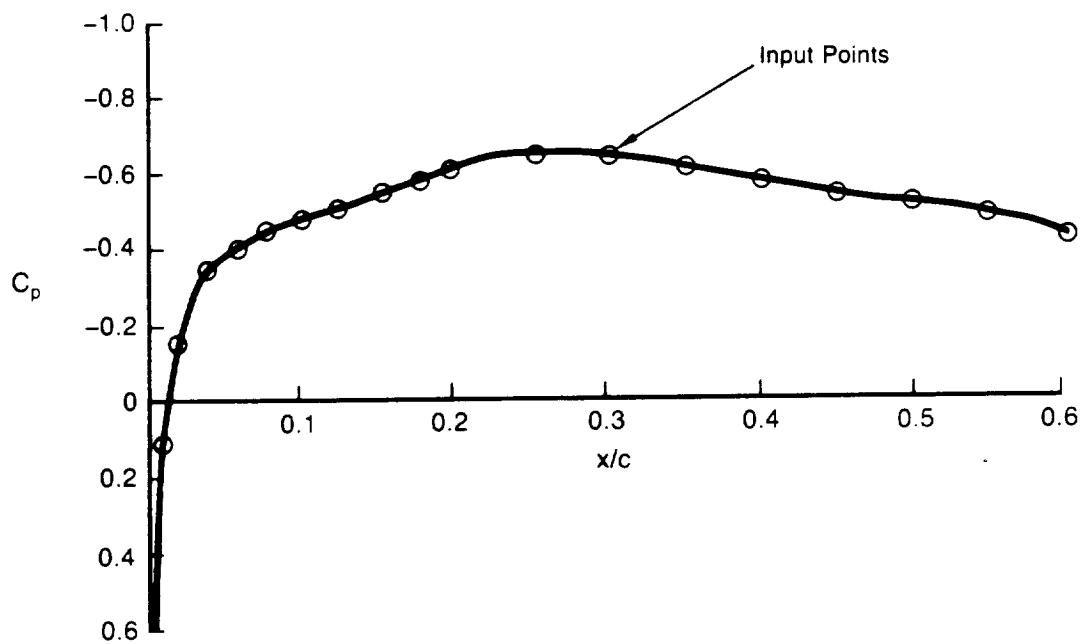
Figure A9. — *Pressure Distribution and Compressible Stability Results for Case V6*
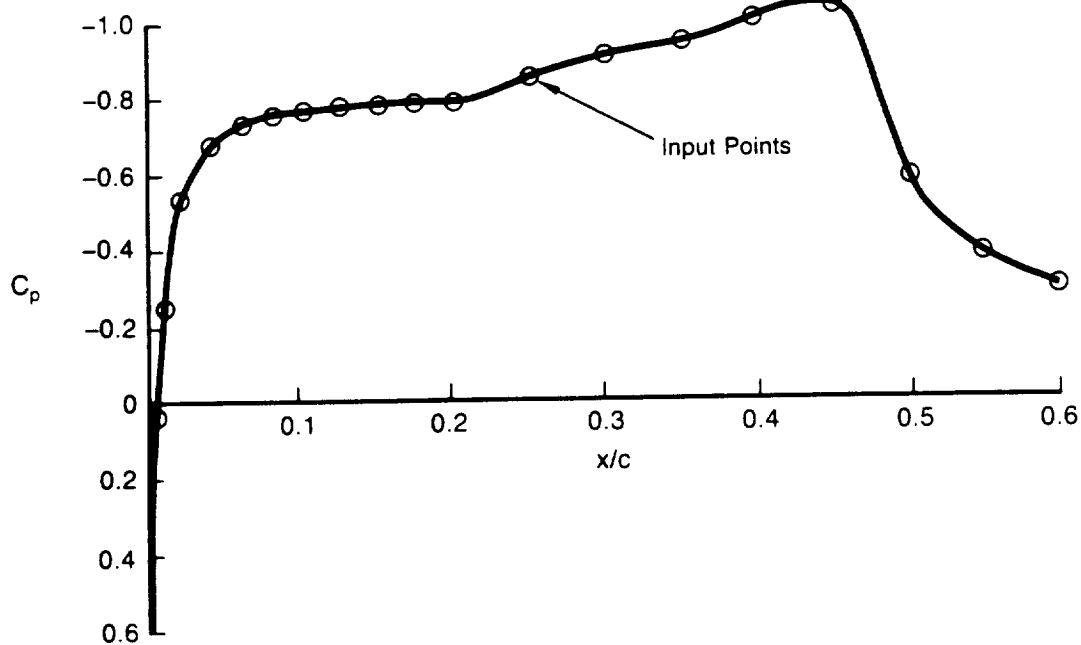
(a) Pressure Distribution
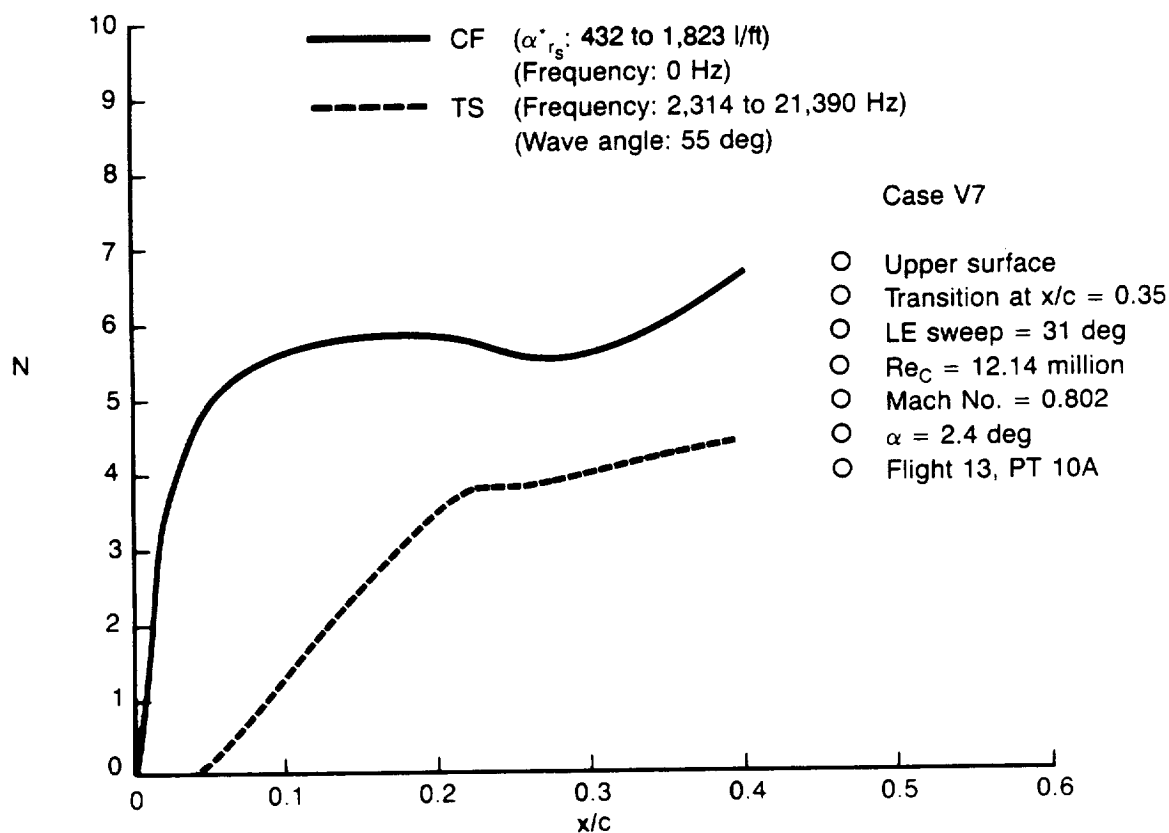
(b) Compressible Stability

Figure A10. — Pressure Distribution and Compressible Stability Results for Case V7
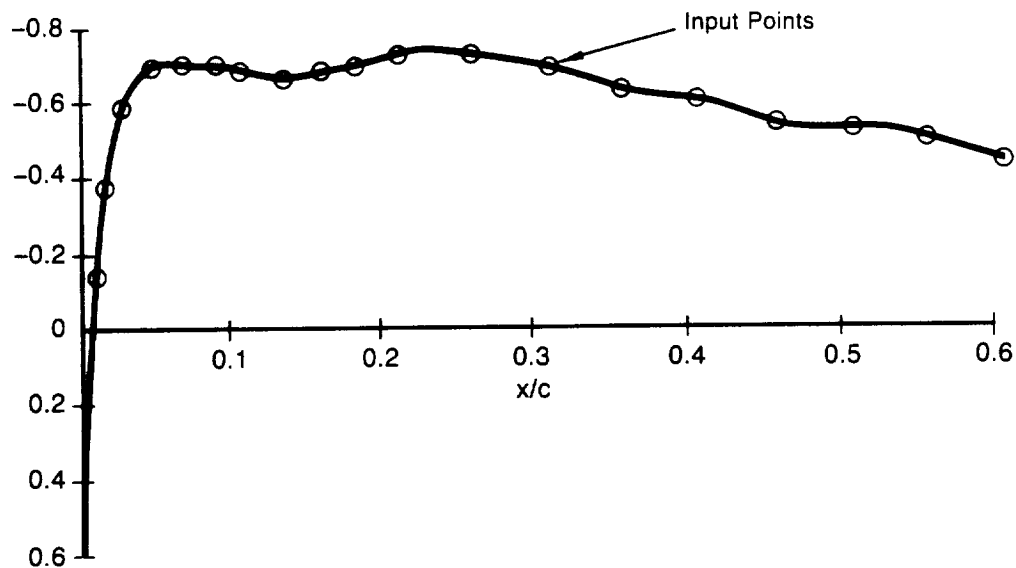
(a) Pressure Distribution
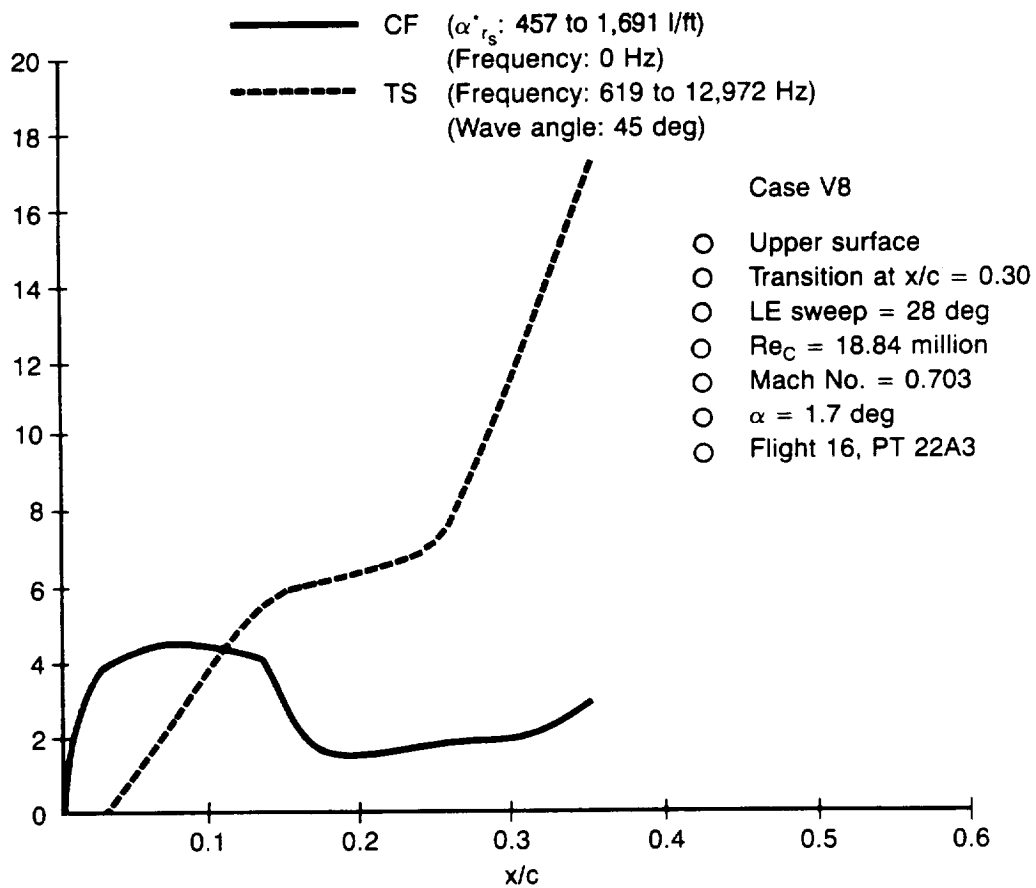
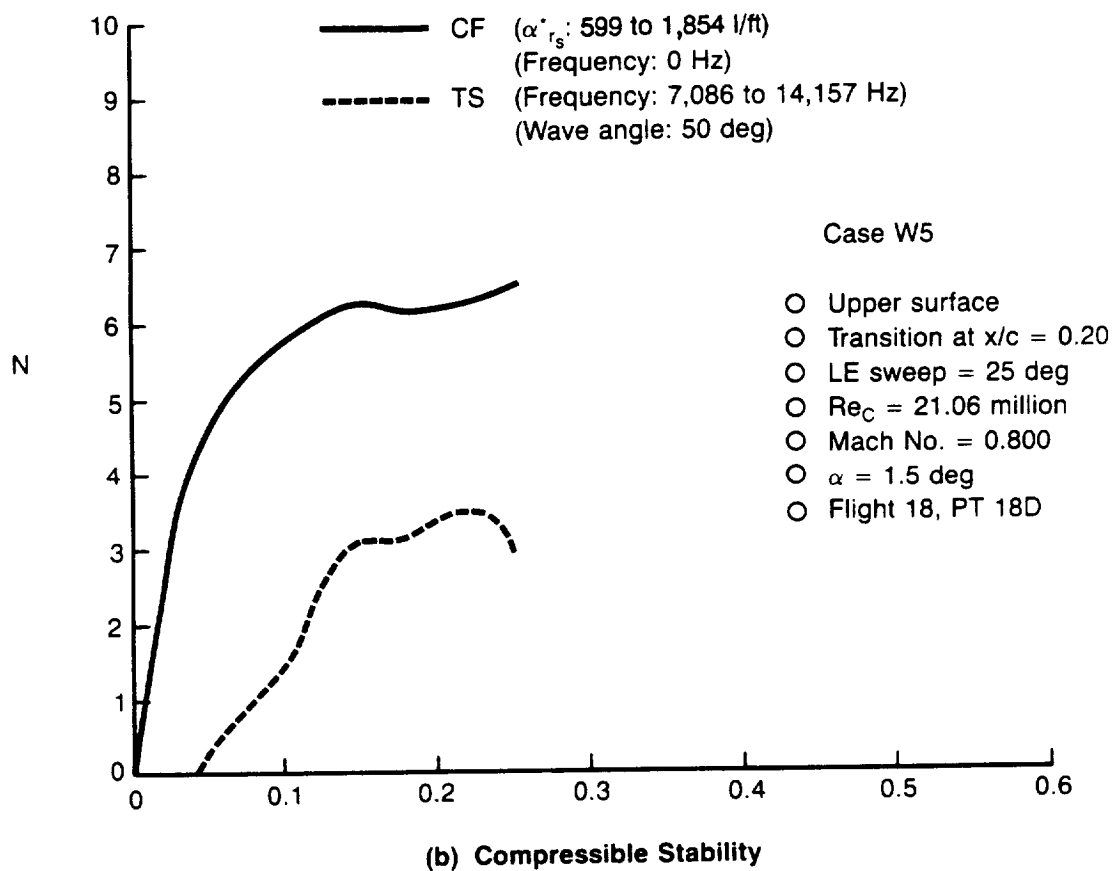**(b) Compressible Stability**

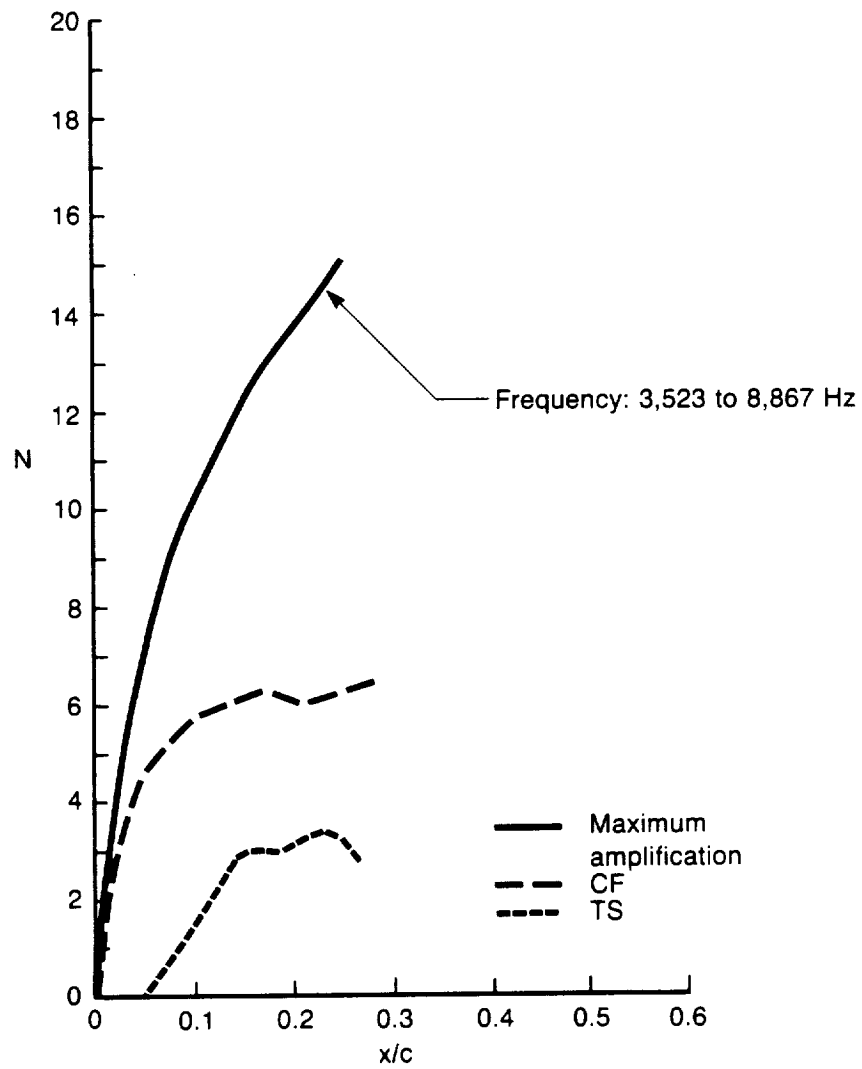*Figure A11. — Pressure Distribution and Compressible Stability Results for Case V8*

Figure A12. — *Compressible Stability Results for Case V8 Including the Maximum Amplification Method*
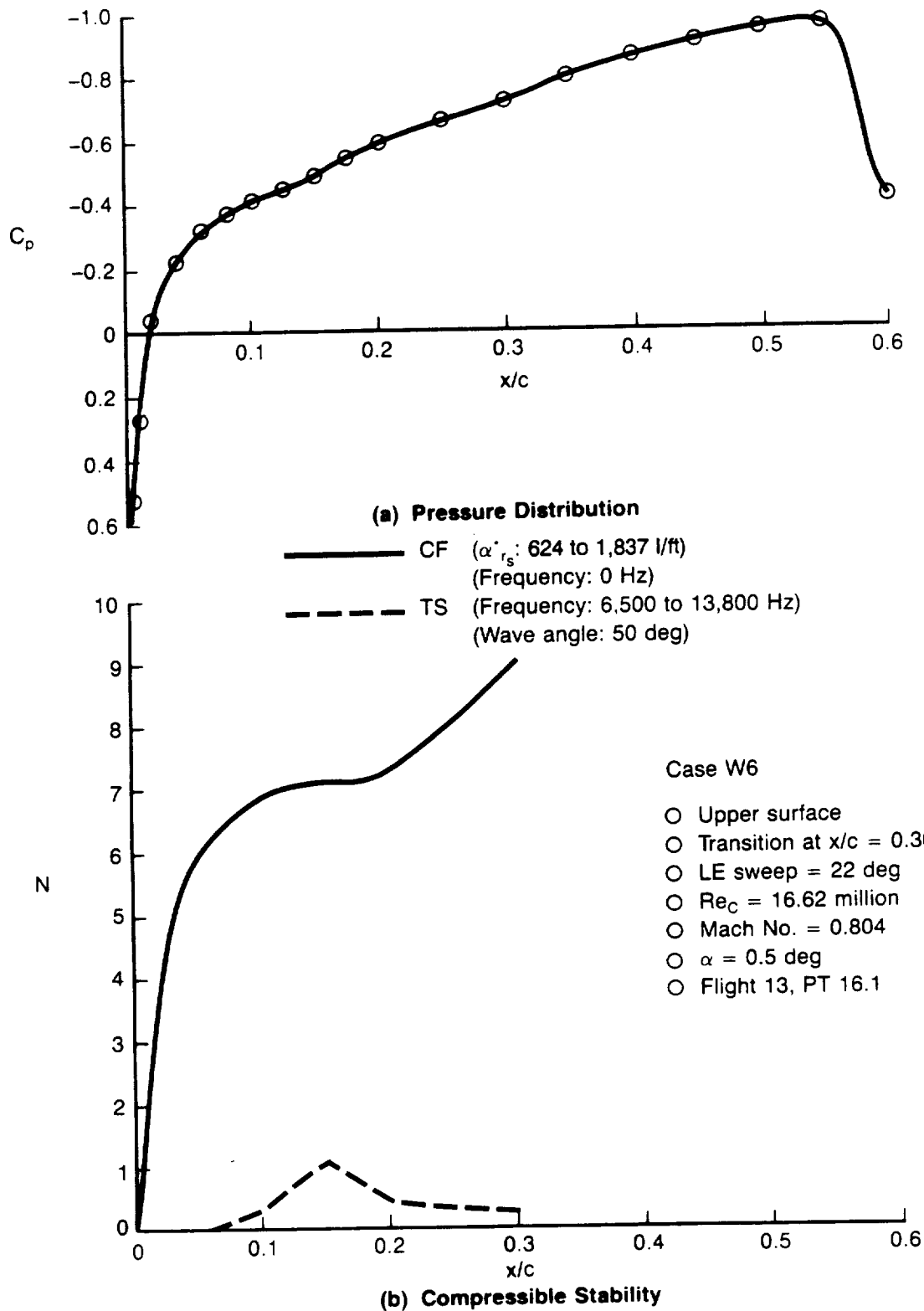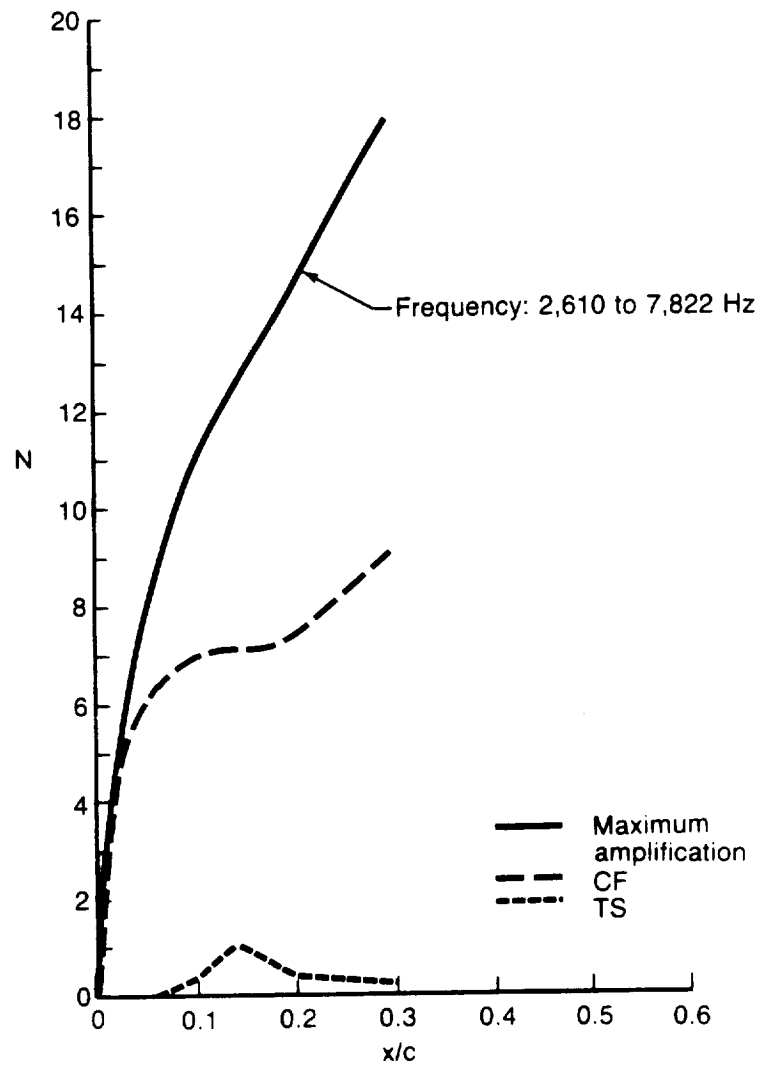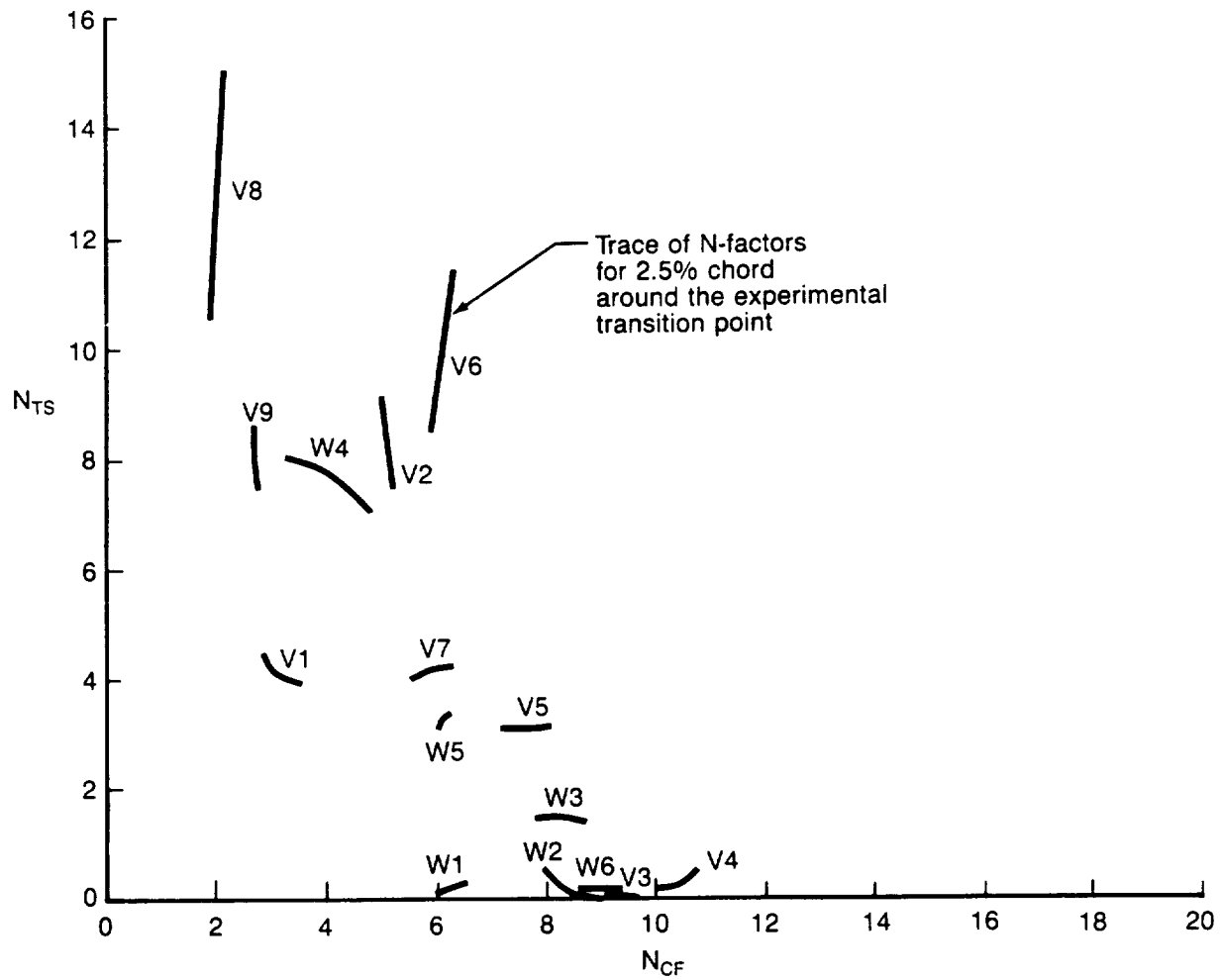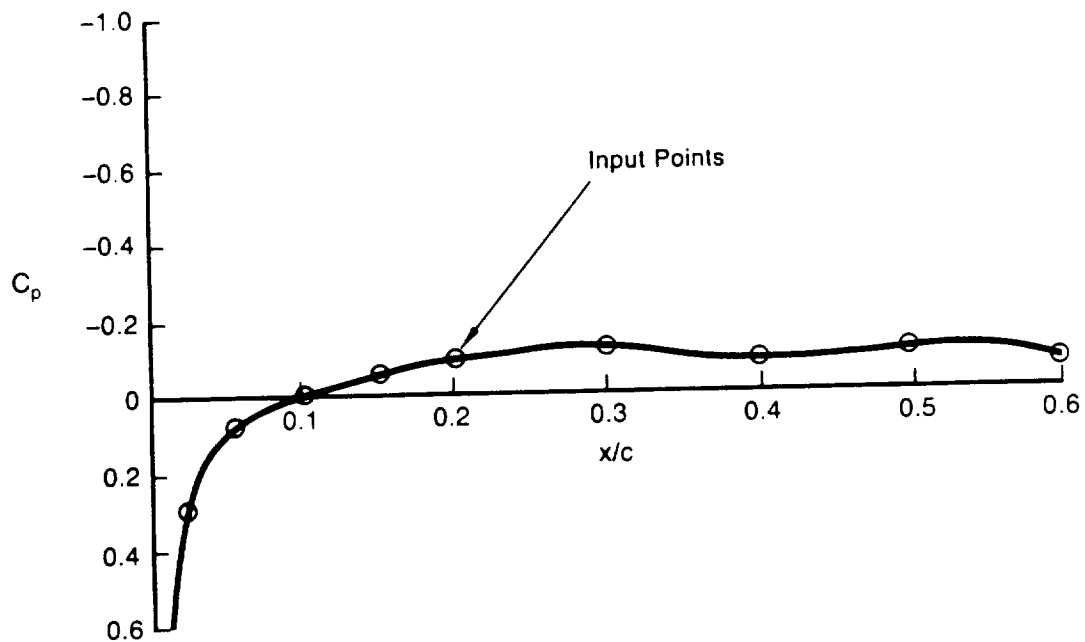
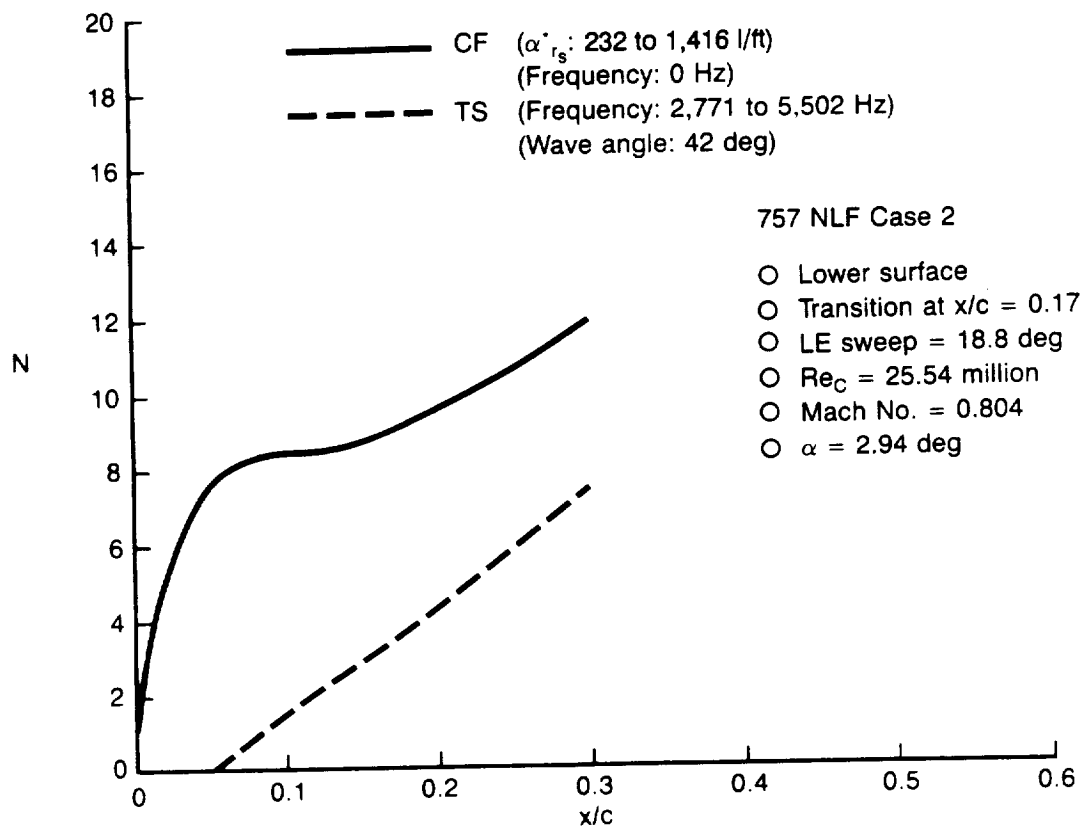**(a) Pressure Distribution**

(b) Compressible Stability

Figure A13. — Pressure Distribution and Compressible Stability Results for Case V9

(a) Pressure Distribution

CF $(\alpha^{\cdot}{}_{r_s}$: **437 to 1,757 l/ft)**
(Frequency: 0 Hz)

TS (Frequency: 4,008 to 22,086 Hz)
(Wave angle: 50 deg)

Case W1

○ Upper surface
○ Transition at x/c = 0.45+
○ LE sweep = 20 deg
○ Re$_C$ = 11.72 million
○ Mach No. = 0.803
○ α = 0.18 deg
○ Flight 13, PT 12C

(b) Compressible Stability

Figure A14. — Pressure Distribution and Compressible Stability Results for Case W1

90

(a) Pressure Distribution

(b) Compressible Stability

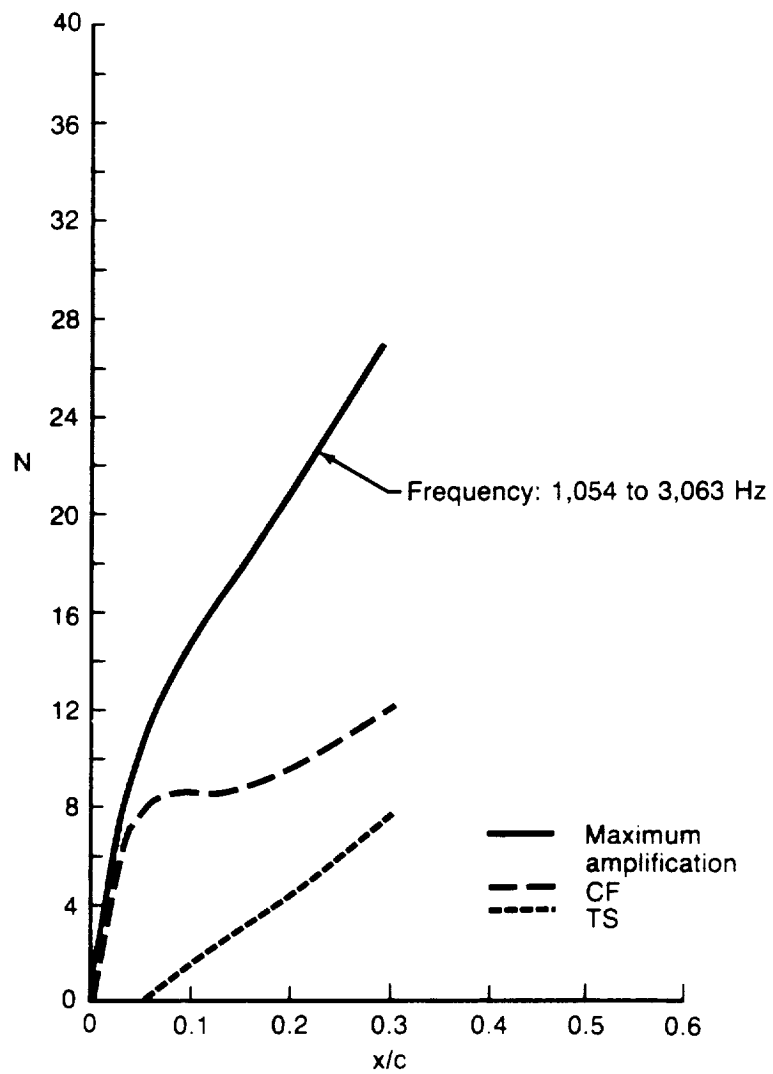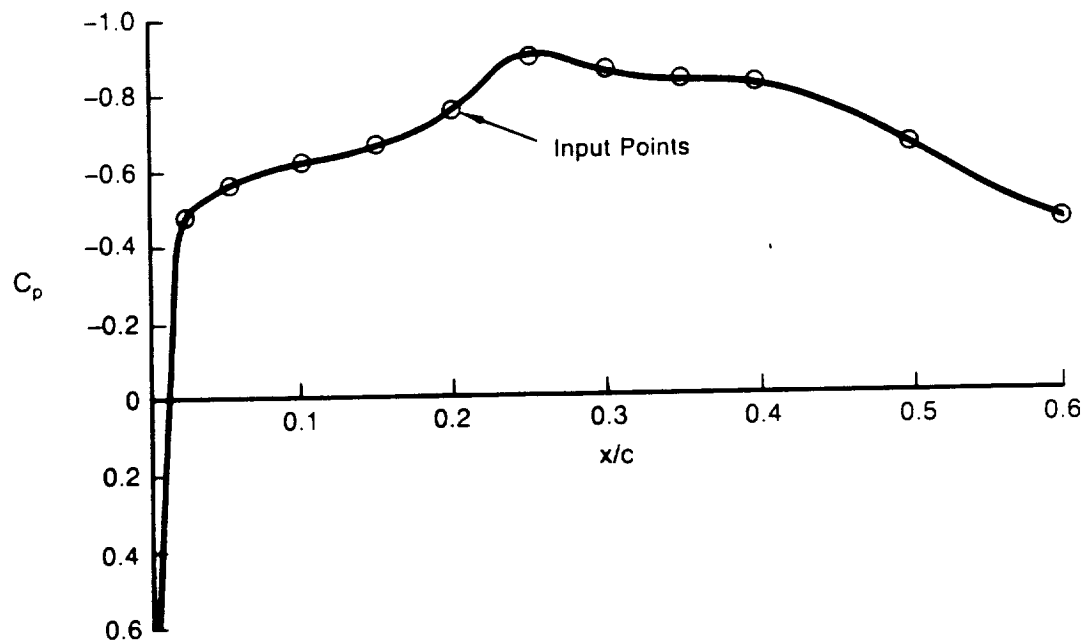Figure A15. — Pressure Distribution and Compressible Stability Results for Case W2

(a) Pressure Distribution

CF ($\alpha^*_{r_s}$: 389 to 1,462 l/ft)
(Frequency: 0 Hz)

TS (Frequency: 4,121 to 21,683 Hz)
(Wave angle: 55 deg)

Case W3

O Upper surface
O Transition at x/c = 0.45
O LE sweep = 25 deg
O Re_C = 12.06 million
O Mach No. = 0.801
O α = 1.4 deg
O Flight 13, PT 11C

(b) Compressible Stability

Figure A16. — Pressure Distribution and Compressible Stability Results for Case W3

(a) **Pressure Distribution**

(b) **Compressible Stability**

CF ($\alpha^*_{r_s}$: 1,418 to 1,739 l/ft)
(Frequency: 0 Hz)

TS (Frequency: 6,782 to 15,901 Hz)
(Wave angle: 20 deg)

Case W4

O Upper surface
O Transition at x/c = 0.15
O LE sweep = 31 deg
O Re_C = 18.70 million
O Mach No. = 0.702
O α = 2.0 deg
O Flight 16, PT 22A2

Figure A17. — Pressure Distribution and Compressible Stability Results for Case W4
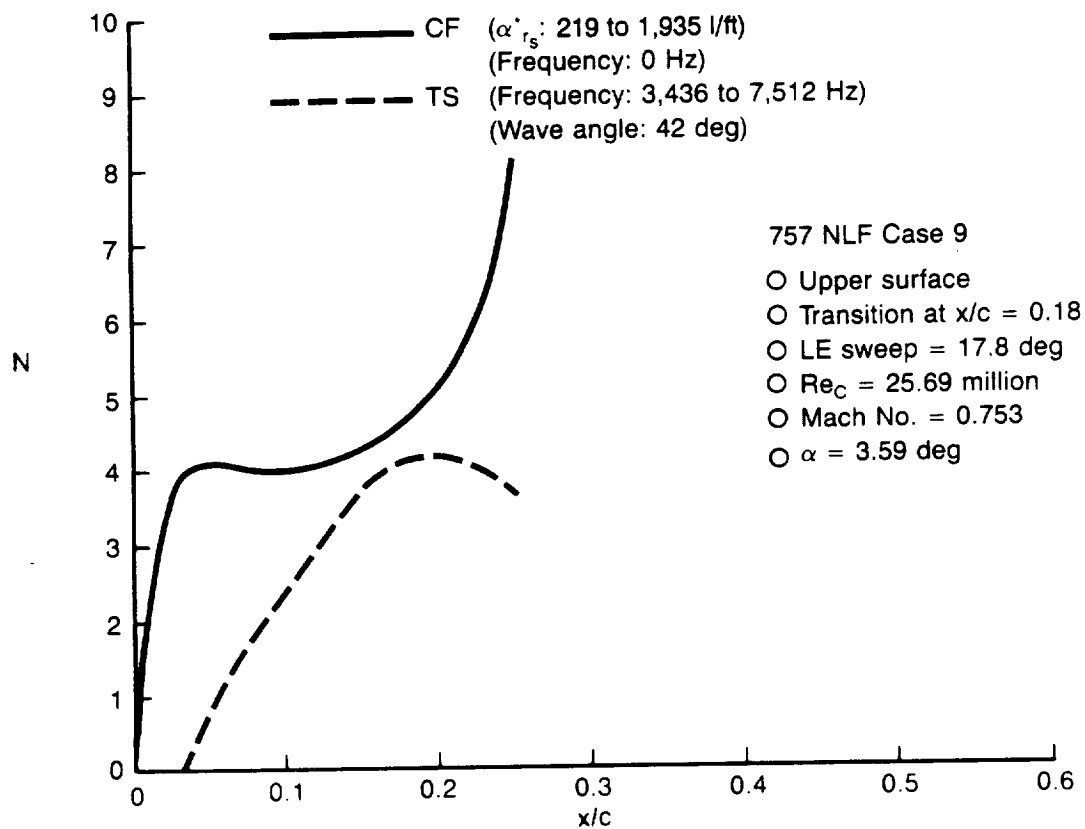
Figure A18. — *Compressible Stability Results for Case W4 Including the Maximum Amplification Method*

C-2

(a) Pressure Distribution

CF $(\alpha^*_{r_s}$: 599 to 1,854 l/ft)
(Frequency: 0 Hz)

TS (Frequency: 7,086 to 14,157 Hz)
(Wave angle: 50 deg)

Case W5

O Upper surface
O Transition at x/c = 0.20
O LE sweep = 25 deg
O Re_C = 21.06 million
O Mach No. = 0.800
O α = 1.5 deg
O Flight 18, PT 18D

(b) Compressible Stability

Figure A19. — Pressure Distribution and Compressible Stability Results for Case W5

Figure A20. — *Compressible Stability Results for Case W5 Including the Maximum Amplification Method*

(a) Pressure Distribution

————	CF	$(\alpha^{*}_{r_s}$: 624 to 1,837 l/ft) (Frequency: 0 Hz)
– – – –	TS	(Frequency: 6,500 to 13,800 Hz) (Wave angle: 50 deg)

Case W6

O Upper surface
O Transition at x/c = 0.30
O LE sweep = 22 deg
O Re_C = 16.62 million
O Mach No. = 0.804
O α = 0.5 deg
O Flight 13, PT 16.1

(b) Compressible Stability

Figure A21. — Pressure Distribution and Compressible Stability Results for Case W6

Figure A22. — *Compressible Stability Results for Case W6 Including the Maximum Amplification Method*

Figure A23. — VSTFE F-14 Cleanup Glove Transition N-Factors

(a) Pressure Distribution

CF (α^*_{rs}: 232 to 1,416 l/ft)
(Frequency: 0 Hz)

TS (Frequency: 2,771 to 5,502 Hz)
(Wave angle: 42 deg)

757 NLF Case 2

O Lower surface
O Transition at x/c = 0.17
O LE sweep = 18.8 deg
O Re_C = 25.54 million
O Mach No. = 0.804
O α = 2.94 deg

(b) Compressible Stability

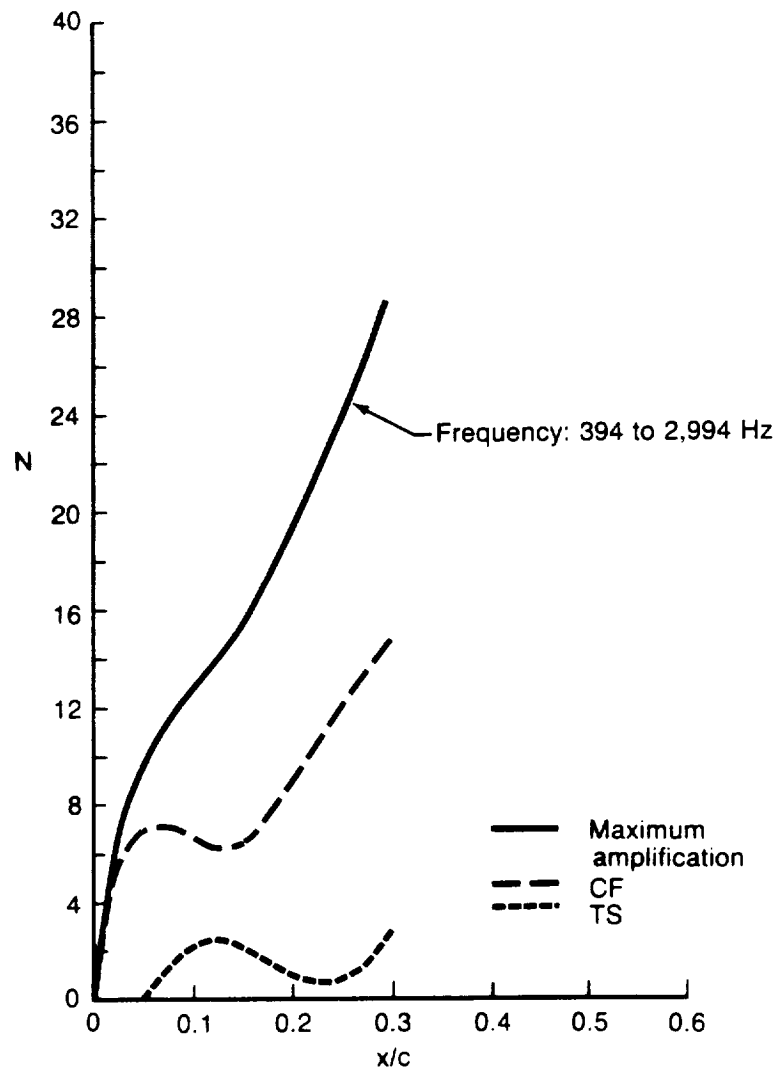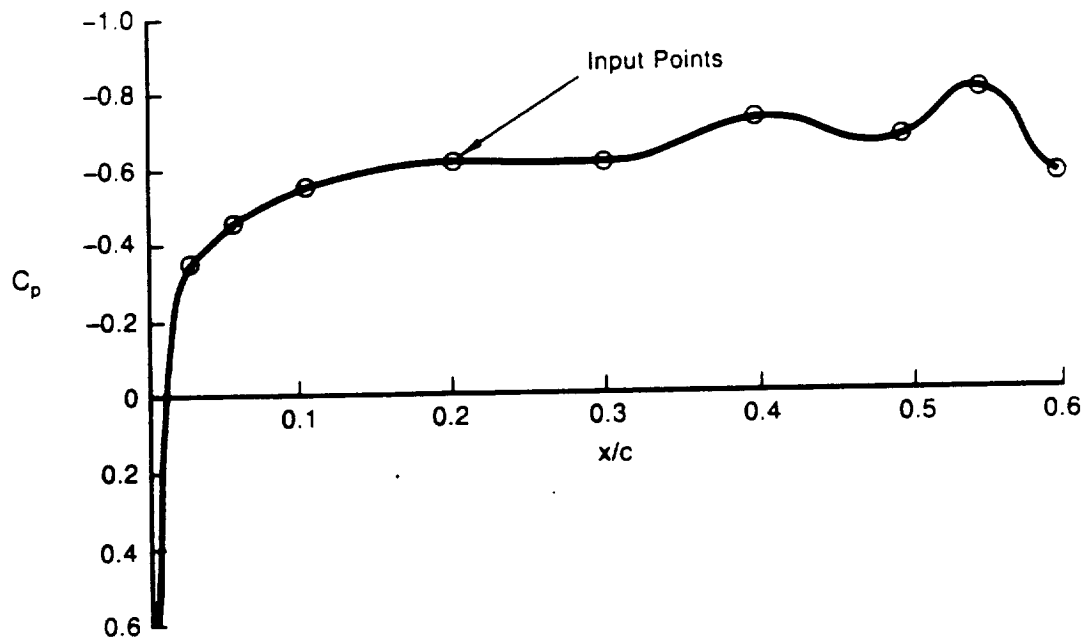*Figure A24. — Pressure Distribution and Compressible Stability Results for the 757 NLF Glove Case 2*

Figure A25. — Compressible Stability Results for 757 NLF Glove Case 2 Including the Maximum Amplification Method

(a) **Pressure Distribution**

CF ($\alpha^*_{r_s}$: 219 to 1,935 l/ft)
(Frequency: 0 Hz)

TS (Frequency: 3,436 to 7,512 Hz)
(Wave angle: 42 deg)

757 NLF Case 9

O Upper surface
O Transition at x/c = 0.18
O LE sweep = 17.8 deg
O Re_C = 25.69 million
O Mach No. = 0.753
O α = 3.59 deg

(b) **Compressible Stability**

Figure A26. — *Pressure Distribution and Compressible Stability Results for the 757 NLF Glove Case 9*
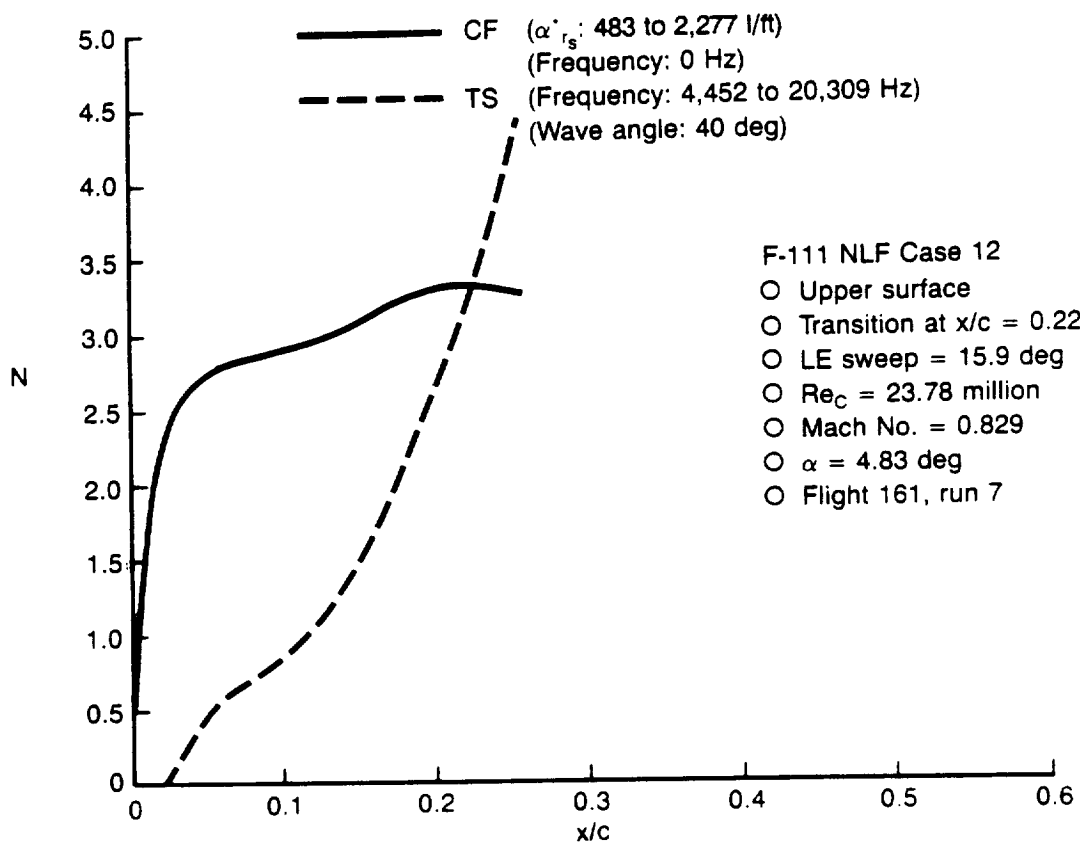
102
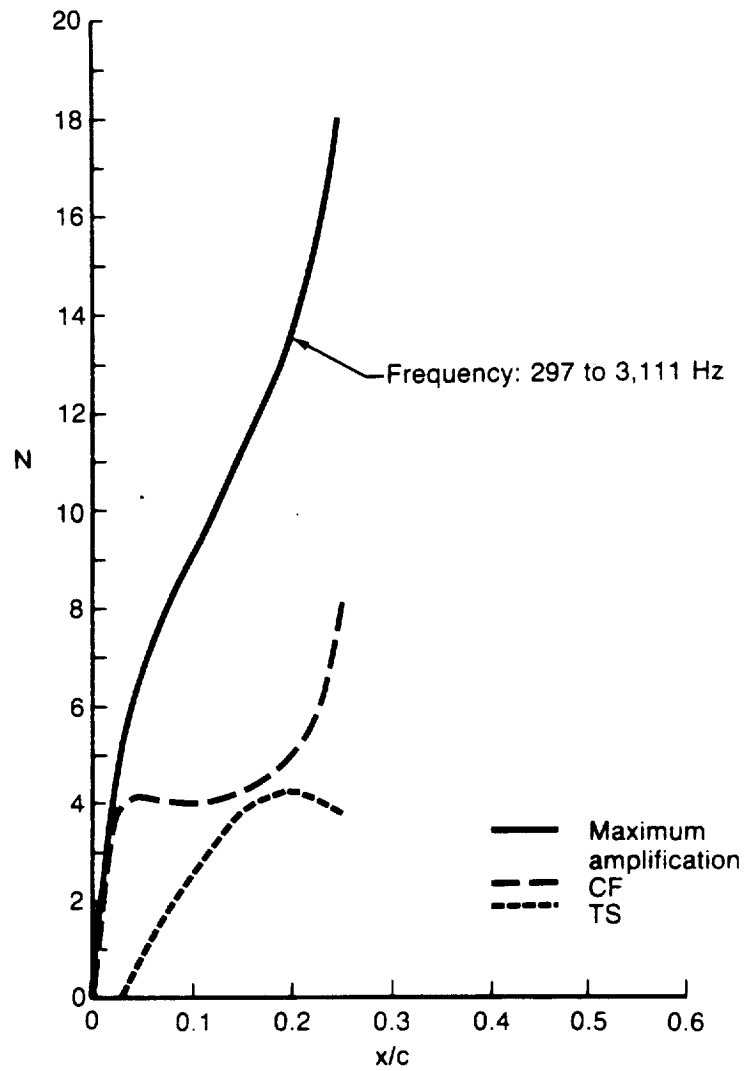
Figure A27. — *Compressible Stability Results for 757 NLF Glove Case 9 Including the Maximum Amplification Method*

(a) Pressure Distribution

(b) Compressible Stability

CF ($\alpha^{\cdot}{}_{r_s}$: 300 to 1,738 l/ft)
(Frequency: 0 Hz)

TS (Frequency: 2,797 to 8,002 Hz)
(Wave angle: 42 deg)

757 NLF Case 11

O Upper surface
O Transition at x/c = 0.27
O LE sweep = 19.9 deg
O Re_C = 29.99 million
O Mach No. = 0.801
O α = 2.61 deg
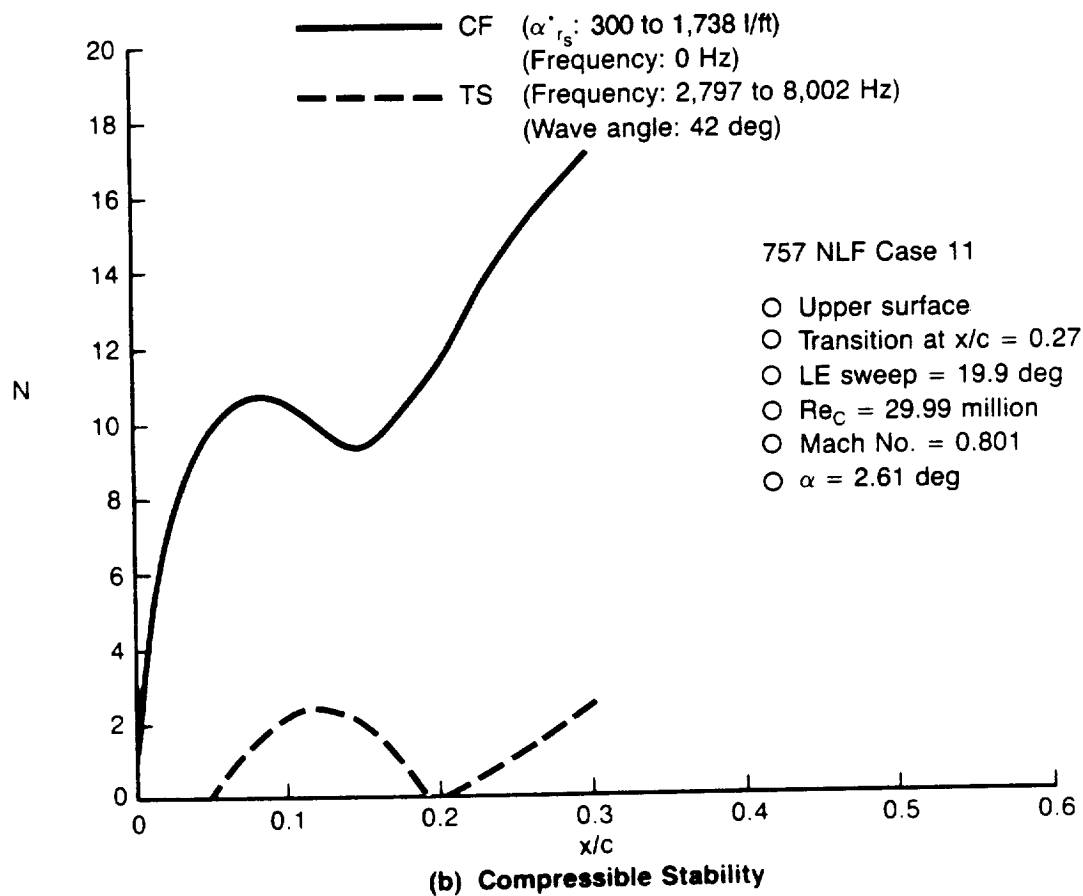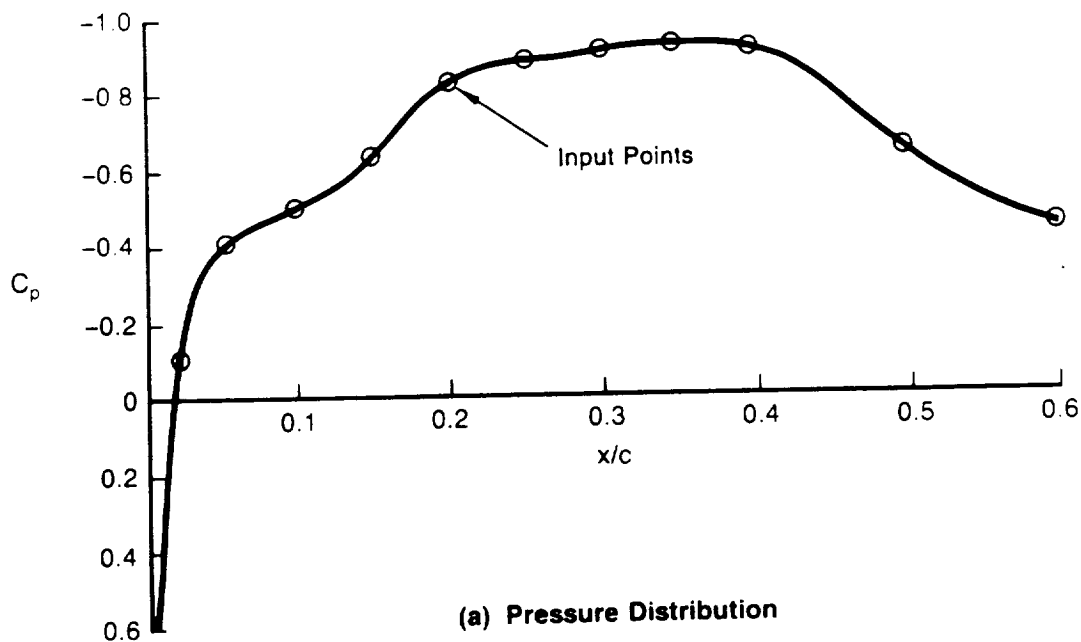
Figure A28. — Pressure Distribution and Compressible Stability Results for the 757 NLF Glove Case 11

104
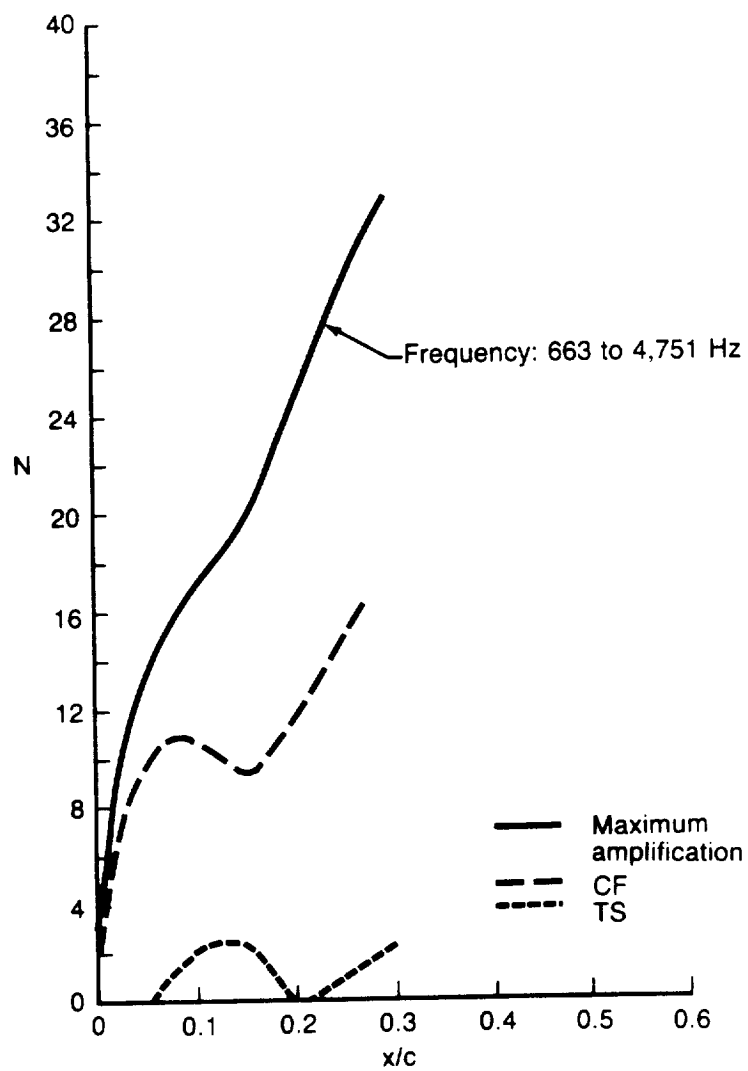
Figure A29. — Compressible Stability Results for 757 NLF Glove Case 11 Including the Maximum Amplification Method
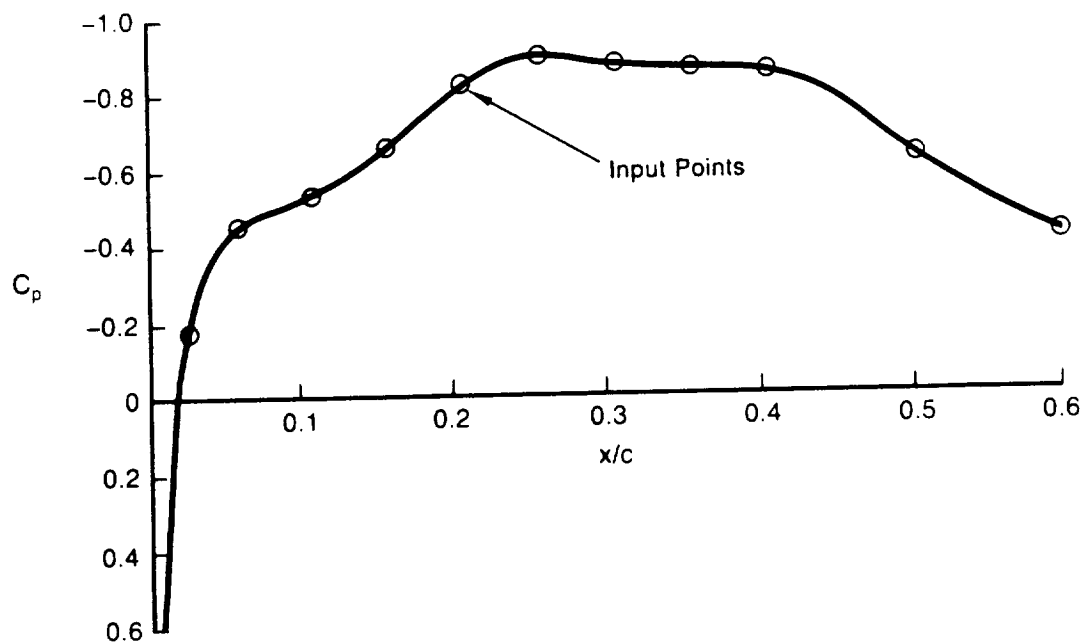
(a) Pressure Distribution
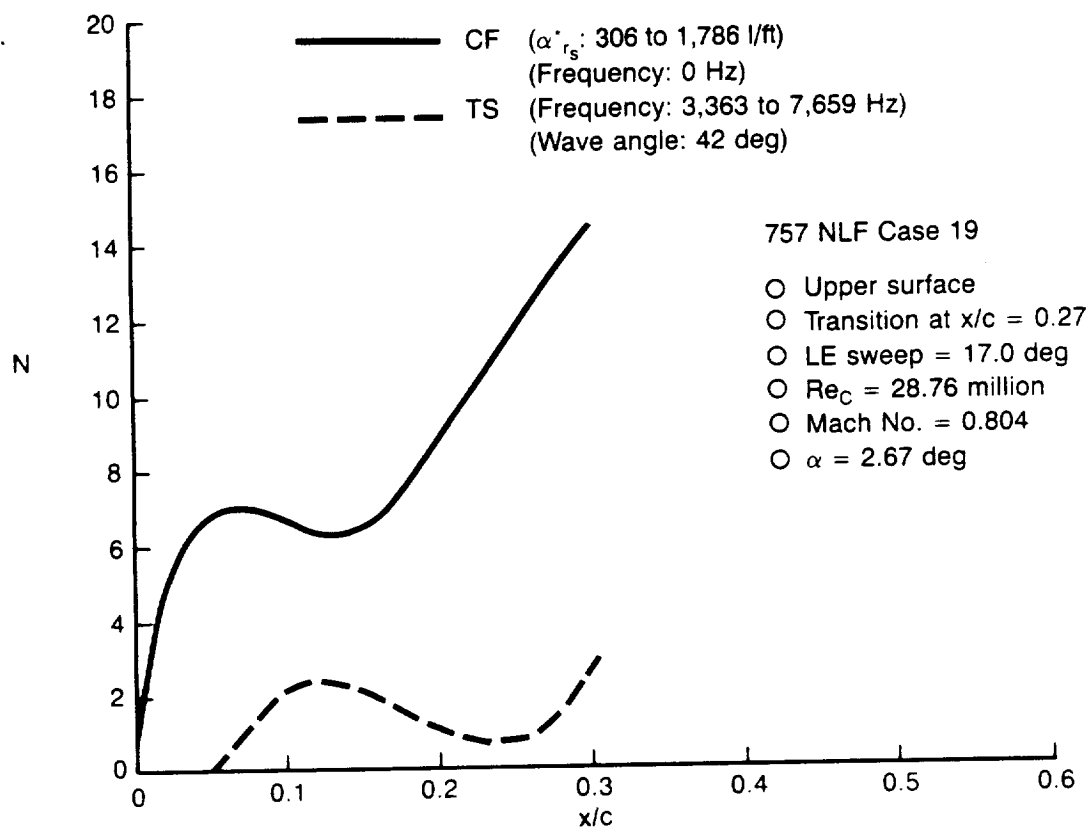
(b) Compressible Stability

Figure A30. — Pressure Distribution and Compressible Stability Results for the 757 NLF Glove Case 19
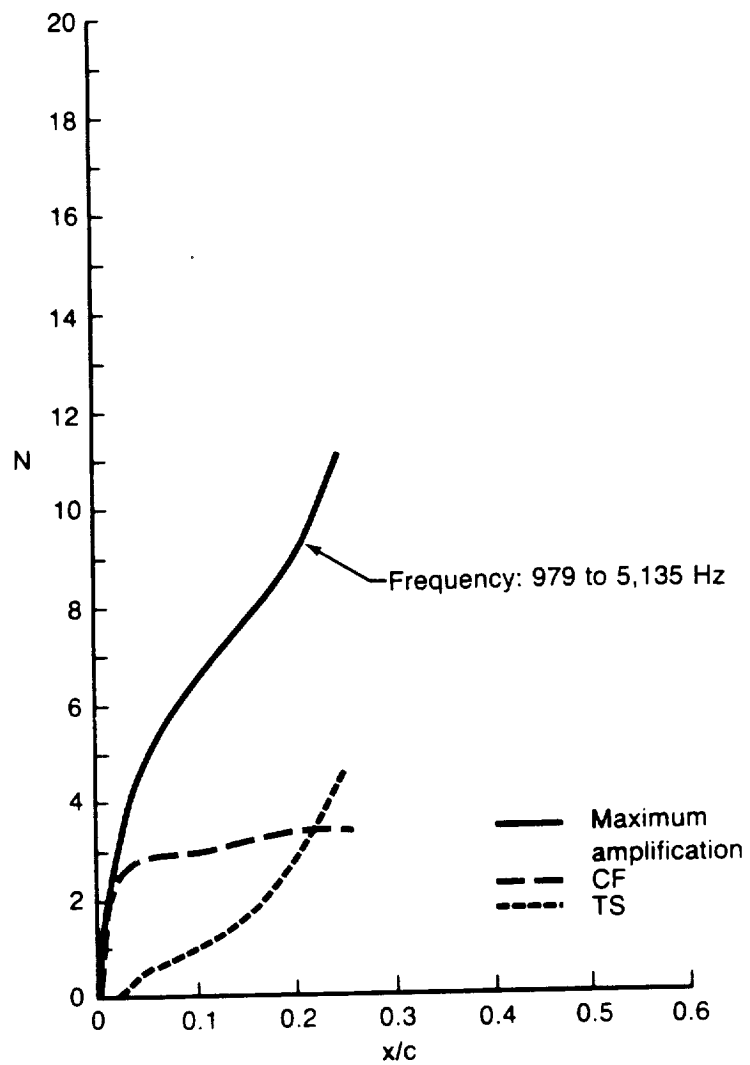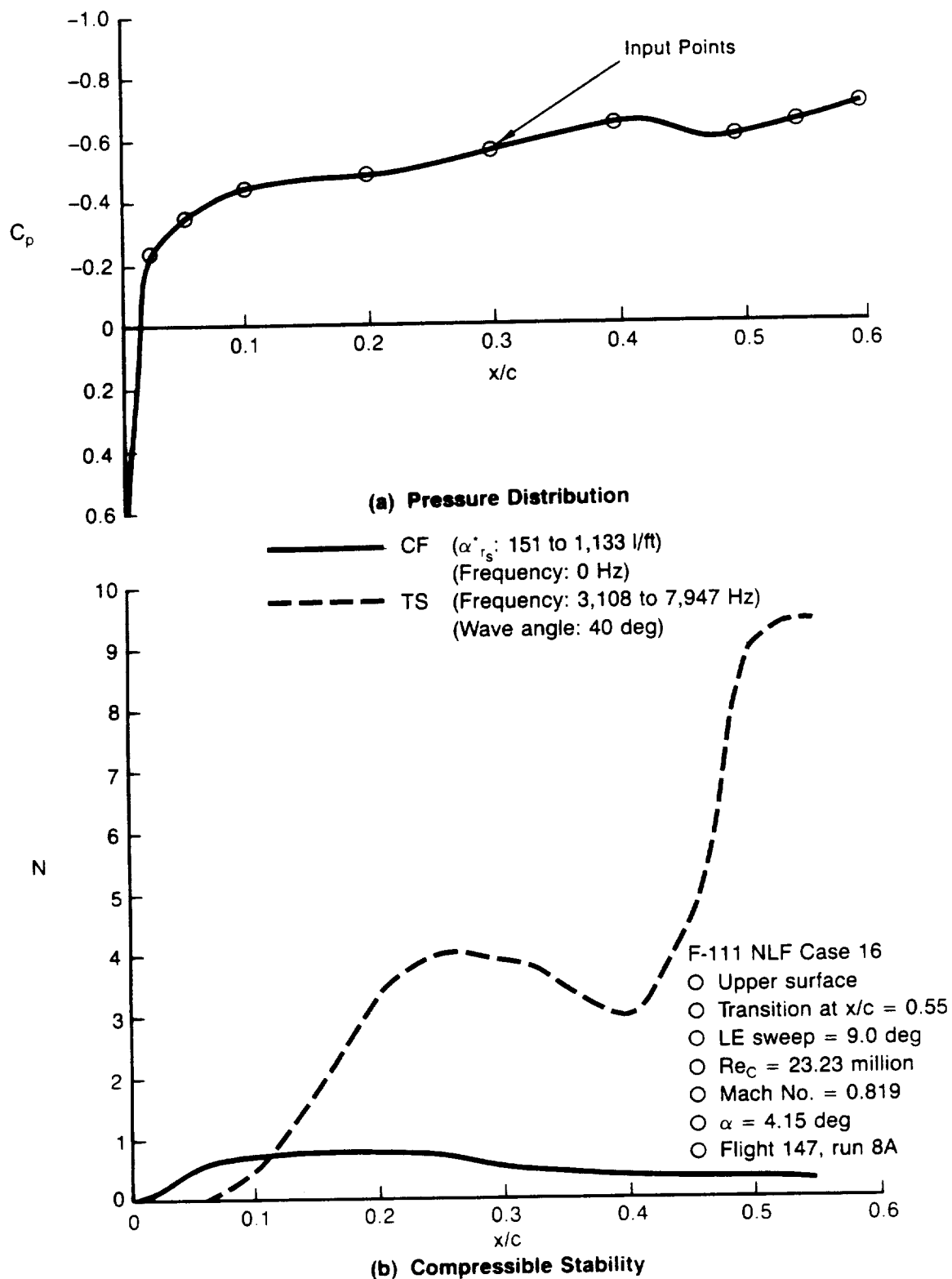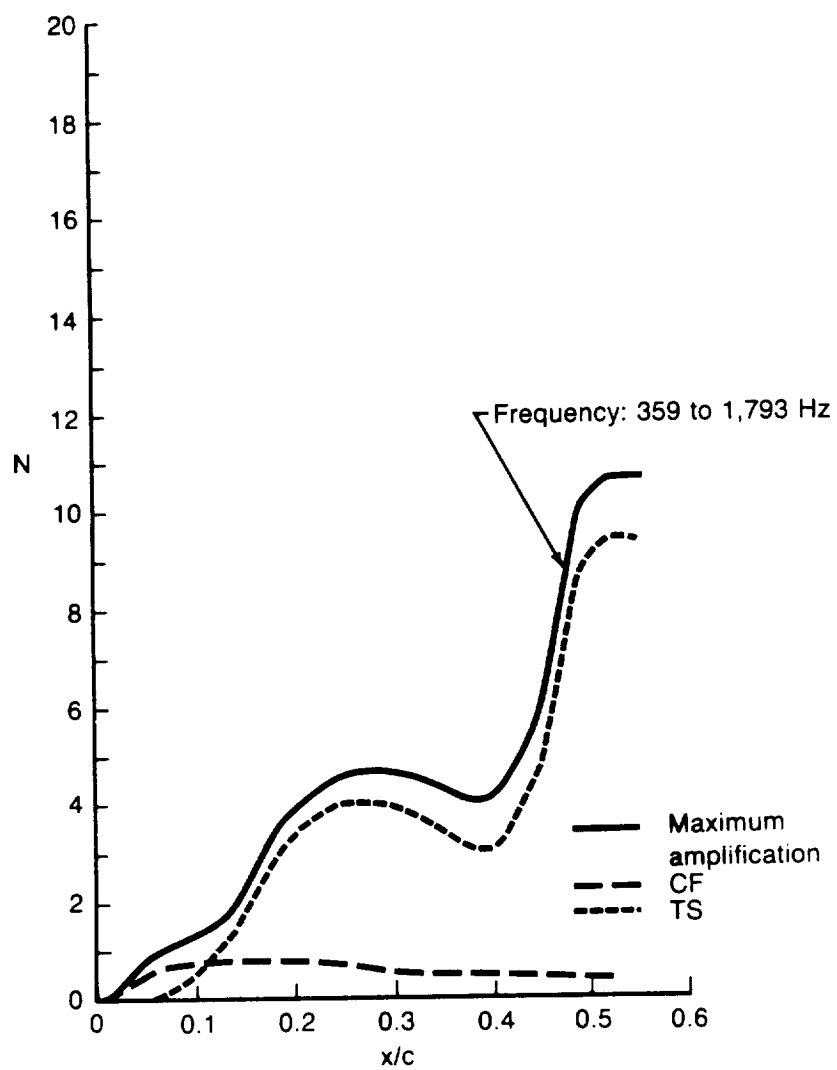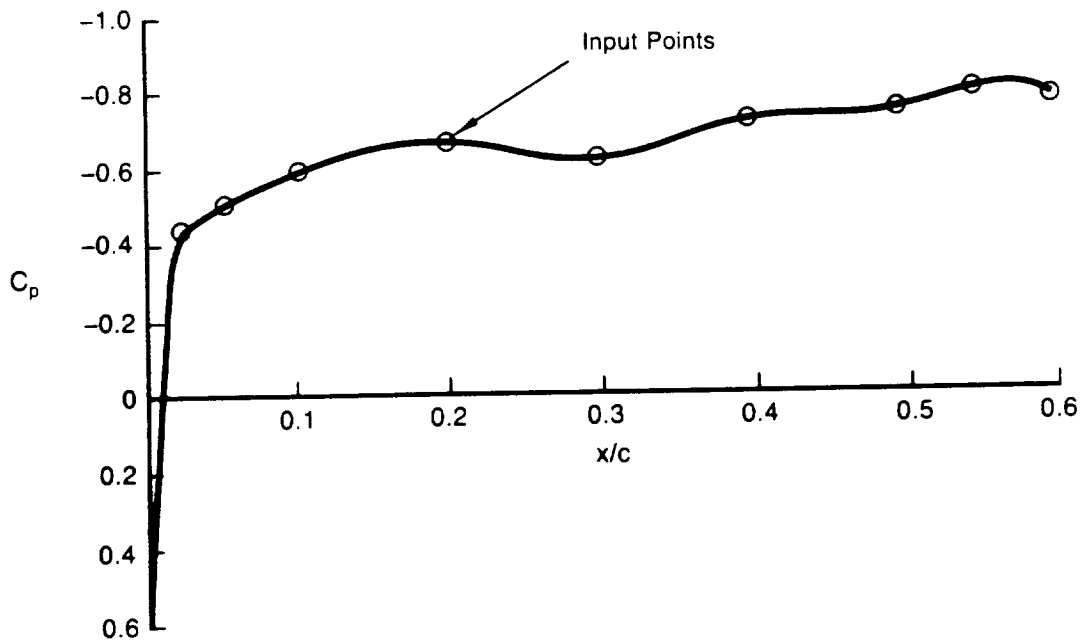
Figure A31. — *Compressible Stability Results for 757 NLF Glove Case 19 Including the Maximum Amplification Method*

(a) Pressure Distribution

(b) Compressible Stability

CF $(\alpha^{*}_{r_s}$: 483 to 2,277 l/ft)
(Frequency: 0 Hz)

TS (Frequency: 4,452 to 20,309 Hz)
(Wave angle: 40 deg)

F-111 NLF Case 12
O Upper surface
O Transition at x/c = 0.22
O LE sweep = 15.9 deg
O Re_C = 23.78 million
O Mach No. = 0.829
O α = 4.83 deg
O Flight 161, run 7

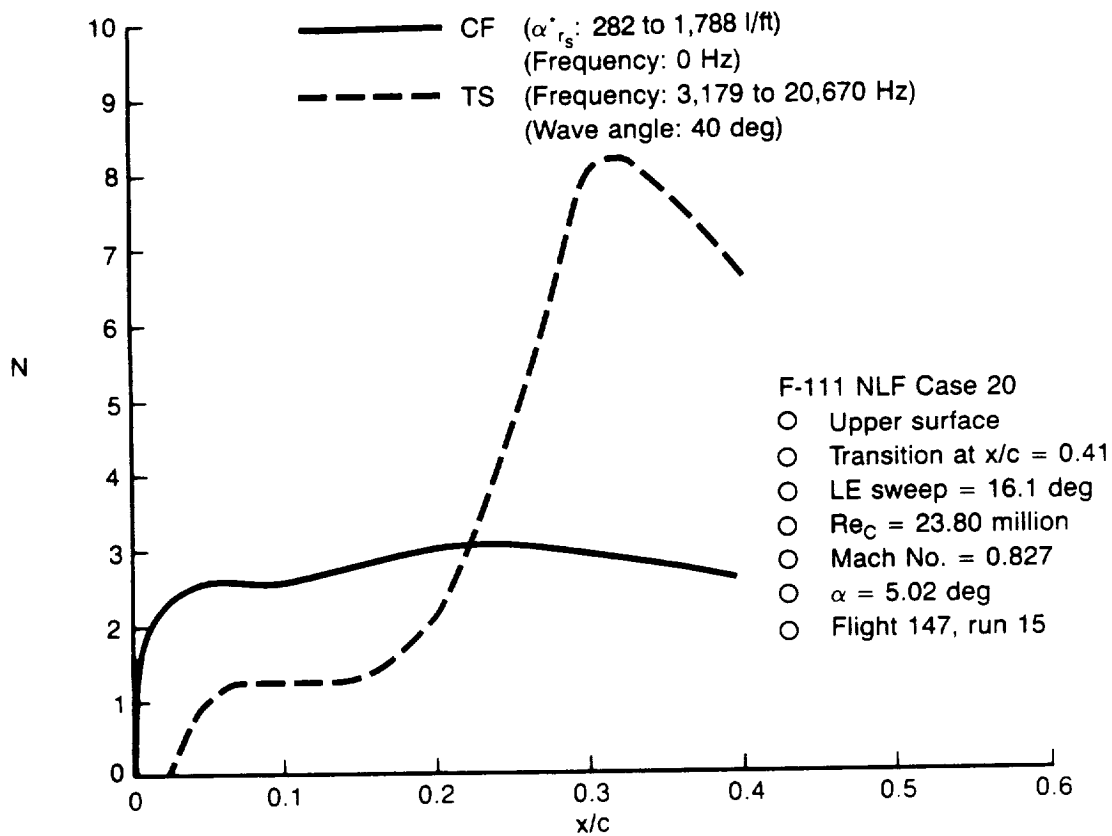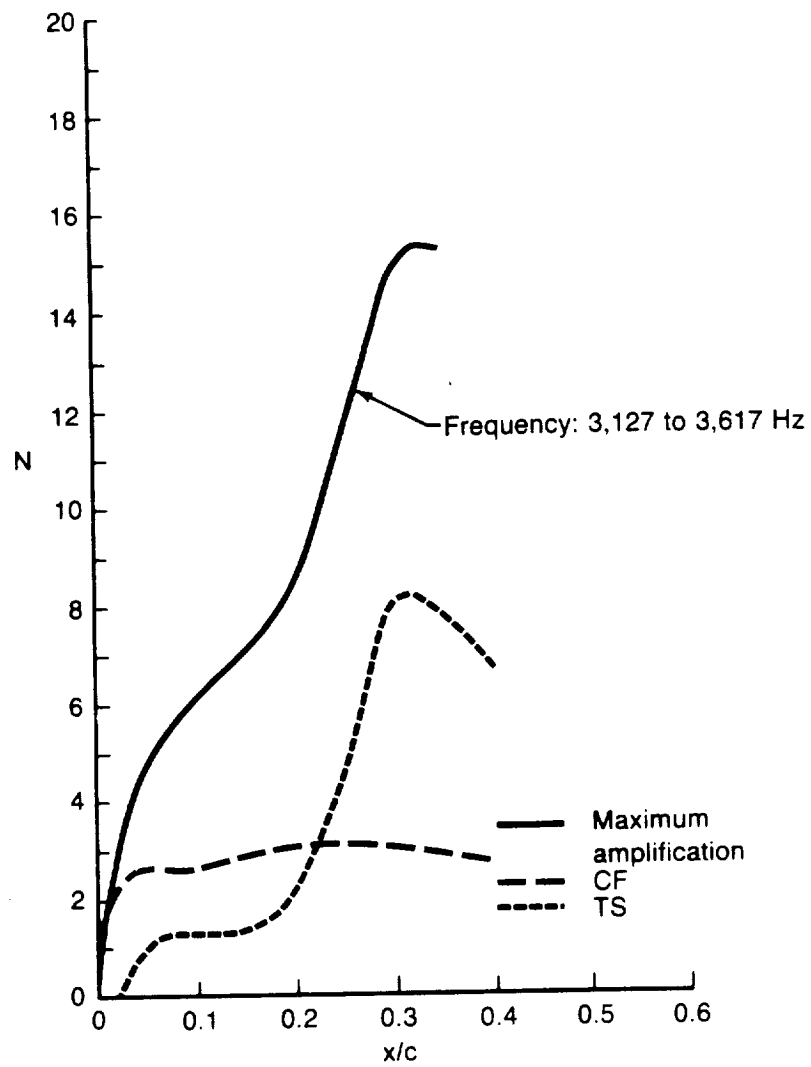*Figure A32. — Pressure Distribution and Compressible Stability Results for F-111 NLF Glove Case 12*

Figure A33. — *Compressible Stability Results for F-111 NLF Glove Case 12 Including the Maximum Amplification Method*

(a) **Pressure Distribution**

———— CF (α*$_{rs}$: 151 to 1,133 l/ft)
(Frequency: 0 Hz)

– – – – TS (Frequency: 3,108 to 7,947 Hz)
(Wave angle: 40 deg)

F-111 NLF Case 16
O Upper surface
O Transition at x/c = 0.55
O LE sweep = 9.0 deg
O Re$_C$ = 23.23 million
O Mach No. = 0.819
O α = 4.15 deg
O Flight 147, run 8A

(b) **Compressible Stability**

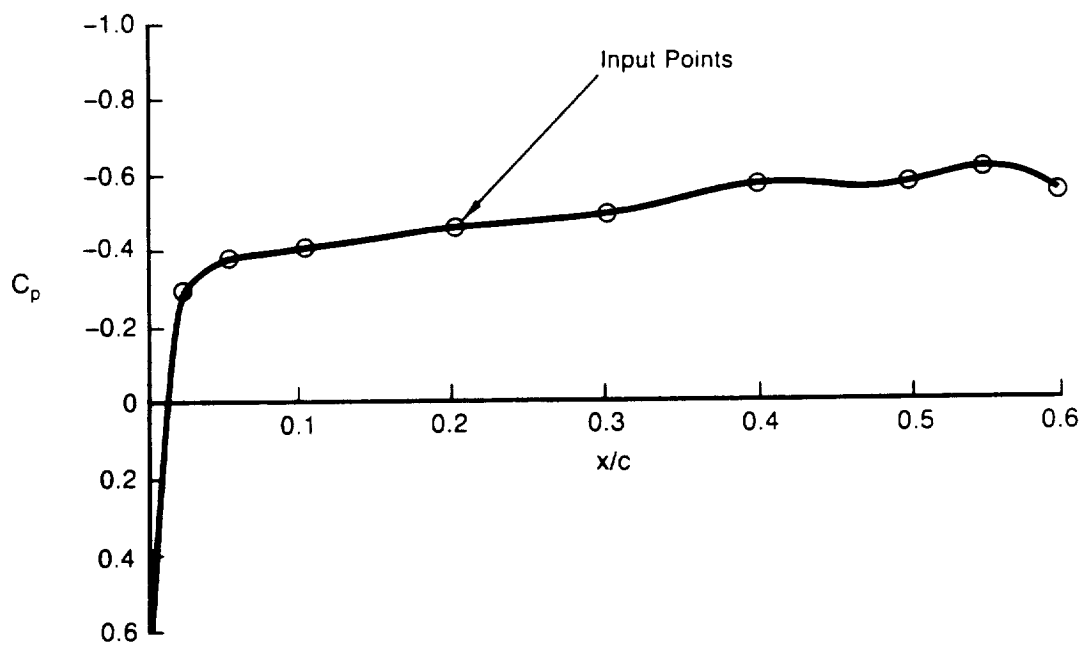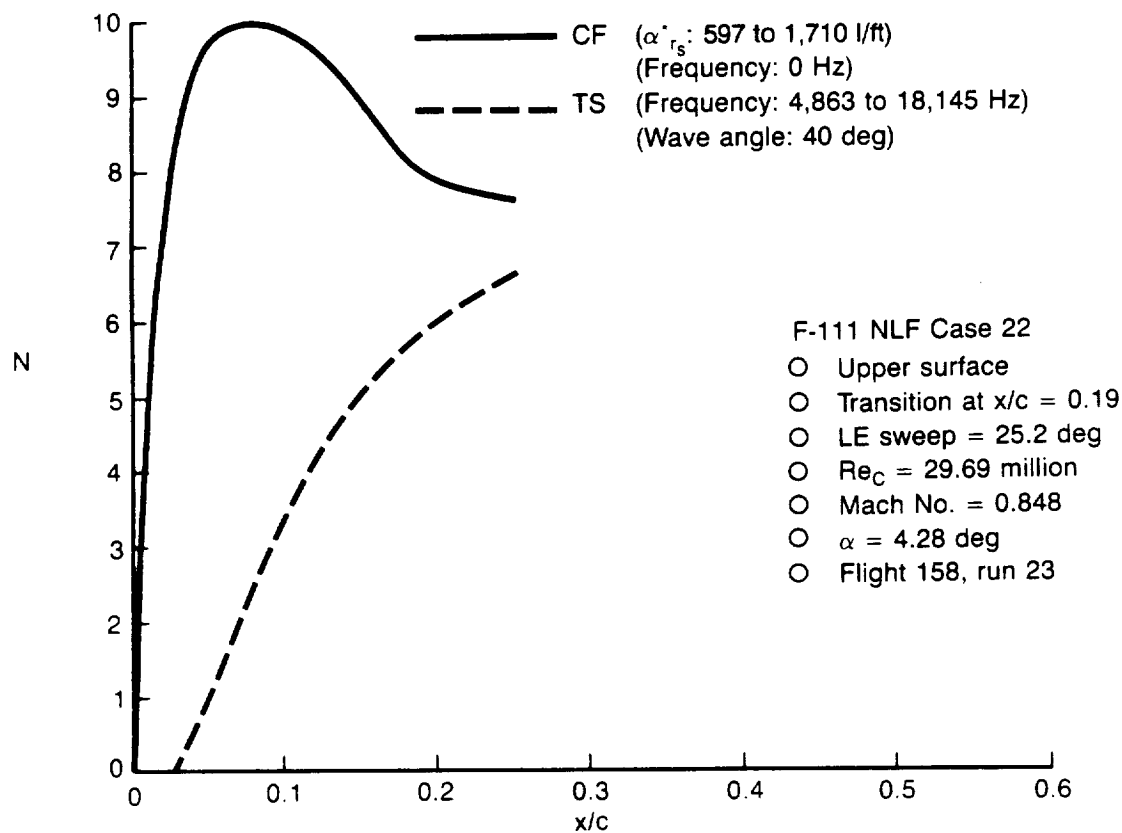Figure A34. — *Pressure Distribution and Compressible Stability Results for F-111 NLF Glove Case 16*

Figure A35. — *Compressible Stability Results for F-111 NLF Glove Case 16 Including the Maximum Amplification Method*

(a) Pressure Distribution

(b) Compressible Stability

CF ($\alpha^{*}_{r_s}$: 282 to 1,788 l/ft)
(Frequency: 0 Hz)

TS (Frequency: 3,179 to 20,670 Hz)
(Wave angle: 40 deg)

F-111 NLF Case 20
O Upper surface
O Transition at x/c = 0.41
O LE sweep = 16.1 deg
O Re_C = 23.80 million
O Mach No. = 0.827
O α = 5.02 deg
O Flight 147, run 15

Figure A36. — Pressure Distribution and Compressible Stability Results for F-111 NLF Glove Case 20

Figure A37. — *Compressible Stability Results for F-111 NLF Glove Case 20 Including the Maximum Amplification Method*

(a) Pressure Distribution

(b) Compressible Stability

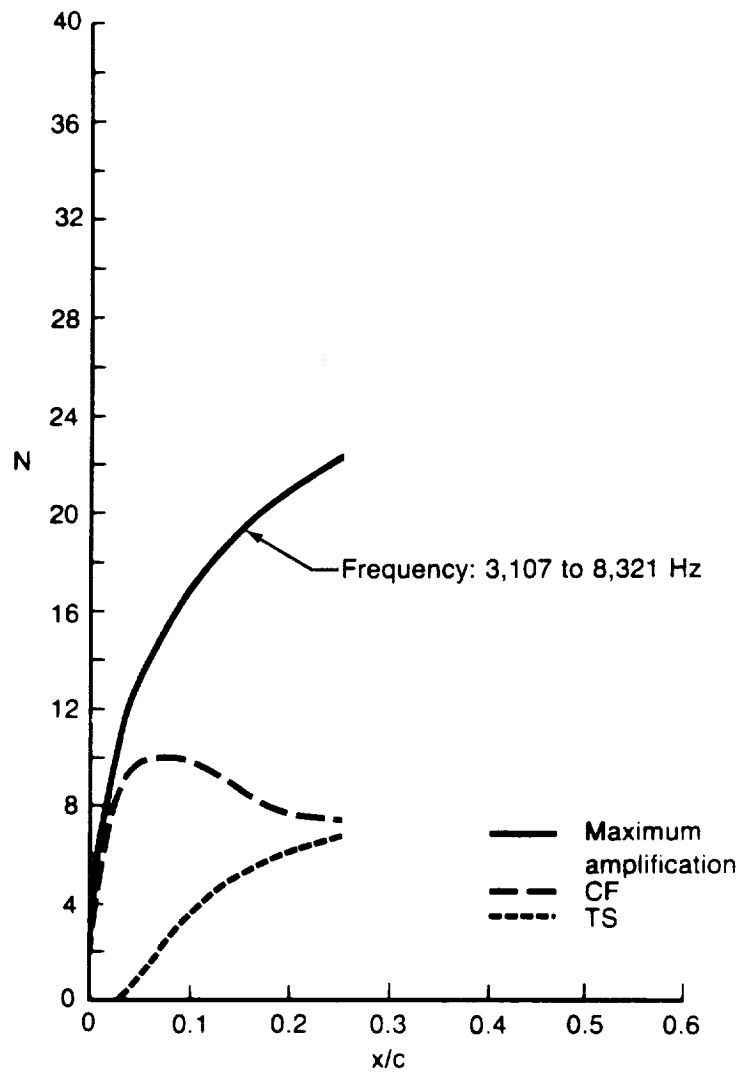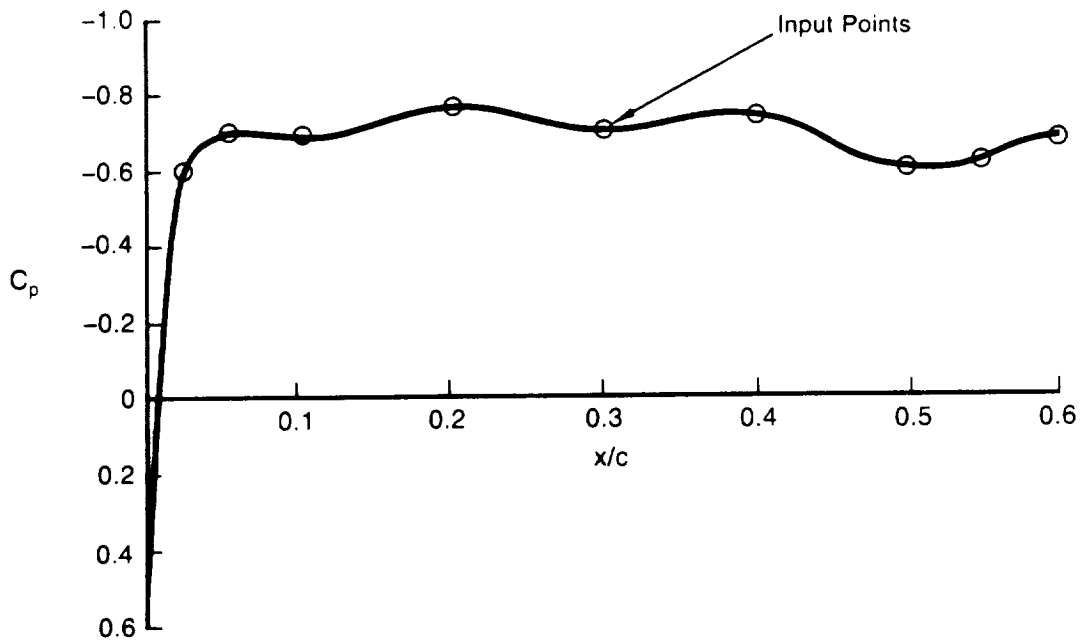Figure A38. — *Pressure Distribution and Compressible Stability Results for F-111 NLF Glove Case 22*
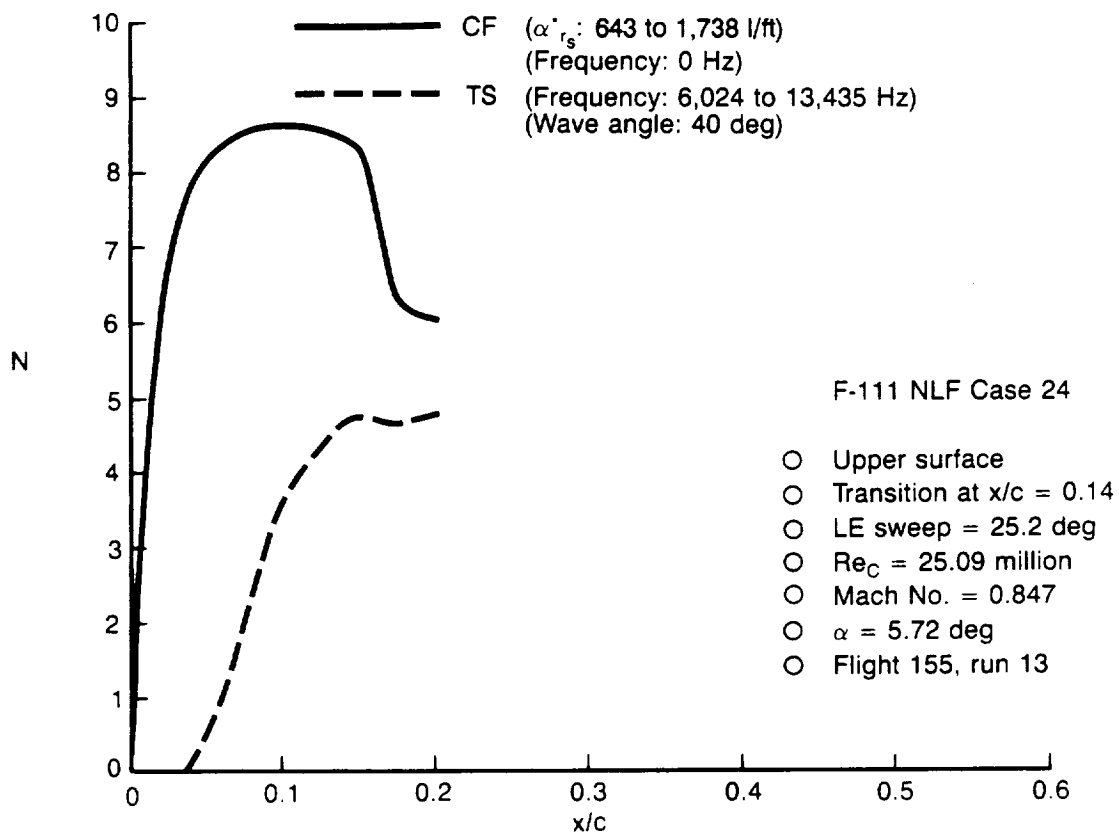
114

Figure A39. — Compressible Stability Results for F-111 NLF Glove Case 22 Including the Maximum Amplification Method

(a) **Pressure Distribution**

(b) **Compressible Stability**

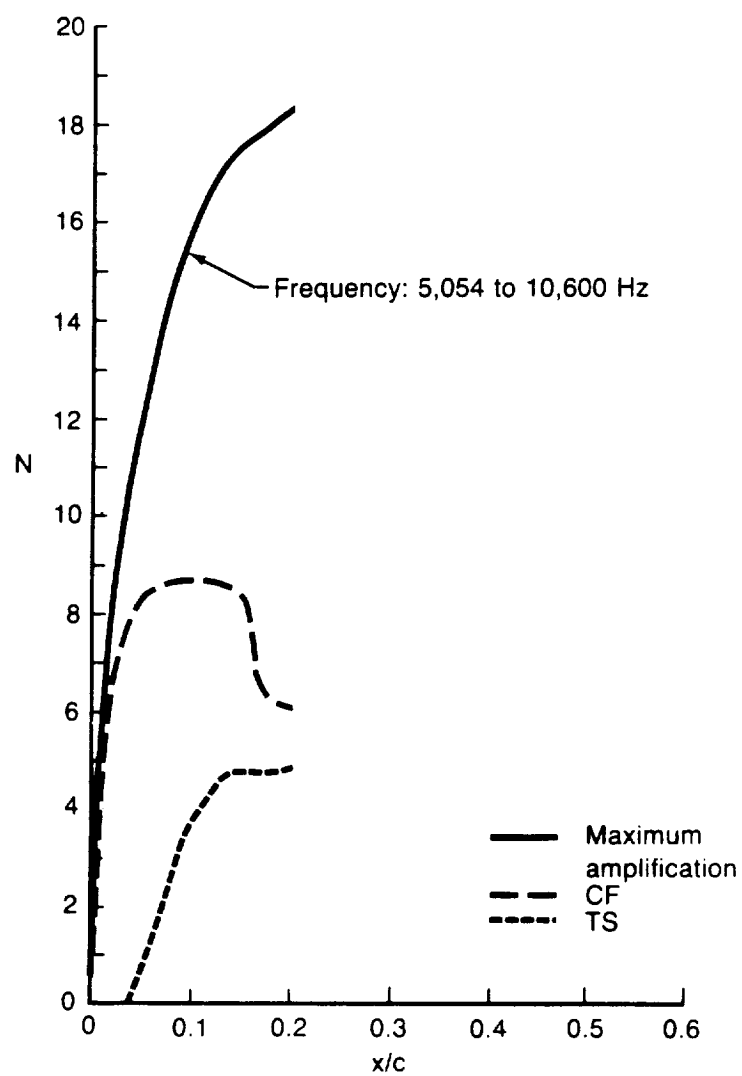*Figure A40. — Pressure Distribution and Compressible Stability Results for F-111 NLF Glove Case 24*

Figure A41. — *Compressible Stability Results for F-111 NLF Glove Case 24 Including the Maximum Amplification Method*

Table A-2. — Summary of 757 NLF Glove Cases

Case ID	Surface	WBL, in	Λ_{LE}, deg	M_∞	Re/ft x 10^{-6}	x/c_{TR}	Local chord, ft	Re_{TR} x 10^{-6}	N_{TS}	N_{CF}	$N_{Max.amp.}$	α, deg
2	Lower	308.5	18.8	0.804	1.511	0.17	16.9	4.34	3.5	9.1	18.9	2.94
9	Upper	308.5	17.8	0.753	1.520	0.18	16.9	4.62	4.2	4.6	12.4	3.59
11	Upper	308.5	19.9	0.801	1.775	0.27	16.9	8.10	1.7	15.8	31.0	2.61
19	Upper	308.5	17.0	0.804	1.702	0.27	16.9	7.77	1.3	12.9	25.7	2.67

Table A-3. — Summary of F-111 NLF Glove Cases

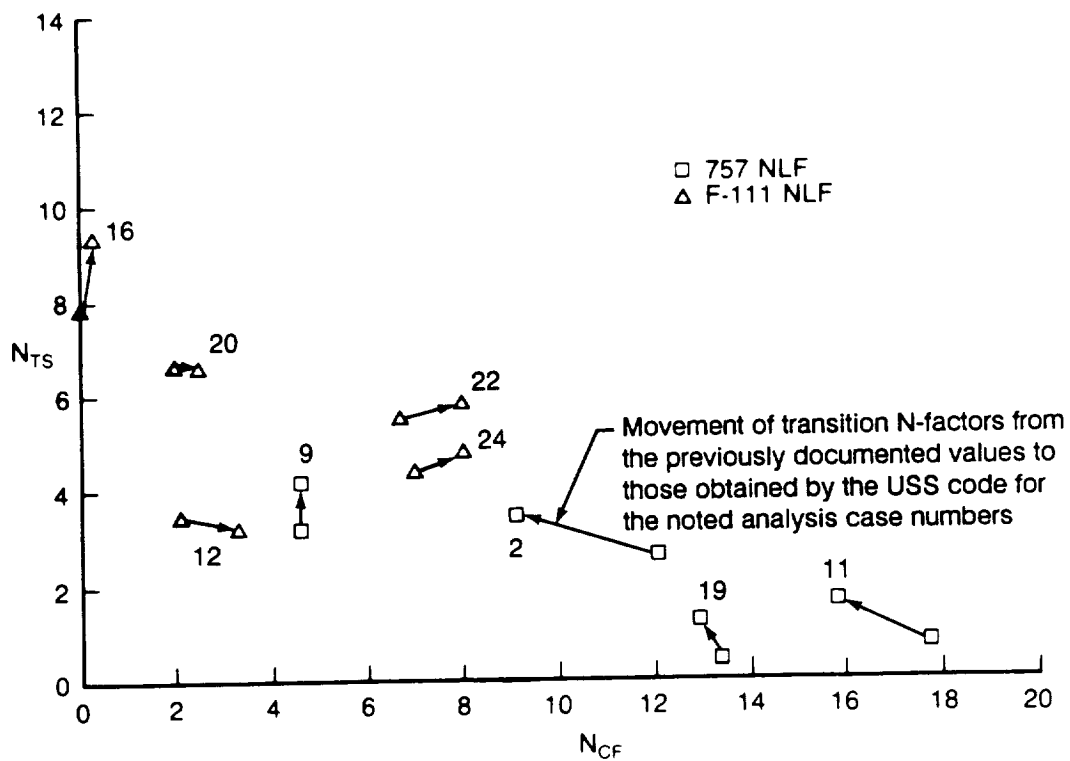| Case ID	Flight No.	Run	Λ_{LE}, deg	M_∞	Re/ft x 10^{-6}	x/c_{TR}	Local chord, ft	Re_{TR} x 10^{-6}	N_{TS}	N_{CF}	$N_{Max.amp.}$	α, deg
12	161	7	15.9	0.829	2.35	0.22	10.14	5.24	3.2	3.3	9.5	4.83
16	147	8A	9.0	0.819	2.32	0.55	10.03	12.80	9.3	0.3	10.6	4.15
20	147	15	16.1	0.827	2.35	0.41	10.14	9.77	6.6	2.5	13.5	5.02
22	158	23	25.2	0.848	2.83	0.19	10.50	5.65	5.8	8.0	20.5	4.28
24	155	13	25.2	0.847	2.39	0.14	10.50	3.51	4.8	8.0	17.5	5.72

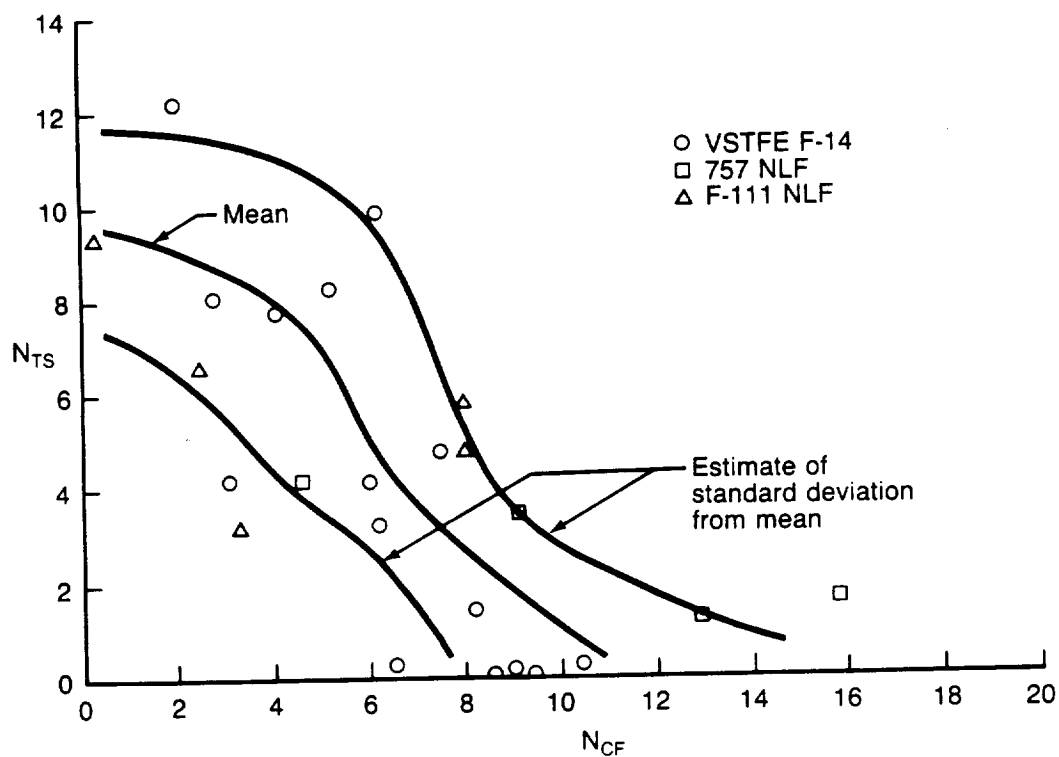Figure A42. — Change in Transition N-Factors Using USS

Figure A43. — Transition Mean Line and Standard Deviation From Mean

119

1. Report No. NASA CR-181918	2. Government Accession No.	3. Recipient's Catalog No.
4. Title and Subtitle Variable Sweep Transition Flight Experiment (VSTFE) — Unified Stability System (USS) Description and Users' Manual		5. Report Date June 1990
		6. Performing Organization Code
7. Author(s) Rodger A. Rozendaal and Roxanna Behbehani		8. Performing Organization Report No. D6-54961
		10. Work Unit No. 505-60-41-01
9. Performing Organization Name and Address The Boeing Company P.O. Box 3707 Seattle, WA 98124		11. Contract or Grant No. NAS1-15325
12. Sponsoring Agency Name and Address National Aeronautics and Space Administration Washington, DC 20546-0001		13. Type of Report and Period Covered Contractor Report October 1985-May 1990
		14. Sponsoring Agency Code

15. Supplementary Notes

Technical Monitors: D. W. Bartlett
D. V. Maddalon
NASA/Langley Research Center

16. Abstract

NASA initiated the Variable Sweep Transition Flight Experiment (VSTFE) to establish a boundary layer transition database for laminar flow wing design. For this experiment, full-span upper surface gloves were fitted to a variable sweep F-14 aircraft. The Boeing Company is under contract to NASA to provide design and analyses support for the program. This report documents the development of an improved laminar boundary layer stability analysis system called the Unified Stability System (USS) and shows results of its use on the VSTFE flight data. The USS consists of eight computer codes. The theoretical background of the system is described herein, as is the input, output, and usage hints. The USS is capable of analyzing boundary layer stability over a wide range of disturbance frequencies and orientations, making it possible to use different philosophies in calculating the growth of disturbances on sweptwings.

17. Key Words (Suggested by Author(s)) • Computational fluid dynamics • Crossflow disturbances • Transition • Linear stability theory • Boundary layer • Natural laminar flow (NLF) • Wing glove • Tollmein-Schlichting disturbances • F-14 • Flight test • Computer code	18. Distribution Statement ━━━━━ Subject Category 02

19. Security Classif. (of this report) Unclassified	20. Security Classif. (of this page) Unclassified	21. No. of pages 120	22. Price*